POLITECNICO
MILANO 1863

SCHOOL OF CIVIL, ENVIRONMENTAL
AND LAND MANAGEMENT ENGINEERING

High temperature industrial processes and mapping of their potential for solarization

MASTER'S THESIS IN ENVIRONMENTAL AND LAND PLANNING ENGINEERING

Author: **Riccardo Cuneo**

Student ID: 103276
Advisor: Giampaolo Manzolini
Academic Year: 2023-24

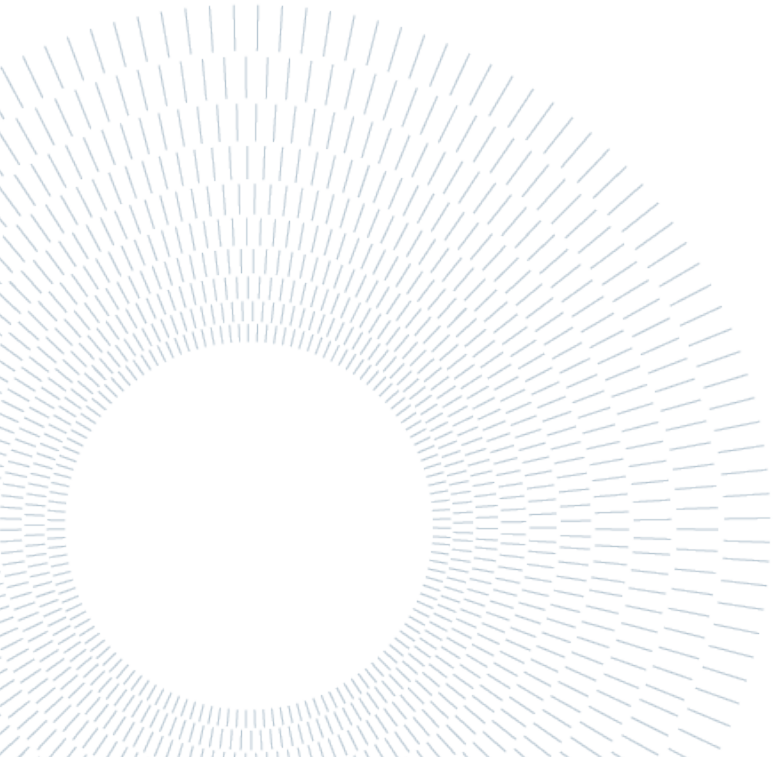

Acknowledgments

Ringraziamenti

Abstract

Climate change is already affecting human society on several aspects, however the CO_2 concentration in the atmosphere is continuously increasing. To achieve a carbon-neutral society, emissions from energy production of any form have to be cut.

This thesis examines the potential of concentrated solar thermal (CST) energy as a technology to provide heat to high temperature industrial processes, like metals manufacturing. These processes are relevant in the most important sectors both for economic and societal development. A detailed look at the production of some commodities with a thermal energy demand above 600 °C shows their cost- and emission-composition. A possible replacing of fossil fuels with solar energy is evaluated in 25 countries around the world that have an abundant solar resource in terms of Direct Normal Irradiance (DNI), namely: Argentina, Australia, Bolivia, Chile, Egypt, Mexico, Morocco, Portugal, Peru, South Africa, Spain, USA, Angola, Botswana, Brazil, Iran, Israel, Madagascar, Namibia, Saudi Arabia, Tanzania, UAE, Turkey, Zambia and Zimbabwe. The impact of carbon taxes is taken into consideration as several governments are implementing them more and more in order to encourage cleaner processes. A comparison between the CST option and a PV implementation is also calculated to assess which is more attractive based on the location. Results show that CST can be a competitive source of industrial heat in most of the countries that have been analysed. In particular, the CST option appears to be the most cost-efficient path for production in some areas like Spain, Portugal, Israel and Chile where for example the recycling of a tonne of aluminium costs 1235 EUR/t using coal and 1228 EUR/t using a solar technology[1]. Therefore, CST proves to be a very promising player in the decarbonization path of industry.

Key-words: Concentrated Solar Thermal Energy, CST, solar heat, high-temperature processes, decarbonization, industry.

1: Production costs based on Tarapacà Region, Chile (-21.86°, -69.93°) with a DNI of 3000 kWh/m^2 and coal price based on Appendix Table 2.

Abstract in italiano

Gli effetti del cambiamento climatico sono già visibili nella società sotto vari aspetti, nonostante questo la concentrazione di CO_2 nell'atmosfera è in continuo aumento. Per raggiungere una società *carbon-neutral*, è necessario ridurre le emissioni derivanti dalla produzione di energia sotto qualsiasi sua forma.

Questa tesi esamina il potenziale dell'energia solare a concentrazione (CST) come tecnologia per fornire calore ai processi industriali ad alta temperatura, i quali rientrano nei settori più importanti sia per l'economia che per lo sviluppo della società, come la produzione di metalli. Uno sguardo dettagliato alla produzione di alcuni materiali al di sopra di 600 °C mostra la loro composizione in termini di costi e di emissioni, e viene valutata la possibilità di sostituire i combustibili fossili con l'energia solare in 25 Paesi del mondo che presentano un'abbondante risorsa solare: Argentina, Australia, Bolivia, Cile, Egitto, Messico, Marocco, Portogallo, Perù, Sud Africa, Spagna, USA, Angola, Botswana, Brasile, Iran, Israele, Madagascar, Namibia, Arabia Saudita, Tanzania, Emirati Arabi Uniti, Turchia, Zambia e Zimbabwe. Viene preso in considerazione l'impatto delle tasse sulle emissioni di anidride carbonica che diversi governi stanno introducendo in misura sempre maggiore per incoraggiare processi più puliti. Viene inoltre effettuato un confronto tra l'opzione CST e un'implementazione fotovoltaica per valutare quale sia più conveniente in base alla località. I risultati mostrano che il CST può essere una fonte competitiva di calore industriale in molti Paesi analizzati. In particolare, l'opzione CST risulta essere l'opzione più efficiente in termini di costi in aree come la Spagna, il Portogallo, Israele e il Cile dove per esempio il riciclo di una tonnellata di alluminio costa 1235 EUR/t usando carbone e 1228 EUR/t usando la tecnologia solare[1]. Pertanto, il CST si rivela essere un attore importante nel percorso di decarbonizzazione dell'industria.

Parole chiave: energia solare a concentrazione CST, processi ad alte temperature, decarbonizzazione, industria.

1: Costi di produzione calcolati nella Regione Tarapacà, Cile (-21.86°, -69.93°) con DNI di 3000 kWh/m2 e prezzo del carbone basato sulla Tabella 2 in Appendice.

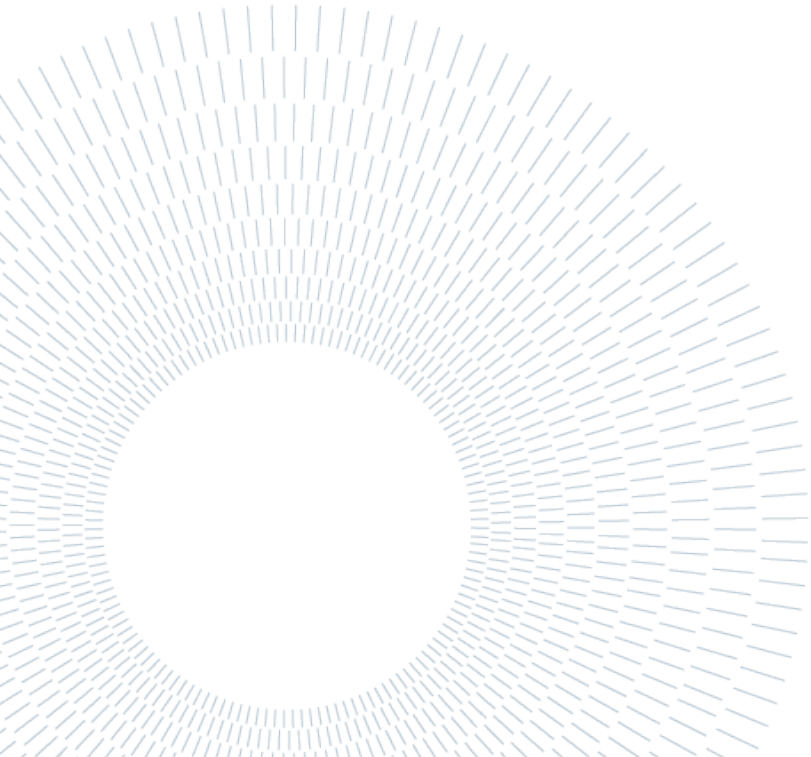

List of abbreviations

Variable	Description	SI unit
DNI	Direct Normal Irradiance	kWh/m^2
GDP	Gross Domestic Product	EUR/a
LCOE	Levelized Cost Of Electricity	EUR/kWh
LCOH	Levelized Cost Of Heat	EUR/kWh
CAGR	Compound Annual Growth Rate	-
CST	Concentrated Solar Thermal	-
DLR	German Aerospace Centre	-
IRENA	International Renewable Energy Agency	-
GHG	Greenhouse Gas Emissions	-

Contents

Acknowledgments ..... **i**
Abstract ..... **ii**
Abstract in italiano ..... **iii**
List of abbreviations ..... **v**
Contents ..... **vii**
Introduction **1**
1 Industrial heat **3**
1.1. Energy demanding industries 4
1.2. Process analysis 4
1.2.1. Aluminium recycling 5
1.2.2. Bricks production 6
1.2.3. Calcium compounds 8
1.2.4. Carbon-based materials 8
1.2.5. Cement production 10
1.2.6. Copper recycling 11
1.2.7. Glass recycling 12
1.2.8. Gypsum – Anhydrite II-E 13
1.2.9. High speed steel 14
1.2.10. Lithium recycling 15
1.2.11. Steel production 16
1.2.12. Sulfuric acid recycling 17
1.2.13. Zinc roasting 17
1.3. Synthesis table 19
1.3.1. Choice of three processes 21
2 CST technology **22**
2.1. Overview 22
2.2. Concentrating solar technologies 22
2.2.1. Parabolic trough (PT) 23
2.2.2. Central receiver solar tower (ST) 23
2.2.3. Parabolic dishes 24
2.2.4. Linear Fresnel 24
2.3. Heat production 24
3 Process analysis **26**
3.1. Spatial distribution 26

3.2. Aluminium recycling 28
3.3. Bricks production 32
3.4. Zinc production 35
4 LCOH calculation 38
5 Calculations and elaborations 41
5.1. Carbon tax 41
5.2. CST production 43
5.2.1. Calculation of CST production 44
5.3. PV comparison 45
5.3.1. From LCOE to LCOH map 45
5.3.2. Calculation of PV production 46
5.4. Results 47
5.4.1. Base scenario 47
5.4.2. Carbon tax and renewable production 49
5.5. Sensitivity analysis 52
6 Conclusion and future developments 57
References 59
A Appendix A 67
A.1. Supplementary tables 67
A.2. Supplementary figures 71
List of Figures 79
List of Tables 81

Introduction

In May 2023, a new record was set for the concentration of carbon dioxide (CO_2) in the atmosphere with a value of 423.68 ppm (NASA, 2023). Despite international efforts like the Paris Agreements in 2015 to decrease the global greenhouse gas emissions, no sign of such turnaround is tangible. At the same time, the effects of climate change are already visible with the increasing frequency of extreme weather conditions that leads to heat waves, floods, droughts and wildfires.

Cleaner ways to produce energy and goods have to be found and adopted, while still keeping pace with the growing population and general improvements of living conditions, which increase the demand of mostly all commodities. Ensuring a sustainable future is a challenge that humanity is facing now and that sees the industrial sector as one of the major involved entities.

Whilst the issue of climate change is dominating the future energy agenda, the fact that demand for oil may have now passed the level of supply from conventional sources is well accepted and, despite large levels of fluctuation, the overall trend is rising prices. This has the potential to be a significant force behind technological advancement, boosting demand for solar power and promoting innovations like solar fuels.

While the public opinion is mostly focused on the electric generation via renewable sources, industrial heat demand is massive and the greenhouse gases emissions related to it are enormous as well, especially when dirtier fuels like coal are the major source of energy [1]. The electrification of high temperature processes is extremely costly and therefore a carbon-free production is difficult to reach. However, the use of Concentrated Solar Thermal energy (CST) for the production of heat could be part of the solution because of its ability to provide high temperatures to reactors only thanks to solar radiation.

In this thesis, conducted at the Institute of Future Fuels of the German Aerospace Centre (DLR), a review of high temperature industrial processes and their potential for solarization was carried out. In particular, after a first broad research about industrial heat and the identification of the most important processes requiring thermal energy at temperatures above 600 °C, three production paths are chosen in order to analyse their potential for solarization. Their cost-composition is studied in detail and a comparison is done between the conventional production using fossil fuel and the production in which high temperature heat is provided by the CST technology. In particular, maps have been elaborated to show the cheapest fuel option in different locations around the world and how it changes based on solar source, country-specific parameters such as fuel prices, various carbon tax values and different CST technology costs. An additional renewable option, i.e. photovoltaics plus electrical heaters, is also part of the analysis to get a broader vision.

1 Industrial heat

Industry is often cited as the global greatest energy-consuming and greenhouse gas-emitting end-use sector. In particular, its demand for energy and fossil fuels is mostly driven by the need for heat [1].

Approximately 30% of the world's energy was used by industry in 2015, three quarters of it in heat form, as shown in Figure 1.1. As a result, in 2015 36% of worldwide carbon dioxide emissions from fuel combustion were attributable to global industry which burned 73% of total used coal in that year, and 38% of total natural gas [1]. In fact, heat production is still strongly fossil dependent, with fossil fuels accounting for 90% of the energy demand, and coal being the main source. Almost half of the heat demand is high temperature heat (above 400 °C for the study by Energy Power Partners, EPP), mostly required by material transformation processes.

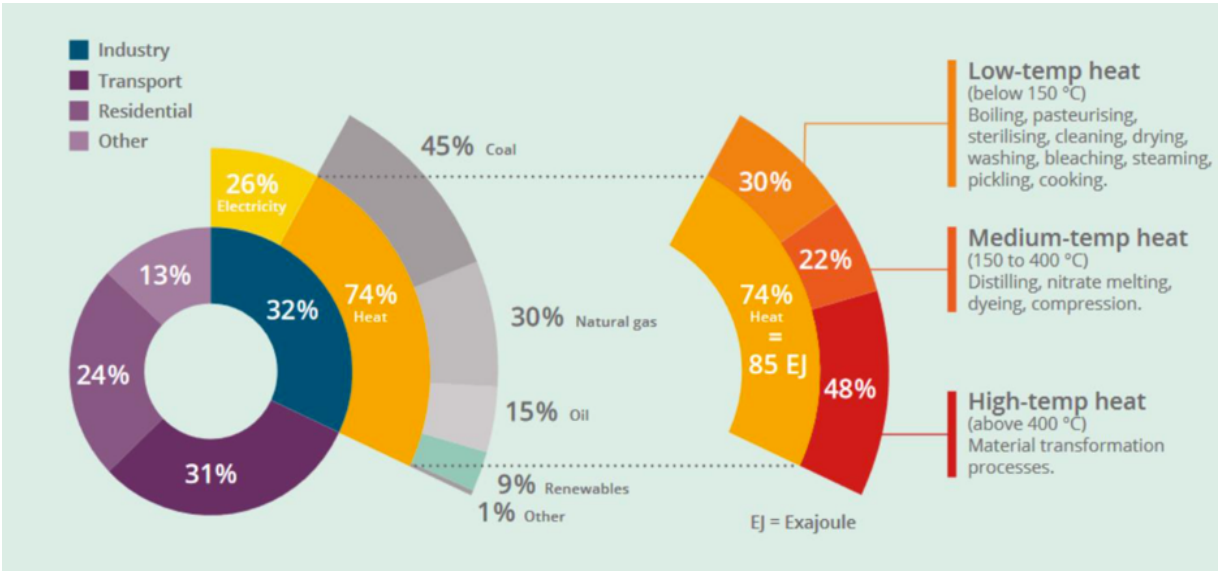

Figure 1.1: Total final energy consumption world-wide in 2015 (EPP 2017).

After these data, one thing becomes clear: to decarbonize industry, we must decarbonize heat, as the title of the article written by Thiel and Startk in 2021 states [2]. The direct substitution of fossil fuels with zero-carbon heat sources is a strategy well known to researchers. Thiel and Startk affirm that this is a relatively straightforward option for applications where the fuels are used solely to produce heat. Zero-carbon heat approaches such as the utilization of sustainable hydrogen or CST can be employed with one of their most important benefits being that there is no need to capture CO_2 (potentially also from many diluted point-sources) in order to be greenhouse gas neutral. This benefit is not present for example in fuels that use CO_2 as carbon source, e.g. synthetic natural gas.

Nevertheless, research and development are required to make it possible to reach cost-competitiveness with fossil fuels.

However, in some cases direct fuel substitution is not straightforward. For many industrial processes, fossil fuels provide not only thermal energy but serve as a reactant as well. In steel production, for example, iron ore is reduced to atomic iron by a reaction with metallurgical coke. For operations where the carbon-fuel is intrinsic to the process chemistry, it is necessary either to design new process chemistries employing carbon-free reactants, or to sequestrate the emitted CO_2 [2].

1.1. Energy demanding industries

According to the US Energy information administration, most industrial energy use occurs in the manufacturing sector with an 82% share of the total; the other industrial sectors, namely mining, construction, and agriculture, account for approximately 9%, 5%, and 4% of industrial energy use, respectively (data valid for USA in 2017, but it seems reasonable to extend their validity to at least the other Western countries) [3].

According to Naegler et al. the most energy demanding industry in Europe in 2012 was steel making, with an annual thermal demand of more than 500 TWh of which three quarters at temperatures above 1000 °C. The second biggest industry was chemicals with an annual thermal demand of around 445 TWh, followed by minerals with 335 TWh. High temperature heat is needed by steel (three quarters of its demand), non-ferrous metals (three quarters of its demand), minerals (around half of its total demand) and other industries in smaller quantities [4].

Several additional studies have been made about the quantification of industrial heat demand by sector. Among the most recent the article by Rehfeldt et al. estimates the heating and cooling demand in European industry in 2017 [5]. In his study, not just industrial sectors but also the single processes that compose them are analysed under the energy perspective. A table has been elaborated by the authors showing per each process the fuel demand [GJ/t], the electricity demand [GJ/t], and the needed temperature distribution (divided into five intervals namely <100 °C, 100-200 °C, 200-500 °C, 500-1000 °C, >1000 °C). For the purpose of the thesis, the last two temperature intervals have been taken into consideration in order to obtain a first group of appealing processes. In particular, the following processes require large amount of heat at high temperatures: iron and steel, primary and secondary aluminium, primary and secondary copper, primary zinc, glass, ceramics and bricks, clinker, lime and calcium carbide [5].

1.2. Process analysis

In this section, different high temperature industrial processes are individually analysed. A short evaluation is provided about their potential for solarization according to the thesis´s aim, based on different factors such as required temperature, market size, and process complexity. Past and ongoing studies are also reported about the utilization of solar energy to provide heat, demonstrating the technical feasibility of a cleaner production.

The choice of the processes is based considering both the ones with a large overall energy demand, as presented in Naegler's and Rehfeldt 's works [4] [5], and the ones with an already studied potential for their solarization, as presented in Fernandez-Gonzalez's articles [6] [7].

1.2.1. Aluminium recycling

Aluminium is currently the most common metal after iron because of its outstanding properties, e.g. its low density that is one-third that of steel [8]. It is used in a broad range of sectors, from transportation to construction and from engineering to food packaging.

Production process and market situation

Primary production starts with bauxite rock ($Al_2O_3 \cdot 2H_2O$) which is converted to alumina by the Bayer process and then by the Hall-Heroult process aluminium metal is achieved [9]. The whole process is extremely energy demanding and costly, and in addition the environmental effects of the primary production are enormous, from mining to refining.

On the contrary, secondary production of aluminium requires 95% less energy (from 35300 kWh/t needed for the primary production to 705 kWh/t) and 90% less invested capital costs [10]. According to the International Aluminium Institute, over 30 million tonnes of aluminium scrap are recycled globally every year which in 2021 corresponded to 35% of total aluminium production. Numbers have more than doubled in less than 15 years and estimations predict a steep progress. The global amount of recycled ingots will more than double again in another 20 years – to 67 million tonnes in 2041. In 2070 it is predicted that the global recycled alloyed production amounts to around 120 million tonnes, which corresponds to three times of today´s figure. Scrap is the feedstock and it can be divided into old scrap, e.g. from post-consumer use (cans, car, etc.), and new scrap, e.g. from production processes (cut-off parts, etc.). Today both sources cover around the same share of total recycled quantity, however, by 2036 the availability of old scrap sources is expected to double that of new scrap sources for the first time – 44 million tonnes vs 22 million tonnes – and numbers are estimated to grow further [11].

The recycling process starts with the collection of scraps, which are then sorted and mechanically processed before being melted. Sometimes further pre-treatments such as pyrolysis are needed depending on the quality of scrap and aluminium content. Secondary aluminium smelters typically use gas-fired furnaces, and range in capacity from a couple of thousand tonnes up to 400,000 t for the largest facilities. According to Moya et al. the furnaces use between 0.87 and 1.96 kWh/kg of aluminium [12] [13].

As of 2022, most of recycled ingot production was in China, USA and Europe; it is also worthy to underline that secondary production is prosperous even in locations without alumina deposits such as Italy, which is the biggest European aluminium recycler [14].

Solarization potential

The solar production of recycled aluminium has been studied by DLR since 2001, when the possibility to melt aluminium scrap with solar energy was successfully investigated. It was found that the required temperature to melt 1 kg of scraps is 800 °C [15]. During a second study carried out in 2016, a solar aluminium recycling plant has been designed and sized for the location of Almeria, Spain [16].

Overall, by 2050 recycling is expected to increase by +180% [11], analysing new cleaner production methods is not only interesting but necessary if emissions have to be decreased, and the CST option could be a good candidate.

1.2.2. Bricks production

Fired bricks are among the strongest and longest-lasting building materials and have been used for several millennia; standardised fired bricks were being heavily produced in Rome by the early first century [17]. Nowadays, bricks continue to constitute one of the used materials for the construction of buildings.

Production process

Korones and Dompros [18] did an environmental analysis for a brick production facility in Greece in 2006 exanimating all the materials and energy fluxes characterizing the processes; the followed information is taken from their study. The production process starts with raw material acquisition (mainly clay and sand) from the deposits immediately followed by the transportation to the factory. There, materials are cleaned, smashed and then kneaded with water. The mixture is subsequently shaped and cut to form bricks that are firstly dried at low temperatures and then put on coaches and placed inside the furnace at high temperature. When they exit the kiln and cooled down, they are already ready for packaging and distribution.

The main energy inputs to the production system are electricity, diesel and solid fuel (such as coal) and the main environmental effects are mostly caused by air emissions from the burning of fossil fuels. Machines used in the first phases (mechanical treatment of materials and kneading) mostly use electricity. The drying process usually does not require any fuel; bricks are simply placed in an open space for 4-5 days. Diesel is used by moving machines in order to transport the materials and the bricks from one place to the other. The baking process is the most important and energy intensive phase: dried bricks are placed in a furnace that operates at 980-1030 °C and through a rail truck they are slowly moved for the duration of about 100-130min. The fuel used in the furnace is Pet-coke because of its low price (based on the study [18], Greece 2006). According to Korones and Dompros, the entire production requires 585 kWh/tonne of brick divided as follows: 86% from coal, 11.5% from diesel and 2.5 % from electricity.

Bricks can vary a lot in shape, material types and proportions, weight, and moisture content; the energy demand and the related emissions are therefore very susceptible plant to plant. While investigating a more sustainable brick production in 2018, Murmu [19] affirms that a conventional brick kiln emits about 70–282 g of carbon dioxide, 0.001–0.29 g of black carbon, 0.29–5.78 g of carbon monoxide (CO) and 0.15–1.56 g of particulate matter per kilogram of brick fired, depending on the type of kiln and fuel used for the firing. Further, it consumes about 0.15–0.87 kWh of specific energy per kilogram of brick produced. In his study, Murmu investigates the production of bricks with industrial waste materials (mainly from mines); the results are positive, the quality of these bricks is proved to be high enough and the baking process is no different from conventional brick with a temperature of 980-1050 °C and a resident time of 2 hours.

Market situation

The market for fired bricks is projected to grow steadily in the coming years, owing to increased building and construction activities, especially in the Asia-Pacific region [20]. Nowadays, China only produces about 700–800 billion bricks per year and India, Pakistan, Bangladesh and Vietnam together produce more than 260 billion bricks per year, providing about 75% of the global demand [19].

Solarization potential

The solar potential in bricks production has been already studied [21] [22]. A first case is by Vittoriosi et al. in 2014 [21] that demonstrates the reliability and quality of large solar thermal collector fields to produce industrial heat for a brick company located in Italy. Fresnel collectors were installed to reduce the consumption of natural gas currently employed for the generation of process heat. The solar technology has a planned maximal capacity of 1.2 MW and provides a temperature of about 180 °C that is used during the drying process and in the pre-heating phase before bricks enter the kiln. A second study by Munoz et al. in 2011 [22] analyses a complete solarization of the process where heat is provided by solar technology not only for the drying process, but also for the high-temperature backing. A 1x1m heliostat conveys the sunlight to an off-axis parabolic concentrator which focuses the light on the entrance of the firing chamber. This last one contains a prismatic cavity that absorbs the solar radiation to generate heat which is needed for baking the bricks. A prototype has been built and temperatures over 1000 °C have been reached inside the chamber. Ten bricks have also been produced. The quality of different bricks produced at different temperatures (from 800 to 1100 °C) has been assessed and the best conditions were found between 950 and 1050 °C. In addition, the quality of bricks should even improve due to the fact that the heat inside the firing chamber is uniform, in contrast to the use of traditional kilns. Figure 1.2 depicts the system designed and built by Munoz. It has also been calculated that in order to produce 110 bricks per day, the needed area of the heliostat would be 49 m^2. The solarization of the entire process seems therefore feasible and appealing.

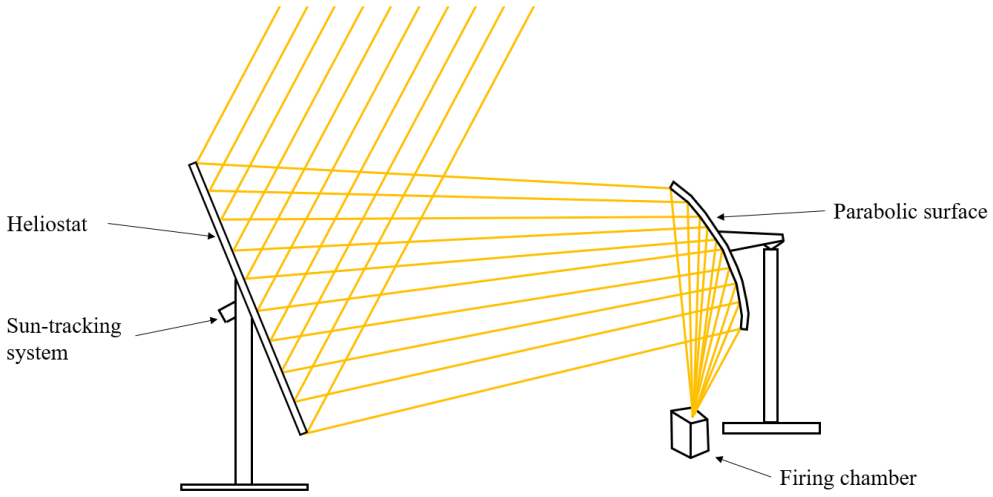

Figure 1.2: Schematic drawing based on the system designed by Munoz (2011).

Since the building industry has a big environmental impact, a more sustainable construction can be achieved through, among others, the use of less energy intensive materials. In fact, material production industries have been attributed to be one of the largest fuel consuming sectors of the economy [18]. Given the irreplaceable importance that bricks have in this sector, studying the potential of a less energy and carbon intensive production of them seems indispensable.

1.2.3. Calcium compounds

Calcium is the third most abundant metal in the earth crust, but it is found only in the form of limestone ($CaCO_3$), gypsum ($CaSO_4 \cdot 2H_2O$), and fluorite (CaF_2). Its compounds are used in several industrial and commercial applications: calcium is used in metal extraction as reducing agent and as an alloying agent for the production of certain metals; in steelmaking it is used to improve the quality of steel; in battery industries it is used to improve the electrical performance and battery life; in food industry it is used as addictive, as supplement in animal feeds and as fertilizer [23].

Production process

Calcium carbide (CaC_2) is one of the most common compounds of calcium. It is industrially produced in an electric arc furnace from a mixture of lime and coke at approximately 2200 °C during an endothermic reaction that requires around 2000 kWh/tonne of energy [24]. However, a more interesting compound is calcium cyanamide ($CaCN_2$), also known as nitrolime, which is produced from calcium carbide. In fact, this last element reacts with nitrogen in presence of high temperatures: $CaC_2 + N_2 \rightarrow CaCN_2 + C$. The reaction is exothermic, but it requires a temperature of 900-1000 °C to initiate. The heat source is then removed and the reaction continues controlled by the addition of nitrogen. This process requires meticulous temperature control since the melting point of calcium cyanamide is only 120 °C lower than the boiling point of sodium chloride [25].

Market situation

The market for calcium cyanamide is expected to grow with a CAGR (Compound Annual Growth Rate) of 2.4% from 2022 to 2028, mostly driven by Asia where the increasing population and agriculture industry are demanding more and more calcium products [26]. On the contrary, in Europe and USA different and cheaper substances are becoming more popular than calcium cyanamide, leading to an uncertain market future of it.

Solarization potential

Overall, calcium cyanamide process presents some weaknesses that lead to not further continue with the analysis of a possible solarization. Firstly, the strict temperature control can be difficult to handle with a CST plant and secondly the market presents some uncertainties, despite the expected growing demand, because of the diffusion of better fertilizers.

1.2.4. Carbon-based materials

Production process and market situation

Carbon-based materials are referred to products which use elementary carbon (C). These materials are more and more used in various industrial sectors, e.g. in the electrochemical sector, where carbon nanostructures offer integrated advantages such as upright electrical conductivity, built-in and structural flexibility, flimsy, and huge chemical and thermal stability [27]. Other important applications are in the construction of airplanes, cars, bikes, canoes, etc., because of excellent strength and low-density characteristics.

A first classification among carbon-based materials is by the dimensionality: in the zero-dimensions category belong nanodiamonds for example, in the one-dimension category belong single or multi-walled carbon nanotubes, in the two-dimensions category belongs graphene, and in the three-dimensions category belong graphite and diamonds [28].

Nanodiamonds are used in biology, medicine and energy sector, but although their production is highly energy intensive, the required temperature is around 300 °C [6].

Graphene is nowadays the carbon-based material with the most promising properties and, consequently, most research in the field of carbon-based materials focuses on it. Carbon fibres can be divided into three categories based on the production temperature that influences the properties:

- Type-I: requires a high-heat treatment in which the final temperature should be above 2000 °C. It is the strongest fibre type
- Type-II: requires intermediate-heat treatment with temperatures around or above 1500 °C. It is a medium-high strength fibre
- Type-III: requires a relatively low-heat treatment with temperatures not greater than 1000 °C. This type is the least strong fibres [29].

Although showing the lowest strength compared to the other types, Type-III is still used in many industrial applications, e.g. for bicycles production.

Carbon fibre energy demand is extremely high and according to Ellringmann et al. who published a cost model of the production, energy accounts on average for 35% of total production costs [30]. According to US Department of Energy, producing one kilogram of carbon fibre needs 87 kWh only in the oxidation/carbonization process, where high temperature heat is required [31].

Solarization potential

In 2022, Hu et al. synthesized graphene nanosheets by photothermal conversion from bio material, i.e. banana and other fruit´s peels, using concentrated solar radiation at temperatures above 1000 °C in 2-3 seconds. After spectroscopic techniques analysis, they were able to affirm that physical and chemical properties were similar to graphene prepared by other approaches [32]. However, although the promising results, the authors themselves stated that their approach could be further improved by more advanced sunlight manipulation techniques; given the early stage of the research it has been considered not suitable to investigate in this work.

Because of its fast-growing market demand, exceptional properties and at the same its high energy consumption, the potential to solarize the production process of carbon fibre is noteworthy and it would be ideal to conduct more research.

1.2.5. Cement production

Cement is intensively used for construction, and its main components are often lime or calcium silicate. It is estimated to be the most widely used material in the world with an annual production of 4.4 billion tonnes (2021 estimation), of which half of it is made in Asia [33].

Production process

There are different types of cement based on composition and hardening mechanisms. By far the most widely used type of cement is Portland cement, which is a type of hydraulic cement (it hardens as a result of hydration). Its highly complex production starts with the calcination: limestone (calcium carbonate) is heated with other materials, often clay, in a kiln to temperatures of approximately 1450 °C. In this phase, carbon dioxide is emitted from the calcium carbonate to form calcium oxide, which then combines with other materials to form calcium silicates and other cementitious compounds. The final mix is a hard substance that is ground into powder with gypsum to form the final product [34].

It is a very energy intensive process which requires around 1100 kWh per tonne of cement and the relative energy costs account for 30-40% of the total production costs because of the big quantity of fuel needed [35]. In fact, is the source of about 8 to 10% of annual emissions: 900 kg CO_2 are emitted per each tonne of cement produced. It has been calculated that 60% of them come from the chemical process and the remaining 40% comes from burning fuel [36]. It is also interesting to highlight that among the main industries, cement generates the most emissions per revenue dollar: 6.9 kg of CO_2 are emitted per dollar of sold product (for comparison, steel industry emits 1.4 kgCO_2/$, oil and gas industry 0.8 kgCO_2/$, data from 2018 [37]). Environmental impacts, however, are not only confined to GHG air emissions but they include also dust, noise and vibration.

Market situation

The production of cement is not ceasing but, on the contrary, it is growing year by year; the International Energy Agency has estimated that cement production will increase by 12 to 23% by 2050 to meet the needs of the world's growing population [34].

Solarization potential

A lot of research has been done and it is still ongoing on the reduction of the environmental impacts and use of fossil fuels for cement production. At DLR studies are carried out about the solarization of calcination. In the CemSol project, for example, researchers from the DLR Institute of Future Fuels are investigating how a solar thermal plant can supply the high-temperature heat for the calcination of calcium carbonate. The project's goal is to demonstrate the industrial-scale, financially viable operation of a solar-heated calcination plant in order to replace fossil fuels, saving large amounts of CO_2 emissions [38].

A lot of research for the decarbonization of the process is already in progress, in particular by DLR; therefore, it has been decided to proceed considering other processes.

1.2.6. Copper recycling

Copper has been an important commodity since 2000 BC and it is still today one of the most used metals in the world. Strong development in emerging economies and a rise in the usage of copper in innovative and clean energy technologies have resulted in a strong market increase in the demand during the last ten years.

Production process

Primary facilities mainly adopt flash smelting Outokumpu process where copper concentrate is roasted and then melted at temperatures around 1200-1250 °C [39]. Considering only the processes that take place at the facility (namely concentrate drying, smelting and converting, fire refining, electrolytic refining and capture of SO_2 as sulphuric acid) the energy demand ranges from 6400 to 7000 kWh/tonne of copper [40]. If the previous phases from the mine to the facility´s gate are taken into consideration, the overall energy demand grows to nearly 9000 kWh/tonne with an emission of 3.3 tonnes of CO_2 per tonne of metal (mining itself uses about 20% of total energy requirement) [41].

Recycling copper instead requires 85% less energy than primary production (resulting in around 1400 kWh/tonne), it can be done repeatedly without any loss of performance and there is no difference with primary products [42]. Once the material is ready (purification is needed based on scrap quality) it is loaded into a furnace where it is melted at 1085 °C and cast into a particular shape [43].

Less than 20% of the world's total copper production in 2005 was accounted for by the secondary sector, in the 2009-2018 period this percentage increased to 32% according to Copper Alliance; however, despite this, primary production had an almost exponential growth that recycling was not able to follow. This is probably because the primary producers have been more successful over time reducing production costs and because of the presence of impurities in the scrap that requires larger electrolyte purification and slimes treatment facilities may be needed [44] [45].

Market situation

Nevertheless, scrap availability has increased enormously in the last years; it is estimated by the Copper Alliance that in 2018 around 13 Mtonnes of copper were available for recycling. Globally, around 50% of copper stocks is in buildings and 15% is in consumer products: it is followed that human settlements have become the biggest source of copper scrap, giving birth to the so-called “urban mines” term. It is calculated that if all the available scrap is recycled, yearly primary production could be cut by half with consequential energy and raw materials savings [42]. It is well known that the recycling path is challenging and urban scrap availability has big overall numbers but it is formed also by little objects and technological items of which the extraction of the metal could be expensive; however, it is also true that raw materials are non-renewable and the accumulation of waste is a non-minor problem.

Solarization potential

In spite of proven technical feasibility, the penetration of renewable energy in the copper sector is low. Among the available technologies, CST is considered the best option to provide heat: a solar heat plant is in use in Chile where a flat plate collector supplies low-temperature heat for

a primary production [46], a study by Cruz-Robles et al. analyses the potential of a solar central tower system to pre-heat the copper before smelting [41]. However, given the lower temperature demand for the recycling path, CST has all the potential to provide the necessary energy and not limiting its function to a pre-heating level.

In order to meet the increasing demand and create a sustainable future for people and the environment, copper recovery and recycling is necessary and the solarization of the processes could play an important role.

1.2.7. Glass recycling

Production process

According to Rehfeldt et al. [5], glass industry can be divided into container-, flat- and fibre-glass and other products and in their assessment all these four categories share almost the same heat demand. Exception made for fibre-glass that requires most of the heat at medium temperature between 200 and 500 °C, the other glass products need around 50% of heat at temperatures greater than 500 °C, with big shares of values above 1000 °C. It is not unexpected that glass industry is among the biggest in terms of energy demand: soda lime glass from virgin raw materials (silica, soda ash and lime) theoretically requires approximately 742 kWh/t [47].

Glass objects are present everywhere, from buildings to small items. Given this huge spread in society and its high energy intensity, recycling this material brings several advantages first of all for the environment. In fact, according to the Glass Packaging Institute [47], recycling glass requires 30% less energy (524 kWh/t) because the chemical energy needed to melt the raw materials has already been expended (primary production requires temperature around 1600 °C). In addition, glass is 100% recyclable and can be recycled endlessly without loss in quality or purity. The process starts with the collecting of glass objects, sometimes it might have to be separated into different colours depending on the end use and processing capabilities, the glass is then crushed in order to form the so-called cullet. This last one is then mixed with sand (5% of cullet quantity) and ready to be heated up to a temperature of 1400-1500 °C and moulded into the desired shape. It is calculated that over a tonne of natural resources are saved for every tonne of glass recycled and one tonne of carbon dioxide is reduced for every six tonnes of recycled container glass used in the manufacturing process.

Market situation

The European market for recycled glass has exceeded one billion USD in 2020 and it is expected to grow by 7% annually in the coming years [48]. Thanks to an interactive map provided by Glass Global Plants [49] the presence of several recycling glass facilities in the South Europe region where the solar source is abundant can be identified (Portugal has 13 facilities, Spain 27, Italy 51 and Turkey 43).

Solarization potential

Few studies can be found about obtaining glass using solar energy: Ahmad et al. (2014) conducted a series of experiments in a high flux solar simulator to investigate the utilization of solar energy in order to produce different types of glass, obtaining the best results for the soda-lime-silica glass; Padilla et al. (2021) produced glass from waste industrial materials. However,

no focus has been done on glass recycling and despite the promising results the cited studies are still on a research level and not yet replicable on large-scale implementations. Therefore, studies aimed at implementing the technology at a larger scale or the investigation of other families of glasses seem to be the fields that will be researched in the following years [7]. Lastly but most importantly, the largest issue to deal with is the very high temperature needed (well above 1200 °C) for the process which is difficult to reach with the solar technologies available today. Therefore, studying the solarization of this industrial process is too premature due to technological constraints.

1.2.8. Gypsum – Anhydrite II-E

Gypsum is a sulphate calcium mineral that is widely used as a fertilizer and as the main constituent in many forms of plaster, drywall and in general in the construction sector. It can be found widely in natural deposits or can be synthetically produced [50].

Production process

Gypsum as an industrial product usually refers to two kinds of minerals: raw gypsum and anhydrite. The first is calcium sulphate dihydrate (($Ca(SO_4)2H_2O$), the second is anhydrous calcium sulphate ($Ca(SO_4)$) and they are both formed through a calcination process. About three-fourths of the total produced gypsum is calcined for use as plaster [51]. The raw material of gypsum powder is natural gypsum ore and the entire process is divided into five stages: crushing (large size gypsum ore is crushed into small particles), screening (separation of incomplete large particles and impurities), grinding (screened gypsum is grinded to form a powder), calcination (gypsum enters a high-temperature furnace) and lastly storage transportation [52].

Different heating settings also affect the structure and properties of dehydrated gypsum. In particular, the (($Ca(SO_4)2H_2O$) system is characterized by five solid phases obtained at increasing temperatures: calcium sulphate dihydrate, calcium sulphate hemihydrate, anhydrite III, anhydrite II and anhydrite I (which only exists above 1180 °C). Above 300 °C anhydrite III becomes anhydrite II, which is insoluble and characterized by high thermal stability and whiteness [53].

In addition, three types of calcined anhydrite II (anhydrous gypsum plaster) are manufactured, depending on burn temperature and time: Anhydrite II-s (produced between 300 and 500 °C), Anhydrite II-u (produced between 500 and 700 °C) and Anhydrite II-E (produced above 700 °C).

While gypsum is among the least toxic coating materials for the environment when compared to cement mortars, the extraction method can still be highly refined to significantly lessen the effects that it produces. According to the Italian company Fluorsid, which produces synthetic anhydrite, the energy demand for one tonne of product is 215 kWh. This value is considerably low compared to the other investigated industrial processes [54].

Market situation

Global gypsum and anhydrite markets are expected to reach a combined production of over 900 Mtonnes by 2030 (the total production in 2022 was 675 million tonnes). In particular, the anhydrite market is expected to reach 400 billion dollars by 2033, increasing at a CAGR of 4.1% from 2023 to 2033; the market is mainly driven by growing demand from the agricultural sector which is looking for more and more soil treatments [55]. Although separated data for the market demand of the different anhydrites, it seems reasonable to associated anhydrite II to these high demands because of its unique characteristics and the fact that it is often cited in literature when gypsum products are considered.

Because of its good physical properties which are beneficial in many industrial applications and its versatility, anhydrite production is undoubtedly an interesting process that deserves attention. Gypsum deposits occur in many countries, but Spain, Thailand, USA, Turkey and Russia are among the leading producers. This is particularly interesting because most of these countries have a high solar irradiation. However, it has not been possible to find clear data about the market share of anhydrite II-E which is produced in a temperature range considered appealing for the purpose of this thesis.

1.2.9. High speed steel

High-speed steels are alloys that are created by adding different alloying metals to carbon steel, usually tungsten and molybdenum or a mixture of both. The main use of high-speed steels is the manufacturing of various cutting tools because of their extraordinary hardness, toughness, and tolerance to high temperatures, making them able to tolerate high mechanical loads and maintain their cutting edge even in hard conditions.

Production process

Conventional production process starts with already manufactured steel bars that are firstly subject to segmentation, turning and milling. Then a heat treatment at high temperature around 1200 °C improves the quality before further cuttings and the final cleaning and coating phases. The production process is extremely energy intense; according to a life cycle assessment by Catalano et al. in 2022, the cradle-to-gate energy demand for a 30g high-speed steel tools is around 2.12 kWh which are equal to 70,000 kWh/tonne. It is also calculated that 30% of this energy is needed for the heat treatment, which is the most energy-consuming operation of the process investigated in the study [56].

Market situation

The high-speed steel market is segmented by type (tungsten high-speed steel, molybdenum high-speed steel, and others), product (metal cutting tools, cold working tools, and others), and end-user industry (automotive, aerospace, energy etc.) [6]. The demand is expected to grow with a CAGR greater than 5% by 2028 and it is high almost in every continent, in particular in the Asia-Pacific region [57].

Solarization potential

Innovative energy techniques can be exploited for the production of prototypes and short series tooling, reducing both time and costs. Some research has suggested to use concentrated solar energy, which was used to manufacture high-speed steels from powders and by means of a sintering process giving outstanding results. Herranz et al. in 2013 sintered steel powders under N_2-H_2 atmosphere in a solar furnace. They have analyzed the effects of processing parameters, the use of CST on densification process, and the mechanical properties of products; experimental results have demonstrated the activating effect of concentrated solar energy on the sintering process. In addition, it was found that solar energy production improved mechanical characteristics, i.e. high hardness values, with a lower temperature and in a shorter time than in the conventional process. Optimum densification has been achieved at 1150 °C in just 30 to 90 minutes while the conventional method in the tubular furnace requires an optimum temperature of 1290 °C and a total cycle time of around 10 hours. The solar furnace they used consisted of a flat 160 m^2 heliostat that followed the sun reflecting the solar beam towards a parabolic concentrator, following the same principle illustrated in Figure 1.2, placing a reactor with a quartz glass on the focal point [58]. Very similar results have also been obtained by Garcia et al. in 2016: they prepared mixtures of high-speed steel and vanadium carbide through powder metallurgy and concentrated solar energy observing a reduction in processing times and improvements of the materials compared to the one obtained in a tubular electric furnace [59].

Finally, the material appears to have interesting properties and it has been demonstrated that the solarization of the manufacture is feasible and produces excellent results. However, the scaling-up of experimental prototypes to large-scale industrial productions could still be challenging and therefore would require further analysis.

1.2.10. Lithium recycling

Known as “white gold”, lithium has become one of the most appealing commodities in recent years, mainly because of the electrification of transport sector. In fact, the metal is a fundamental component of rechargeable batteries that power cars and technological devices like smartphones.

Production process

The current recycling rate is around 1% (2022), and there are no large-scale plants but only small companies. Automotive Li-ion batteries have only been in commercial use for less than 10 years and because of their lengthy product life not enough batteries have reached the end of their useful lives to enable large-scale recycling facilities [60]. It will take some time before they are employed in huge proportions. The different recycling processes available for lithium batteries are:

- Pyrometallurgical process (smelting): batteries are fed to a high-temperature furnace (around 1000 °C) where they are smelted. While valuable metals like Co, Fe and Ni are easily recovered, lithium is present in the slag together with aluminium and its recovery is extremely expensive and energy intensive
- Hydrometallurgical process (leaching): ions are dissolved by means of acids. Metals are recovered in the solution in high rates, especially Li with 90% recovery rates. The temperature required for the process is around 350 °C

- Direct recycling (physical process): batteries are simply physically disassembled with no use of thermal or chemical energy. The recovered pieces of the cathode are then recovered and reused in new batteries. The technology is new and not so developed.

Additional processes using high temperatures are under development by some companies interested in maximize the recovery of lithium, however additional research is needed in order to have large-scale installations [60].

Market situation

Global demand for lithium has grown exponentially, however current reserves struggle to keep up the pace; the recycling of this material is more and more fundamental and will play a major role in the next decades [61].

Solarization potential

Technologies to recover Lithium are still in the research phase, despite the extraordinary interest industry has for it. The pyrometallurgical process, which requires high temperature heat that can be provided by CST, turns out not to be attractive because overall more expensive and energy demanding than the hydrometallurgical process. This last one has temperatures below the interested range of the thesis.

1.2.11. Steel production

Production process

Steel is the most used metal and its production is the biggest energy demanding industry in the world; according to Naegler et al. steel manufacturing requires more than 500 TWh per year of energy only in Europe, 75% of which is process heat above 1000 °C [4]. Nowadays there are two methods for primary production: Blast Furnace and Electric Arc Furnace. The first one uses coke, iron ore and limestone to produce pig iron at very high temperatures (also over 1500 °C). The second option is relatively new but accounts now for over 70% of steel production in the Western countries, an electrical current is used to melt scrap steel, direct reduced iron and/or pig iron to produce molten steel at similar temperatures [62]. However, electric arc steelmaking can only be cost-effective in areas with an established electrical infrastructure and plenty of reliable power.

Solarization potential

A 2018 estimate stated that each tonne of steel produces on average 1.85 tonnes of CO_2, corresponding to about 8% of global carbon dioxide emissions [63]. The decarbonization challenge is therefore huge and urgent at the same time. Given the incomparable impacts on society, environment and economy that this industry has, numerous studies have already been carried out and some companies are already starting to adopt more sustainable solutions. Among the different decarbonization measures, hydrogen seems the most promising and spread option both for the implementation of new facility sites (the so-called “greenfield sites”) or for upgrading existing facilities (“brownfield sites”).

One example among others can be found by SSAB, a Swedish steel-making company that in 2021 produced the first steel manufactured without the use of fossil fuels. Traditional methods that require the coking process have been replaced with a hydrogen-based process [64].

Hydrogen is now thought to be the most practical choice and the long-term solution to achieve carbon-neutral steel production, particularly in Europe. Therefore, a deeper analysis in order to investigate the potential for solarization is considered not worthy.

1.2.12. Sulfuric acid recycling

Sulfuric acid (H_2SO_4) is an extremely significant commodity chemical used in a wide range of industries like fertilizer manufacture, oil refining, and iron and steelmaking industry. Since it is difficult to find pure in nature, its production and recycling play a major role [65]. In fact, many industrial facilities produce spent sulfuric acid by-products that can be regenerated into full strength high-quality sulfuric acid.

Production process

Nowadays there are three main different methods to recycle it:

- Atmospheric distillation: the acid is distilled and impurities are removed. Although the recovery rate is 95%, operation costs and energy demand are very high. The required temperature is 340 °C
- Low pressure distillation: the acid is distilled and impurities are removed under low pressure in order to improve efficiency. The resulting energy consumption is lower since the required temperature is around 200 °C
- Thermal cracking: the spent acid is thermally cracked in a furnace to separate the different compounds. The temperatures needed are between 1000 and 1200 °C and the spent acid is broken down into sulfur dioxide gas SO_2 and steam while the dissolved organics act as a fuel. A very strict control of quantities of fuel and air is required to maximize the production (nearly a stochiometric control) [66] [67].

Other recovery processes requiring temperatures around 700 °C have been studied [68], however they are still on a preliminary phase with no industrial-wide use.

Solarization potential

Overall, the recycling of sulfuric acid is not considered appealing for further analysis for its solarization because most used processes are not suitable (low temperatures (distillation), combustion and oxidation reactions required (thermal cracking)).

1.2.13. Zinc roasting

Production process and market situation

Zinc is the fourth most common metal in use after iron, aluminium and copper, with an annual global production of about 13 million tonnes in 2021. The most common applications of zinc are being an anti-corrosion agent (galvanization, which is the coating of steel or iron) and being part of alloys such as brass and bronze [69]. The top countries for zinc mine production output

in 2019 were: China (4.2 Mt), Peru (1.4 Mt), Australia (1.3 Mt), USA (0.75 Mt), India (0.7 Mt) and Mexico (0.7 Mt) [70].

The production of zinc starts with the acquisition of raw material in the mines where zinc concentrate is extracted. Once the material has reached the industrial plant, it is fed into a fluid bed roaster, sometimes zinc oxides recycled from the steel industry are added too. During roasting which takes place at 950 °C, the materials are turned into zinc oxide called "zinc calcine" (ZnO) in a granular form like sand. In the following step the produced calcine is dissolved in sulphuric acid through a process called leaching. In this phase zinc is purified from other substances, especially metals like lead, gold, silver, copper, cadmium and cobalt, that is why this phase also assumes the name of purification phase. The zinc sulphate consequently enters the stage of electrolysis where the metal contained in the solution is deposited onto aluminium cathodes; this happens by passing an electric current through cathodes and anodes. After the cathodes are taken out of the cells, after 22 hours, the zinc sheets are separated from them and transported to the casting process where the metal is melted and ingots of the desired shape are produced [71].

The overall process is very energy and carbon intensive, according to Qi et al (2017) from mining to casting the energy demand is 78.1 MJ/kg with a carbon footprint of 6.12 kg CO_2/kg of zinc (in the Chinese production chain), with electrolysis being the highest demanding phase [72]. However, for this thesis scope, the most interesting process is roasting because it is where most of the heat is needed. Despite the chemical reactions that occur in the roasting phase are strongly exothermic, fossil fuel is used to reach the needed temperature of 950 °C. Based on the roaster type, the amount of fuel changes; in the "Overpelt" roaster the consumption is 15 kg of fuel per tonne of raw material (around 200 kWh/t) [73].

Solarization potential

The application of solar energy in the production of zinc has been widely reported in literature both with PV and CST technologies, particularly focusing on the utilization of Zn as a metal fuel. According to Yadav et al. that in 2022 compared the production of zinc using fossil fuels, PV and CST, there is a significant reduction of 95% of CO_2 emissions for both solar technologies [74].

Zinc is a fundamental material for modern society and its demand is increasing. Although the roasting process, which is run at high temperatures, does not have very high energy requirements, it is considered worthy to further investigate the solarization of the process. If the industry has to decrease or better set to zero its emissions, it is important to consider all processes, not just the major ones. In addition, most of the top zinc producer countries mentioned at the beginning are in locations with high annual direct normal irradiation values, in particular Peru, Australia, USA and Mexico; this fact is an additional favourable factor to proceed.

1.3. Synthesis table

Table 1.1 summarizes the main information regarding the industrial processes that have been illustrated. In particular are reported:

- the temperature needed in the high-temperature phase
- the specific energy demand
- possible constrains on the location of the plants due for example to the proximity of raw material deposits
- doubts regarding uncertainties about the process itself or market related uncertainties
- cons, namely elements that are technical obstacles to the solarization of the process such as too high temperatures or other elements that discourage further analysis such as the presence of already big numbers of both past and ongoing researches
- a possible reactor type that can be used for the solarization. This information comes from a very general and rough observation of the industrial processes, but it can be considered realistic to a certain extend based on the state and composition of materials and products.

Table 1.1: Synthesis of high temperature industrial processes information (source for the data are specified in the previous sections).

Process	**T**	**Energy demand**	**Locations**	**Doubts**	**Cons**	**Feedstock type**
-	°C	kWh/t	-	-	-	-
Aluminium recycling	800	700-800	No constrains	-	-	Liquid
Bricks production	1000	150-870	Clay/materials deposits	-	-	Solid
Calcium compounds (Cyanamide)	850-950	No data	Calcium production	Reaction is exothermic and self-sustaining after initiation	Meticulous temperature control	Solid, particles
Carbon fibre (carbonization process of Type III)	1000	87800	No constrains	Only type III production is possible (having lower quality)	Higher quality requires T > 1500 °C	Solid
Cement	>1300	1015	Raw material deposits	-	Already many ongoing studies	Solid, particles
Copper recycling	1085	1400	No constrains	-	-	Liquid
Glass recycling	1400-1500	1100-4700	No constrains	-	Temperature too high	Liquid
Gypsum Anhydrite II-E	700-1180	215	Gypsum production	Market demand not certain compared to the other types of Anhydrites	-	Solid, particles
High speed steel (powder metallurgy)	1150	70000	Steel production	-	-	Solid
Lithium recycling	350-700	Highly dependent on process	No constrains	Pyrometallurgical process not attractive	-	-
Steel production	>1000	5500-7500	Iron mines	-	Already many ongoing studies, especially with hydrogen	Liquid
Sulfuric acid recycling	200-1200	Highly dependent on process	Sulfuric acid sources	Process not attractive	Temperature too low for the most used processes	-
Zinc roasting	950	180-250	Zinc mines	Exothermic process, energy is used to reach the temperature (low demand)	-	Solid, particles

1.3.1. Choice of three processes

Three processes have been chosen among the thirteen described to be further analysed and in particular to study their potential for solarization. The choice was based on different factors including the future market demand, temperatures in an acceptable range (above 600 °C but below 1200 °C, as the complexity of the system increases significantly with higher temperatures), process complexity and attractiveness.

It has been decided to focus on aluminium recycling, bricks and zinc production. They cover relatively wide ranges of temperature, between 800 and 1100 °C, and energy demand, between 180 and 900 kWh/t. Some processes have location constrains e.g. the production of bricks and zinc, which are depending on clay and zinc deposits. In contrast, aluminium recycling in not limited to precise areas because scrap availability is mostly spread by human activities. They also cover all the three different reactor types: molten for aluminium because it requires to be melted inside it, moving structure for bricks because they enter as solid objects and particles for zinc because the concentrate enters the reactor to be roasted in a granular state.

2 CST technology

2.1. Overview

Concentrating solar power (CST) technologies use combinations of movable mirrors or lenses to concentrate direct beam solar radiation on a small area, to provide high temperature thermal energy for electricity production or other heat-demanding processes.

The first commercial development for CST technology was between 1984 and 1995, however, deployment stopped for a decade despite a great deal of research, development, and demonstration took place during that period. Since 2005, the implementation of CST has resumed and accelerated significantly even though the total installed capacity is an order of magnitude smaller than solar photovoltaic (PV). According to IRENA *Renewable Capacity Statistics 2022*, the spread of CST is led by Spain with 2300 MW installed, followed by USA with 1496 MW installed (2021 values) [75]. Other countries involved in CST projects are in North Africa (Algeria, Morocco), Middle East (Egypt, Israel), Australia, South Africa and South Europe (Portugal, Italy, Greece, Cyprus, Malta) and China (although the solar source is not as high as in the previous countries, in terms of annual DNI) because of their high solar potential [76].

In fact, unlike PV that uses also diffuse radiation, CST systems are only able to exploit the direct irradiation component of solar radiation reaching the earth surface. For this reason, CST systems are must suitable in locations with low cloud coverage and low smog or dust concentrations. The main parameter affecting CST production is therefore the Direct Normal Irradiance (DNI) which represents the quantity of direct radiation received per unit area on a surface perpendicular to the sun [kWh/m^2]. Usually, the values of DNI are calculated and expressed daily or annual (as it will be the case in this thesis).

2.2. Concentrating solar technologies

Concentrating solar systems can assume different configurations, mainly four, each of them with its proper technical and output characteristics. Figure 2.1 reports the schematic drawings of Parabolic Trough (1), Solar Tower (2), Parabolic dish (3) and Linear Fresnel (4) which are technically explained in the following subsection. The sources of the information reported are from *Concentrating solar power technology* by Lovegrove and Stein, 2012 [76] and *Progress in research and technological advancements of commercial concentrated solar thermal power plants* by Khan et al, 2023 [77].

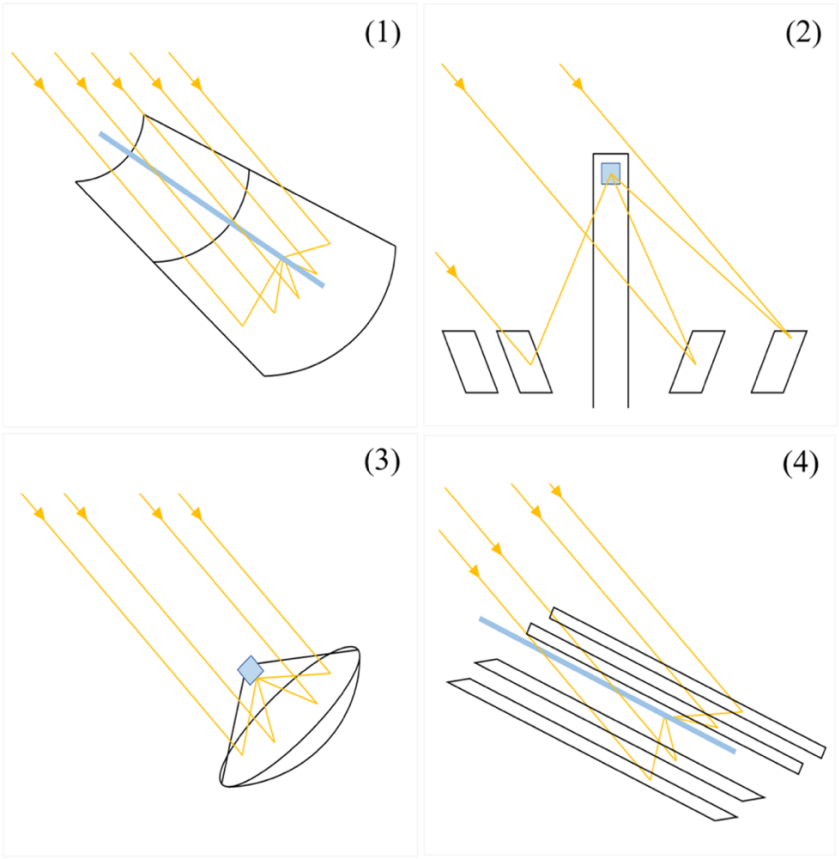

Figure 2.1: Configuration of the four CST technologies: (1) Parabolic Trough, (2) Solar Tower (3) Parabolic dish and (4) Linear Fresnel. In black the physical components (mirrors, tower), in blue the receiver, and in yellow solar radiation.

2.2.1. Parabolic trough (PT)

Parabolic-shaped mirrors focus the radiation on a linear receiver tube along the parabola's focal line, drawing (1) in Figure 2.1 shows the configuration. Mirrors and receiver are mounted on a frame that tracks the movement of the sun throughout the day (one-axis movement); the addition of a second-axis sun tracker to PT technology has been studied to have no economic justification. The heat is collected from a heat transfer fluid, like synthetic oil, that are present in the receiver tubes and then transported to a central power block. Normal operating temperatures are around 400 °C [76] [77].

2.2.2. Central receiver solar tower (ST)

Central receiver tower systems are composed by a certain number of mirrors (called heliostats) that have a two-axis tracking and concentrate the sunlight onto a single point at a fixed receiver mounted at the top of a tower as shown in drawing (2) in Figure 2.1. This configuration permits to reach high concentration ratios allowing the thermal receiver to operate at higher temperatures with reduced losses; values above 1000 °C can be obtained. The heat transfer fluid in this case is usually a molten salt for electricity applications.

In order to optimizes optical efficiency, especially in large-scale plants, the height of the tower should be greater than 100 m above the ground. It's important to note that while PT plants make up more than 77% of CST plants now in operation, 52% of CST installations that have recently (since 2018) been commissioned are ST systems [76] [77].

2.2.3. Parabolic dishes

Dish systems exploit the geometric properties of a three-dimensional paraboloid concentrating the radiation to a point-focusing receiver, as depicted in drawing (3) in Figure 2.1. Among all the CST technologies, parabolic dish collectors have the highest ability to concentrate the sun rays. High temperatures over 1000 °C can be achieved, similar to tower systems. However, it is the least developed of the four CST technologies; it is still at the demonstration stage and the cost of a large-scale production are uncertain due to technical challenges [76] [77].

2.2.4. Linear Fresnel

Linear Fresnel reflector systems produce a linear focus on a downward facing fixed receiver mounted on a series of small towers. Flat or slightly curved mirrors are displayed in long rows and they can move independently on one axis in order to reflect the radiation onto the stationary receiver. Its simpler design with flat mirrors and less supporting structure outweighs the lower overall optical and thermal efficiency. Operating temperature depends on the working fluid, and when molten salts are used, they can reach up to 600 °C, otherwise values are around 400 °C. Drawing (4) in Figure 2.1 represents a schematic of the technology [76] [77].

2.3. Heat production

Since PV production costs of non-dispatchable electricity are lower than concentrating technologies, most of the attention to CSP's potential is turning to thermal energy. In fact, according to IRENA *Renewable Power Generation Costs report 2022* [78], CSP is the most expensive renewable source of electricity, however heat production with the same technology is five times cheaper. On the contrary, producing heat with PV becomes more expensive than producing electricity because of the need of electrical heating elements (and PV systems do not include any storage in the price) [79]. In addition, sun-to-electricity efficiency of solar tower systems is between 18 and 21% while sun-to-heat efficiency is between 42 and 46% [80]. Also, when producing heat there is no need of all the typical plant parts of a CSP solar plant, e.g. the steam turbine, resulting in a reduction of costs per produced heat kWh in comparison to produced kWh of electrical energy. The environmental impacts are also lower: it has been calculated by Ong et al. that when producing heat, CST towers are by far the least land-consuming renewable electricity technology with just 0.65 hectares required per GWh/a while PV range around 1.6 hectares [81]. Moreover, the CO_2 emissions for heat provided with a solar tower are around 5-6 g/kWh [79]. In comparison, the other two most used renewable heat sources that are biomass and geothermal produce respectively 5–200 and 10 grams of CO_2 per kWh of heat [82], while the values for PV are around 40 g/kWh of electricity, to which the emissions of the heat parts have to be added [83].

Thus, CST seems to be the best solution for heat supply where conditions such as high solar potential are met. Research is ongoing on the implementation of this technology in different sectors, as it has been mentioned in the previous chapter where even prototypes have been built showing very good results. Still, it is too early for CST to be widely used in industry for heat supply. Concentrating solar technologies for provision of process heat is an important research topic in particular at DLR where the CentRec receiver has been designed and developed. In particular, CentRec is a centrifugal particle receiver which is considered one of the most promising central receiver technologies for high temperature heat generation for power production, cogeneration and heat applications, Figure 2.2 reports its structure and components. In his study, Frantz et al. aim at studying and maximizing the techno-economic performance of

this technology in order to achieve commercial competitiveness with fossil fuels (the capacity is 20 MW_{th}). A thermal storage with a size of 12 h is considered and temperatures around 1000 °C can be reached. Especially when the added value of storage is considered, the estimated LCOH are in a very appealing range when compared to other possible sources [84].

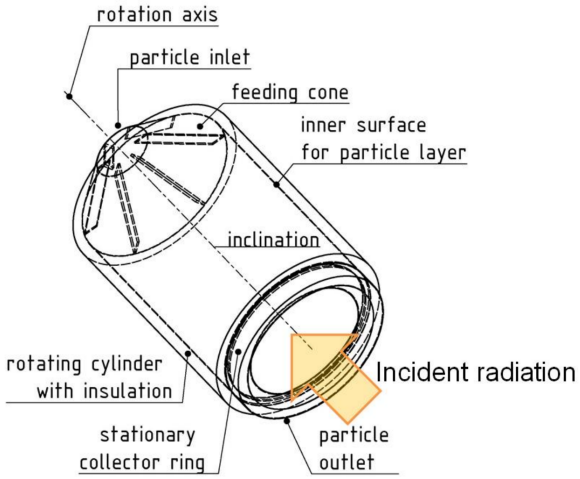

Figure 2.2: Basic concept of CentRec receiver (Frantz et al., 2020 [84]).

When solar renewable technologies are considered, the presence of thermal energy storages are fundamental due to the natural intermittence of radiation which opposes to usual constant energy demand in industry. A balance between cost for storage and solar system and possible emissions (due to back-up fossil fuels, when used) has to be found. However, CSP technology has proven to have lower costs for storage compared to PV, which allows a 24/7 production [85].

Other projects for high temperature industrial processes coupled with CST include for example Prema, a solar reactor for the production of manganese alloy (manganese ores are preheated at 600 °C before entering the furnace). A pilot plant in South Africa has been designed at DLR for an already existing sinter plant (Kalagadi location, where there is a high direct solar irradiation) [86].

The use of this innovative sustainable technology in industry has proven to be promising; in the following chapters the impacts of its implementations in three industrial processes is analysed and compared to other options.

3 Process analysis

In this chapter, an economic analysis for the three chosen processes is done. The aim of this section is firstly to have plausible production costs for each process and secondly to have a geographical distribution of them so that each country is associated with a certain cost. The approach that has been followed to obtain the production costs is to find economic data from scientific literature. To be able to characterize these with the location, the production costs are therefore broken down into single elements and some of them are considered as varying with the location in order to obtain more realistic geographical distributed data; the most striking example is fuel price which is highly dependent on the location. One of the simplifications is to consider the fossil fuel cost constant within a country; however, an exception is made for the United States where available data for single States were possible to find.

3.1. Spatial distribution

It is important to specify that this techno-economic study is not done for each country in the world but just for those that share two requirements: enough available solar source and economic interest for the analysed industrial processes. The first point is achieved where a significant area of a country has a high annual DNI and the second point where the industries are already present or there is a potential for them. It should be emphasized as well that this study does not aim at finding the cheapest place to produce bricks or recycle aluminium but to analyse whether the CST option can be economically attractive based on the location.

A world daily DNI map has been downloaded by the *Global Solar Atlas* [87] and imported to the software where all the onwards spatial analyses are made. The annual values are simply obtained multiplying the original raster file by 365. A threshold of 2000 kWh/m^2 per year has been imposed to identify the best locations in terms of solar source; the resulting map is shown in Figure 3.1.

In order to investigate the industrial potential of a certain area, a database has been created with collected information about the location of different interesting sites: for secondary aluminium data was collected about existing recycling plants and scrap collecting companies (which make up significant deposits of raw material) for a total of 158 points. For bricks the biggest production companies and clay deposits were found, for a total of 210 points. With regard to zinc, the biggest producing companies, which are almost always close to zinc ore mines, and zinc deposits that are not already in use have been identified, with a total of 209. An extraction of the dataset is reported in Appendix Table 1 and in Figure 3.1 the points are shown in the map together with areas having a high solar resource. The created collection is certainly not an exhaustive one; however, with a total of 577 samples, it is believed that it can provide a good overview of reality (considering the biggest companies sites and deposits of raw materials). The geographical coverage of the data is reasonably wide and the locations are to a certain extent homogeneously spread, with certain hotspots in more industrialized regions such as North

America and Europe. However, if an intersection between these locations and the areas with high DNI is done, few macro-regions are found:

- Western United States and Mexico (all three industries equally present).
- South America, especially along the Andes Mountains where the highest DNI values are reached (mostly zinc but also bricks industries).
- South Europe and North Africa (especially aluminium recycling industries).
- South Africa region (mostly bricks but also some zinc industries).
- Australia (all industries present, zinc most of all).

In particular, the following countries are considered in the study: Angola, Argentina, Australia, Bolivia, Botswana, Brazil, Chile, Egypt, Iran, Israel, Madagascar, Mexico, Morocco, Namibia, Peru, Portugal, Saudi Arabia, South Africa, Spain, Tanzania, Turkey, United Arab Emirates, USA, Zambia and Zimbabwe.

The production costs of the three industrial processes are therefore calculated for these 25 countries.

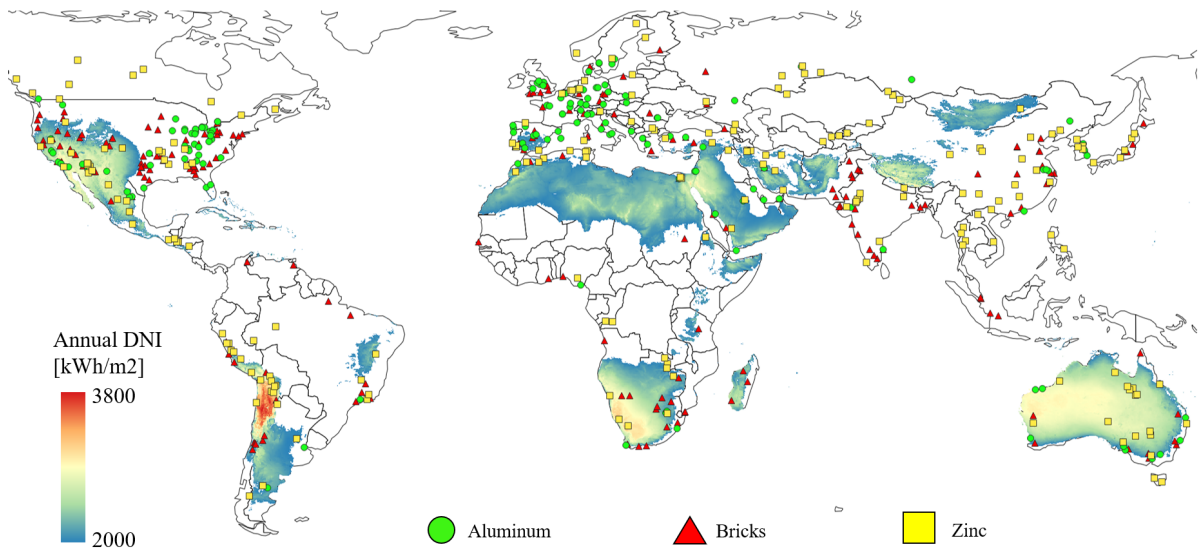

Figure 3.1: World map showing areas with DNI over 2000 kWh/m^2 and the main locations for the three industrial processes.

As mentioned at the beginning of this chapter, some elements in the cost compositions are considered dependent on the location so the uncertainty of the results is reduced. These factors are: fossil fuel price (coal, heating oil and natural gas) [EUR/kWh], diesel price [EUR/l], electricity price [EUR/kWh], median income [EUR/person/year] and raw material prices used for each process, specified in the following sections. Therefore, a dataset containing all these data was created and it is reported in the Appendix Table 2, Appendix Table 3 and Appendix Table 4 with the respective sources.

The median income of a country is used as a parameter to calculate the personnel costs (values from *World Population Review*, 2022 [88]); it is considered to be a better indicator than GDP per capita, that would overestimate the labour costs. In fact, the relationship between these two indicators is less than linear; after a certain value of GDP per capita, the median income of the same country stays essentially constant, as it can be seen in the Appendix Figure 1 where data of several countries have been collected and plotted. In addition to the production costs, each

process is also associated with the emissions of CO_2 based on the fossil fuel used, according by data in Table 3.1.

Table 3.1: Specific carbon dioxide emissions of various fuels (Quaschning and Siegel, 2022 [89]).

Fuel type -	**Emissions** kg CO_2 /kWh
Coal	0.338
Natural gas	0.201
Heating oil	0.267
Diesel	0.267

3.2. Aluminium recycling

In this section, the aluminium recycling process is analysed under an economical perspective. A first study held by Alexopoulos in 2003 [90] shows the comparison between a conventional recycling plant and a solar plant in California. Investments and operational costs of the two options are compared; however, the work is already twenty years old and the CST technology has improved significantly and therefore those numbers should be handled with caution. The fossil furnaces, on the contrary, have not experienced such development and looking at their costs can be considered reasonable. Alexopoulos' results show that the slag treatment consists of almost half of the total operational costs, personnel is the second element and the third, very close in numbers, is natural gas to provide heat.

A more in-depth study by Martin Roeb from DLR compares a conventional and a solar aluminium recycling process [91]. Investments and operational costs are calculated for a solar plant, a fossil and a hybrid one; the last case utilizes both sun and fossil fuels to reduce the fluctuations due to the natural conditions of sunlight (weather, clouds, seasons…) that influence CST output. The location of the facility is Almería, South of Spain. Different annual production quantities are also included as parameters, in particular two outputs are analysed for the fossil production: 6300 t/year and 22000 t/year. The size of the plant is designed as follows: since an aluminium scrap throughput of up to 5 t/h is to be ensured and the typical melting times for conventionally operated furnaces of medium size are 2-3 hours, the furnace size is selected so that the capacity is 8-10 tonnes of scrap. Table 3.2 shows the production costs of a fossil fuel plant for the two production outputs. The plant size has proved to be relatively important: an increase of 250% in the production quantity means a decrease of 28% in the costs per tonne due to the economy of scale. In this case also, slag treatment represents the biggest share of costs, followed by melting salt (not present in Alexopoulos study) while personnel and energy costs are similar but their behaviour is different due to their nature (natural gas is not dependent on the output): energy costs represent 13% of costs both in the 6300 and 22000 t scenarios, on the other hand, personnel costs decrease from 17% to 10% of total costs.

Table 3.2: Production costs for a fossil fuel plant in Spain, 2000 (Roeb, 2000 [91]).

	Annual production [tonnes]					
	6300			22000		
	EUR	EUR/t	Share of total costs	EUR	EUR/t	Share of total costs
Annuity	121894	19.35	9.9%	222262	10.10	6.6%
Insurance/maintenance	87074	13.82	7.0%	158759	7.22	4.7%
Slag treatment/disposal	386543	61.36	31.3%	1349831	61.36	40.2%
Melting salt	225483	35.79	18.3%	787402	35.79	23.4%
Additive (NaHCO3 + coke)	11453	1.82	0.9%	16975	0.77	0.5%
Change refractory material	28121	4.46	2.3%	51130	2.32	1.5%
Personnel	214746	34.09	17.4%	322119	14.64	9.6%
Energy	160037	25.40	13.0%	449432	20.43	13.4%
Total production [EUR]	1235351			3357910		
Production costs [EUR/t]		196.09			152.63	

Roeb´s work is seen as valid, rich in data and detailed enough: it is therefore considered as the starting point for calculating the 2022 production costs of recycling aluminium in various countries.

Values have been then adjusted by inflation to 2022 via *inflationtool.com* with the exception of energy costs that follow a different trend. For these, the table mentioned in Section 3.1 containing the 2022 fuel prices in the countries is used (collection of 2022 energy prices Appendix Table 2-4). The specific energy required is obtained dividing the total energy costs (in 2000) by the price of natural gas of 0.026 EUR/kWh used by Roeb (Spain, 2000); the resulting energy demand is 768.5 kWh/t of aluminium, which agrees well with the range presented in Table 1.1.

In order to obtain a proper production cost, however, it is necessary to include also the raw material impact; according to Deng 2022, the major cost contribution for remelt and recycling aluminium processes is the material cost [92]. According to the study held by Moya in 2015, scrap price makes up around 75% of secondary aluminium costs Figure 3.2. In the study they affirm scrap prices vary from 344 EUR/t to 982 EUR/t depending on quality and location; considering an average value of 700 EUR/t they conclude the final production cost is 950 EUR/t (2015) [12]. During the last years and especially starting from 2021, scrap price has increased sharply and after consulting different sources the following values are used in this study: a value of 1100 EUR/t is associated to countries in Europe, North America and Australia, a value of 1000 EUR/t to countries in Central and South America and a value of 900 EUR/t to countries in Africa, Middle East and Bolivia (Fastmarkets [93], ScrapMonster [94]).

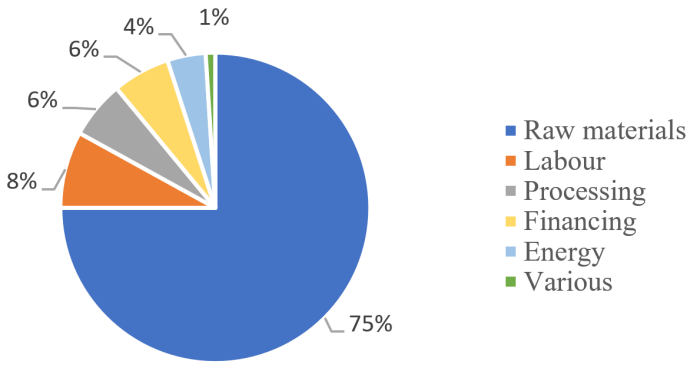

Figure 3.2: Cost breakdown of Western refineries of secondary aluminium (Moya, 2022 [12]).

Based on these assumptions and data, the production costs of fossil fuel recycling aluminium in a certain country and the corresponding CO_2 emissions were calculated. Table 3.3 shows the example of a production in Spain with coal: the total costs are 1365 EUR/t of which 82% are due to the aluminium scrap and 2.8% the fuel (which are 15% of operational costs namely production costs minus raw material costs). In the table, the values that are changing are highlighted: green values are changing with the country (scrap price, personnel and fuel costs) and orange values are changing with the fossil fuel used (fuel costs of course and CO_2 emitted per tonne of aluminium produced). Cost values that are in white cells are considered not changing with the location because some are connected to capital costs (annuity, maintenance) which are considered constant among countries and some have such a small contribution that their effect is negligible (additive and refractory material for example that are together 0.4% of total costs). The constant costs are therefore just inflation adjusted values from Roeb´s study. With regard to personnel costs, a direct proportion is made among labour cost calculated by Roeb, the median income of the location of the plant (Spain) at the study´s time (2000) and the median income of the country considered in 2022. The emissions are 100% coming from the smelting furnace and in Table 3.9 the specific emissions based on the fuel used are reported.

Table 3.3: Production costs calculation based on country and fuel used for a 15000 t/year plant.

Country	Spain	**Fuel**	Coal

Product	**Quantity**	**Unit**	**Cost**	**Unit**	**Total cost**	**Unit**	**Quantity/t_Al**	**Cost/t**	**%**
Aluminum Scrap	15300.0	t/year	1100	EUR/t	16830000	EUR/year		1122.00 EUR/t	82.2%
Annuity			253300	EUR/year	253300	EUR/year		16.89 EUR/t	1.2%
Insurance/maintenance			180930	EUR/year	180930	EUR/year		12.06 EUR/t	0.9%
Slag treatment/disposal	11250.0	t/year	120	EUR/t	1354725	EUR/year	0.750 t/t_Al	90.32 EUR/t	6.6%
Melting salt	7500.0	t/year	105	EUR/t	790200	EUR/year	0.500 t/t_Al	52.68 EUR/t	3.9%
Additive (NaHCO3 + coke)	32.7	t/year	640	EUR/t	20919	EUR/year	0.002 t/t_Al	1.39 EUR/t	0.1%
Change refractory material			58330	EUR/year	58330	EUR/year		3.89 EUR/t	0.3%
Personnel	8.0	people	52685	EUR/year	421480	EUR/year		28.10 EUR/t	2.1%
Coal	11528046.0	kWh/year	0.049	EUR/kWh	568325	EUR/year	768.54 kWh/t_Al	37.89 EUR/t	2.8%
TOT					**20478210**	**EUR/year**		**1365.21 EUR/t**	**100%**

location-variable
fuel-variable

Non-fuel costs	1327.33	EUR/t	97.2%
Fuel costs	37.89	EUR/t	2.8%
TOT	1365.21	EUR/t	100%

Kiln emissions	259.92	kgCO2/t	100%
Other emissions	0	kgCO2/t	0%
TOT	259.92	kgCO2/t	100%

In order to verify the reliability of the obtained results, a comparison with literature data is made. A first look to Moya´s value, cited above, of 950 EUR/t may suggest that the obtained 1365 EUR/t value is too high, however his study is from 2015 and prices have changed; his energy price is 66% cheaper than in 2022 and they used an average scrap price of 700 EUR/t which corresponds to a medium quality aluminium scrap. Price of raw material has increased and a high-quality scrap was taken into consideration in this thesis. After these adjustments the two costs become very similar (Moya's adjusted value becomes around 1380 EUR/t).

According to a second study by Deng from 2022, the production cost of recycled aluminium in India is around 1160 EUR/t and through a sensitivity analysis it has been assessed that scrap price is the most sensitive factor ([92]). The results obtained in the present calculations show production costs ranging between 1100 and 1350 EUR/t, depending on the country. Deng also reports that the price of the scrap is around 950 EUR/t and the selling price of aluminium ingot is 1915 EUR/t. The assumptions and the values found are therefore considered in agreement with literature.

3.3. Bricks production

In this section, the production of bricks is analysed under an economical perspective. Unlike aluminium recycling where the melting temperature is fixed and the product is always a metal ingot, in this process there is a wider range of operation possibilities and variables: raw materials quality and proportions are changing from location to location, firing temperature and time are changing based on materials and product quality. The range of products itself is wide with bricks changing in shape, dimension and weight.

A study by Yüksek in 2020 [95] analyses fired clay brick production under an energy perspective: two different factories located in Turkey are compared by their energy consumptions during all the production phases. A cradle-to-gate approach has been adopted and for each process the fossil fuel energy and electricity demands are reported. The results confirm the high variability of this industry and the Specific Energy Consumption (SEC) has been calculated for both the facilities: the first one has a value of 0.33 kWh per kg of brick produced and the second one 0.45 kWh per kg of brick. The two facilities are approximately located at the same distance from the clay deposit and they both use coal as energy source for the firing process because it is the cheapest fuel in Turkey, as it is underlined in the study (validating the data collected for fuel prices around the world in Appendix Table 2). Different SEC values and specific coal consumption (tonnes/100,000 bricks) are also reported in Yüksek´s study for some countries and different kilns, as Table 3.4 shows.

Table 3.4: Comparison of kilns in terms of energy consumption (Maithel and Heierli 2008 [96]).

Type of kiln		**SEC** (MJ/kg of brick)	**Specific coal consumption*** (tonnes/100,000 bricks)
Continuous kilns	VSBK (India, Nepal, Vietnam)	0.7-1.0	11-16
	Fixed chimney BTK (India)	1.1-1.5	17.5-24
	Moveable chimney BTK (India)	1.1-1.75	19-28
	Tunnel kiln (Vietnam)	1.4-1.6	22-25
	Modern tunnel kiln (Germany)	1.1-2.5	17.5-40
Intermittent kilns	Clamp and other batch kilns (Asia)	2.0-4.5	32-71

*Considering gross calorific value of coal as 18.8 MJ/kg (4500 kcal/kg) and fired brick weight of 3 kg

These studies, however, are only focused on the energy side and no economic data is given to extrapolate for the other cost elements. A study by Youssef from 2020, on the other hand, analyses the economic potential of geopolymer brick manufacturing and data for a conventional brick industry are used [97]. The production cost of clay fired bricks in Bretagne, France, is calculated and divided into the different elements from raw materials to personnel, as Table 3.5 shows.

Table 3.5: Production costs for a clay-fired brick plant in France, 2020 (Youssef, 2020 [97]).

Product	**Quantity**	**Unit**	**Cost**	**Unit**	**Total cost**	**Unit**	**Cost/tonne**		**Share of total costs**
Clay	24113	t/year	20	EUR/t	482260	EUR/year	19.12	EUR/t	15.9%
Sand	10620	t/year	40	EUR/t	424800	EUR/year	16.84	EUR/t	14.0%
Water	3355	m3/year	3	EUR/m3	10065	EUR/year	0.40	EUR/t	0.3%
Natural gas	17500000	kWh/year	0.0589	EUR/kWh	1030750	EUR/year	40.87	EUR/t	34.1%
Electricity	2446125	kWh/year	0.1483	EUR/kWh	362760	EUR/year	14.38	EUR/t	12.0%
Domestic fuel	17911	L/year	0.875	EUR/L	15672	EUR/year	0.62	EUR/t	0.5%
Maintenance			350000	EUR/year	350000	EUR/year	13.88	EUR/t	11.6%
Labour			350000	EUR/year	350000	EUR/year	13.88	EUR/t	11.6%
TOT					3026307	EUR/year	120.00	EUR/t	100%

The annual production output is 25220 tonnes of fired bricks and as it can be seen, natural gas itself covers one third of total costs (pre-pandemic values), the second biggest cost element is raw materials with 30% of the total. This industry utilizes a mixture of clay and sand with a relation of approximately 2:1; as already mentioned, there is a wide variety of possibilities but for simplicity it is assumed as a general brick production process. Given the accuracy and the recent source of the data, Table 3.5 is considered as the starting point for calculating the 2022 production costs of bricks in various countries.

Values have been adjusted by inflation to 2022, for fossil fuel prices Appendix Table 2 is used. The specific energy required is obtained dividing the yearly total energy demand by the tonnes of bricks produced in a year: the resulting value is 694 kWh/t of brick, value inside the range presented in Table 1.1.

Afterwards the production costs of fossil fuel bricks production in a certain country and the corresponding CO_2 emissions were calculated. Table 3.6 shows the example of a production in Australia using natural gas: the total costs are 154.7 EUR/t of which 23% are for raw materials and 40% for the fuel (which becomes 52% if only operational costs are considered). In the table, values changing with the locations are highlighted in green (clay, sand, fuel, electricity and labour), while values changing with the fuel are in orange (specific emissions per tonne of bricks produced). Cost components in white cells are considered constant with the location: water cost is negligible and maintenance cost is related to capital investments, which are considered not variable. For these two components, only an inflation adjustment is done from Youssef´s work. For labour costs, the same approach described for aluminium recycling is adopted (direct proportion with median income). With regard to clay and sand prices, it has been considered necessary to vary with the location because of their cost impact: a direct proportion is made among raw materials cost calculated by Youssef (plant in France), the average price of 1000 bricks provided by Linesight Country Commodity Report [98] in France and the same commodity price for the analysed country.

Table 3.6: Production costs calculation based on country and fuel used for a 25,220 t/year plant.

Country	Australia	**Fuel**	Natural gas

Product	**Quantity**	**Unit**	**Cost**	**Unit**	**Total cost**	**Unit**	**Quantity/t_brick**	**Cost/t**	**%**
Clay	24113	t/year	19.883	EUR/t	479449	EUR/year	0.96 t/t_br	19.01 EUR/t	12.3%
Sand	10620	t/year	39.767	EUR/t	422324	EUR/year	0.42 t/t_br	16.75 EUR/t	10.8%
Water	3355	m3/year	3.330	EUR/m3	11172	EUR/year	0.13 m3/t_br	0.44 EUR/t	0.3%
Natural gas	17500000	kWh/year	0.089	EUR/kWh	1557500	EUR/year	693.92 kWh/t_br	61.76 EUR/t	39.9%
Electricity	2446125	kWh/year	0.249	EUR/kWh	609085	EUR/year	97.00 kWh/t_br	24.15 EUR/t	15.6%
Domestic fuel (Diesel)	17911	L/year	1.175	EUR/L	21045	EUR/year	0.71 L/t_br	0.83 EUR/t	0.5%
Maintenance			389270	EUR/year	389270	EUR/year		15.44 EUR/t	10.0%
Labor			411854	EUR/year	411854	EUR/year		16.33 EUR/t	10.6%
TOT					**3901699**	**EUR/year**		**154.71 EUR/t**	**100%**

	location-variable
	fuel-variable

Non-fuel costs	92.12 EUR/t	60%
Fuel costs	62.59 EUR/t	40%
TOT	154.71 EUR/t	100%

Kiln + drying emissions	97.54 kgCO2/t	70%
Other emissions	41.95 kgCO2/t	30%
TOT	139.49 kgCO2/t	100%

The emissions are split into two categories: those which come from processes that can be solarized and those which cannot. The high-temperature firing in the kiln (that uses 50% of the total fuel demand [97]) and the drying process that occurs at low temperature just after the shaping of bricks (using 20% of total fuel [18]) belong to the first group. The remaining 30% of fuel cannot be substituted with a CST technology and therefore it will be included for the renewable production calculations. Table 3.9 reports specific emissions values based on fuel (total emissions are considered).

In order to verify the reliability of the obtained results, a comparison with other literature data has been made. Firstly, the plant output is calculated based on number of bricks and not on tonnes because most of commodity prices are expressed in this way. The weight of a single brick is not provided in Youssef´s study; the value ranges from 2 to 4 kg and if an average of 3 kg/brick is considered [99] the plant´s output corresponds of 330 bricks/tonne. On a country average (Europe and North America) the production of one brick is therefore between 0.25 and 0.40 EUR/brick. Based on the Linesight Country Commodity Report [98], the selling prices in the same countries is between 0.40 and 0.90 EUR/brick, resulting in a slight underestimation of costs. However, because of the high variability in quality, dimensions, weight and material composition of bricks, limiting the costs validation to only one source would not be too accurate. According to building companies like HomeAdvisor [100] (USA), the average selling price is 0.55 EUR/brick. Using this data, the calculated production costs are around 60-80% of selling price, which is more plausible. A third source by Turgut [101] shows the production costs of a 1000 bricks-plant in the USA which is, adjusted to 2022, 0.33 EUR/brick; according to the calculations made using the calculator presented in Table 3.6, that value is 0.28 EUR/brick. The assumptions and the values found are therefore considered in agreement with literature.

3.4. Zinc production

In this section, the production of zinc is analysed under an economical perspective. Among the three industrial processes, this one is the most complex because of the number and heterogeneity of stages, as it has been shown in 1.2.13 Zinc roasting. The production starts with the acquisition of zinc concentrate and after several plant sections, metal ingots are obtained; it is therefore expected that overall production costs (neglecting raw materials) are higher than for aluminium and bricks that have simpler plant structures.

A book by the Australasian Institute of Mining and Metallurgy [73] reports a detailed overview of zinc production including the capital and operational costs for an electrolytic zinc plant in USA in the year 2000. Two plant outputs are analysed, 100,000 annual tonnes and 200,000 annual tonnes, and the relative costs compared. Table 3.7 reports the data for a plant with the lower output where each plant section is associated with the specific operational costs. Additional data have been added such as energy demands and costs split between electricity and fuel, temperature required for the process and share of fuel (data from the same source [73]).

Table 3.7: Direct operating costs for an 100,000 t/a zinc plant (in USD as at June 2000, [73]).

Plant section	Operational costs USD/ton	% of costs	Electricity [kWh/t]	Fuel [kWh/t]	Electricity cost USD/t	Fuel cost USD/t	Temperature	% of fuel used
Concentrate handling	6.85	1.5%	10	41.67	0.40	0.45	no heat from fuel	16.6%
Roasting	32.00	7.0%	110	111.12	4.40	1.20	950 °C	44.3%
Acid plant	27.50	6.0%	214	-	8.56	-	-	-
Leaching/iron separation	40.60	8.9%	108	55.56	4.32	0.60	90 °C	22.2%
Purification	22.95	5.0%	43	-	1.72	-	-	-
Cadmium production	8.01	1.8%	8	0.56	0.32	0.01	765 °C	0.2%
Gypsum removal	2.30	0.5%	30	-	1.20	-	-	-
Electrolysis	185.60	40.7%	3338	-	133.52	-	-	-
Melting and casting	41.05	9.0%	143	41.67	5.72	0.45	500 °C	16.6%
Effluent treatment	8.40	1.8%	20	-	0.80	-	-	-
Residue disposal	8.60	1.9%	5	-	0.20	-	-	-
Administration	71.65	15.7%	15	-	0.60	-	-	-
TOT	**455.51**	**100%**	**4044**	**250.58**	**161.76**	**2.71**		**100%**

It is clear that in the electrolytic pathway, energy demand under electricity form is high, constituting around 35% of operational costs (year 2000), while on the other side fuel demand is significantly lower, accounting of less than 1% of costs.

As the author affirms, clearly boundary conditions and location would significantly change the values, but operational costs shown in Table 3.7 should provide a guide to major items to be considered and the general order of cost for new facilities under USA conditions. Given the high level of details, these data are considered as the starting point for the calculation of the production costs of zinc in various countries in 2022.

A second table in the Australasian Institute of Mining and Metallurgy´s book provides the direct operating costs for each plant section categorized as follows: energy, labour, maintenance materials, and materials and supply. Values are reported in Appendix Table 5 and after a sum procedure it was possible to obtain the total costs by category and not by plant section.

Maintenance costs are simply estimated by the authors as two per cent of direct construction costs for each section [73]. In order to obtain proper production costs, however, it is necessary to include also the raw material costs. In 2022 concentrate price was difficult to define because of being very susceptible to quality (zinc content), location and period (market was oscillating conspicuously); according to the International Zinc Association, during 2021 values were around 90–105 EUR/t while during the following year the range was between 320 and 470 EUR/t [102]. The Association provides also the prices in different markets: in Europe a value of 280 EUR/t has been associated, in USA and Australia 187 EUR/t and for the remaining countries 121 EUR/t. In Roderick´s work, the following numbers are considered: an average concentrate zinc content of 52% and a 97% recovery of zinc (*raw mineral* to *final product* efficiency) [73]. An overall 50% concentrate-to-zinc product rate is believed to be reasonable: per each tonne of product, two tonnes of raw materials are bought. Based on these assumptions and data, the production cost of fossil fuel zinc production in a certain country and the corresponding CO_2 emissions were calculated. Table 3.8 shows the example of a production in USA with heating oil: the total costs are 1126 EUR/t of which 33% are from the raw materials, 32% from electricity and 18% from personnel. Fuel costs are the smallest contributors with 1.7% share.

Table 3.8: Production costs calculator based on country and fuel used for a 100,000 t/year plant.

Country	USA	**Fuel**	Heating oil

Product	**Quantity**	**Unit**	**Cost**	**Unit**	**Total cost**	**Unit**	**Quantity/t_Zn**	**Cost/t**	**%**
Raw material	200000	t/year	187.00	EUR/t	37400000	EUR/year	2.0 t/t_Zn	374.00 EUR/t	33.2%
Personnel	345	people	58912.64	EUR/year	20324860	EUR/year		203.25 EUR/t	18.0%
Electricity	398500000	kWh/year	0.09	EUR/kWh	36662000	EUR/year	3985.0 kWh/t	366.62 EUR/t	32.6%
Heating oil	25060000	kWh/year	0.07	EUR/kWh	1867548	EUR/year	250.6 kWh/t	18.68 EUR/t	1.7%
Maintenance			6615326.00	EUR/year	6615326	EUR/year		66.15 EUR/t	5.9%
Materials and supply			9733870.00	EUR/year	9733870	EUR/year		97.34 EUR/t	8.6%
TOT					**112603604**	**EUR/year**		**1126.04 EUR/t**	**100%**

Non-fuel costs	1107.36 EUR/t	98.3%
Fuel costs	18.68 EUR/t	1.7%
TOT	1126.04 EUR/t	100%

location-variable
fuel-variable

Fuel to heat	56.23 kgCO2/t	84.2%
Other fuel	10.55 kgCO2/t	15.8%
TOT	66.78 kgCO2/t	100%

Like in the previous cases, the values that are changing are highlighted: in green, country-dependent values (raw material, electricity and fuel prices, and personnel costs) and in orange, fuel-dependent values (specific emissions). Values that are in white cells are considered constant with the location because they are connected to capital costs (maintenance), they are therefore just adjusted by inflation to 2022. With regard to labour costs, the same approach for the previous industrial processes is done. In this case also, emissions are split into two categories: those which comes from processes that can be solarize and those which cannot. To the first group belong the processes that need heat (roasting, leaching and iron separation, cadmium production, melting and casting), as shown in Table 3.7, accounting for 84% of total fuel demand. For the remaining 16% of fuel, heat is not produced, therefore CST technology cannot be used. Table 3.9 reports specific emissions values based on fuel (in a 100% fossil fuel operation).

In order to verify the reliability of the obtained results, a comparison with other literature data has been made also for this process. As already mentioned, the market prices of zinc are changing with a daily basis and in particular during the last two years record values have been reached. However, values were in 2023 close to ones in pre-pandemic period; according to

Boulamanti who studied the production costs of non-ferrous metals in some countries in 2016, zinc production in EU was 450 EUR/t, which adjusted by inflation becomes 510 EUR/t in 2022 [103]. Considering that Boulamanti did not include the cost of raw materials and the energy prices are from 2013, the corresponding results obtained in this thesis for the same countries are around 800 EUR/t. A light overestimation is expected, since taking into consideration the energy prices differences from 2013 and 2022, which was once again a peak year, the range between the two production calculations would reduce further. The assumptions and the values found are therefore considered in agreement with literature.

Table 3.9: Specific emissions for the three processes based on fuel used (no electricity).

	Emissions by fossil fuel required during production kgCO2/t		
Fuel	**Aluminium recycling**	**Bricks production**	**Zinc production**
Natural gas	154.32	139.49	50.32
Heating oil	204.81	185.08	66.78
Coal	259.92	234.84	84.75

4 LCOH calculation

It is well known that DNI resource has a very strong impact on LCOE (Levelized Cost of Electricity) of concentrating solar systems [104]. In their study, Dersch et al. demonstrated the analytical relation between these two variables by calculating the LCOE for CST plants in different countries against the annual DNI specific of the plant´s location. Data were from 2018 and divided based on the technology; an interpolation was made for parabolic trough and one for solar tower. A power law gave a reasonable approximation of the cost dependency on the solar resource: the R2 obtained for the first technology considered was 0.88 and the R2 for the second one was 0.98. The graph they obtained is reported in Figure 4.1. The lower fluctuation for solar tower systems is due to their better tracking of the sun position with heliostats compared to parabolic trough systems.

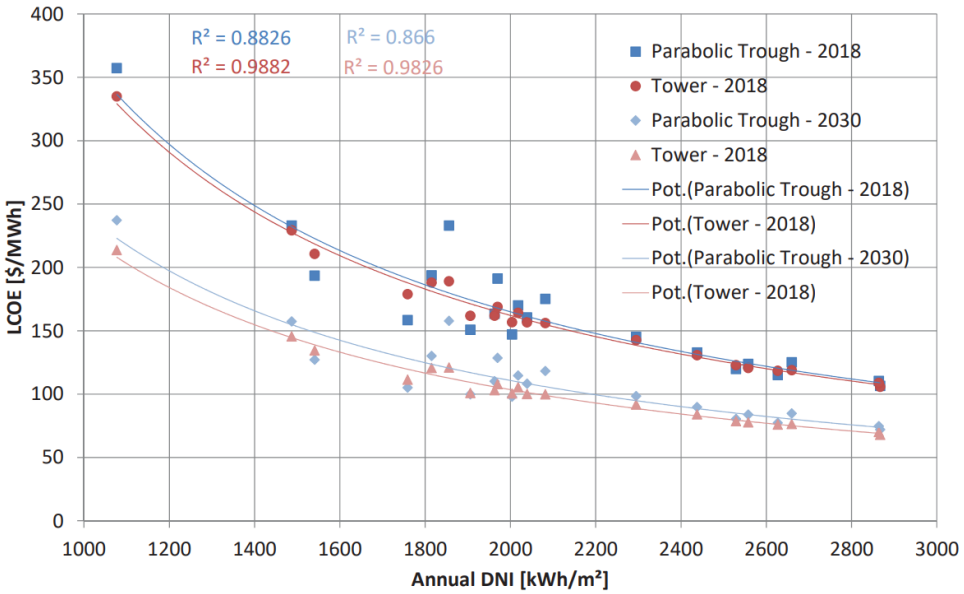

Figure 4.1: LCOE and DNI resource of different plants with potential law fit curves (Dersch et al.)

Since the purpose of thesis is to study the potential of the heat provided by CST, the Levelized Cost of Heat (LCOH) is considered as a parameter instead of LCOE. Because of the promising results of the above study, using the same approach to have an LCOH dependency on DNI, and thus a location dependency, was considered reasonable. It has to be said that the interpolation lines found by Dersch et al. for the two CST technologies do not differ much (blue and red lines), but rather can be considered as one: in this study a single interpolation line was calculated considering data from installations of both technologies. The first step to be done was to collect

data of different plants from as many different locations as possible in order to have a better approximation that is possibly valid for all the world. A total of 51 data points were collected from literature and the different LCOH were all converted to Euro and adjusted for inflation to 2022. Table 4.1 reports the obtained dataset; in the "Type" category ST stands for Solar Tower and PT for Parabolic Trough technologies.

Table 4.1: Dataset used for the interpolation LCOH vs DNI

	Type	**DNI**	**LCOH**	**Storage**	**Location**	**Year**	**Source**
	-	kWh/m²/y	cEUR/kWh	h	-	-	-
1	ST	1915	3.43	12	Australia (Brisbane)	2021	ASTRI, 2021 [105]
2	ST	2168	3.31	12	Australia (Rockhampton)	2021	ASTRI, 2021 [105]
3	ST	2169	3.66	12	Australia (Armidale)	2021	ASTRI, 2021 [105]
4	ST	2178	3.45	12	Australia (Wagga Wagga)	2021	ASTRI, 2021 [105]
5	ST	2212	3.66	12	Australia (Bickley)	2021	ASTRI, 2021 [105]
6	ST	2218	3.76	12	Australia (Orange)	2021	ASTRI, 2021 [105]
7	ST	2248	3.55	12	Australia (Oakey)	2021	ASTRI, 2021 [105]
8	ST	2257	3.24	12	Australia (Townsville)	2021	ASTRI, 2021 [105]
9	ST	2306	3.17	12	Australia (Gladston)	2021	ASTRI, 2021 [105]
10	ST	2344	3.43	12	Australia (Swanbourne)	2021	ASTRI, 2021 [105]
11	ST	2368	3.29	12	Australia (Dubbo)	2021	ASTRI, 2021 [105]
12	ST	2375	3.38	12	Australia (Mildura)	2021	ASTRI, 2021 [105]
13	ST	2431	3.24	12	Australia (Moree)	2021	ASTRI, 2021 [105]
14	ST	2499	3.13	12	Australia (Geraldton)	2021	ASTRI, 2021 [105]
15	ST	2537	3.17	12	Australia (Cobar)	2021	ASTRI, 2021 [105]
16	ST	2622	3.15	12	Australia (Kalgoorlie)	2021	ASTRI, 2021 [105]
17	ST	2632	2.92	12	Australia (Mount Isa)	2021	ASTRI, 2021 [105]
18	ST	2639	3.06	12	Australia (Charleville)	2021	ASTRI, 2021 [105]
19	ST	2648	2.92	12	Australia (Longreach)	2021	ASTRI, 2021 [105]
20	ST	2649	2.99	12	Australia (Halls Creek)	2021	ASTRI, 2021 [105]
21	ST	2649	3.01	12	Australia (Woomera)	2021	ASTRI, 2021 [105]
22	ST	2691	2.80	12	Australia (Tennant Creek)	2021	ASTRI, 2021 [105]
23	ST	2808	2.85	12	Australia (Oodnadatta)	2021	ASTRI, 2021 [105]
24	ST	2856	2.77	12	Australia (Carnarvon)	2021	ASTRI, 2021 [105]
25	ST	2881	2.85	12	Australia (Alice Springs)	2021	ASTRI, 2021 [105]
26	ST	2885	2.82	12	Australia (Pt. Hedland)	2021	ASTRI, 2021 [105]
27	ST	2899	2.94	12	Australia (Newman)	2021	ASTRI, 2021 [105]
28	ST	2913	2.87	12	Australia (Meekatharra)	2021	ASTRI, 2021 [105]
29	ST	2942	2.70	12	Australia (Learmonth)	2021	ASTRI, 2021 [105]
30	PT	1416	5.51	no data	Chile (Puerto Montt)	2016	Cortes, 2018 [106]
31	PT	2168	3.41	no data	Chile (Concepcion)	2016	Cortes, 2018 [106]
32	PT	2197	3.35	no data	Chile (Valparaiso)	2016	Cortes, 2018 [106]
33	PT	2219	3.87	no data	Chile (Santiago)	2016	Cortes, 2018 [106]
34	PT	2373	2.61	no data	Chile (Arica)	2016	Cortes, 2018 [106]
35	PT	2986	2.30	no data	Chile (Atacama)	2016	Cortes, 2018 [106]
36	PT	2373	3.39	no data	California	2015	Kurup, 2015 [107]
37	PT	2008	4.00	no data	California	2015	Kurup, 2015 [107]
38	PT	2738	2.91	no data	California	2015	Kurup, 2015 [107]
39	PT	2008	4.13	no data	USA (California)	2016	Kurup, 2016 [108]
40	PT	2190	3.77	no data	USA (California	2016	Kurup, 2016 [108]
41	PT	2555	3.23	no data	USA (California)	2016	Kurup, 2016 [108]
42	PT	2125	3.71	no data	Morocco (Benguerir)	2019	Mouaky, 2019 [109]
43	PT	2548	3.25	no data	Morocco (Errachidia)	2022	Ouali, 2023 [110]
44	ST	2008	3.27	no data	Israel	2016	Riggs, 2017 [111]
45	ST	2190	3.00	no data	India	2016	Riggs, 2017 [111]
46	ST	2190	3.00	no data	Spain	2016	Riggs, 2017 [111]
47	ST	2300	2.86	no data	Caribbean	2016	Riggs, 2017 [111]
48	ST	2300	2.86	no data	Morocco	2016	Riggs, 2017 [111]
49	ST	2555	2.57	no data	Nepal	2016	Riggs, 2017 [111]
50	ST	2993	2.19	no data	Australia	2016	Riggs, 2017 [111]
51	ST	3468	1.89	no data	Chile	2016	Riggs, 2017 [111]

In Figure 4.2 the scatter plot with the LCOH-DNI data is reported; different technologies (Solar Towers and Parabolic Trough) are highlighted. The interpolation function giving the best approximation is a logarithmical one and it is reported in Equation 4.1. The corresponding R^2 obtained is closed to the value of 0.74, which led to consider the approximation good enough, given the number of data and their geographical diversity. In the continuation of the study, this equation plays a fundamental role since it permits to calculate the LCOH in every location, given the corresponding value of DNI.

$$LCOH = -3.173 \cdot \ln(DNI) + 27.916 \qquad \text{Equation 4.1}$$

It is important to mention that not all data from the plants share the same characteristics of thermal storage; some are from literature works where clear information about it were written, others not. Therefore, their relative LCOH value could slightly change with the addition or improvement of it. However, an additional data was put on the graph and not included in the interpolation: it is the LCOH of the CentRec receiver reported by Frantz et al. for a plant in Morocco [84] (with storage included) which has already been mentioned in Section 2.3. It can be observed that relatively with the DNI of its location, CentRec has lower costs, thus demonstrating that values obtained by the interpolation are not underestimating the costs, also at temperatures of >900 °C.

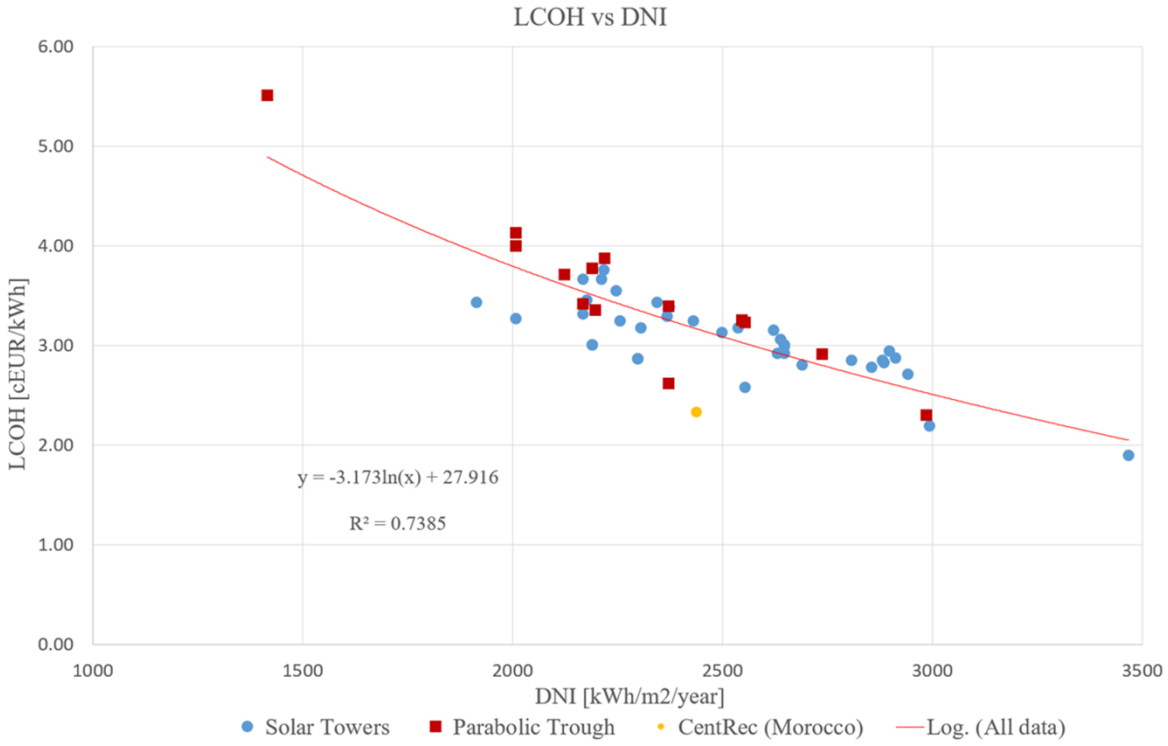

Figure 4.2: Graph with literature data and interpolation line. Different technologies are highlighted (Solar Towers in blue circle and Parabolic Trough in red squares) and the plant studied by Frantz et al. is the yellow circle (not included in the interpolation).

5 Calculations and elaborations

The main outcomes of this work, such as calculations, geographical elaborations, results, and their respective implications, are presented in this chapter.

The production costs of the three different industrial processes are calculated in different countries around the world based on different variables and in various scenarios. The fossil fuel heat production option is compared to the CST heat production under different carbon tax scenarios in order to assess where the renewable option is cheaper and how much the CO_2 price can influence it. In addition, because CST in not the only appealing renewable technology available on the market, a third production method based on heat production through a PV system is studied and compared to the other alternatives. Ultimately, a sensitivity analysis on the CST technology is done in order to observe the effects on production costs in the case of increasing LCOH and whether this alternative can still be attractive.

5.1. Carbon tax

A carbon tax is a fee for the carbon dioxide emissions required to produce a good. The purpose of carbon taxes is to draw attention to the socioeconomic costs associated with carbon emissions, which are felt indirectly through things like more extreme weather or in general global warming. They are intended to raise the cost of the fossil fuels that release greenhouse gases when they are used and therefore both reduce the demand for high-emission products and encourage the production of less carbon-intensive ones [112]. They are considered to be the most effective strategy for combating climate change [113]. Researchers have proved that carbon taxes effectively reduce emissions and according to the World Bank, carbon tax is critical to scaling up climate action [114].

There are different forms of carbon tax depending on which emissions are covered: only carbon dioxide or also other greenhouse gases such as methane or nitrous oxide (based on their CO_2-equivalent global warming potential). The simplest case is considered in this thesis so that only CO_2 emissions are calculated.

More than 20 cities, states, provinces, and almost 40 countries currently utilize carbon pricing methods, and more are planned to do so in the future. Approximately half of their emissions are covered by the current carbon price systems combined, which accounts for roughly 13% of yearly greenhouse gas emissions worldwide (5% direct carbon tax and the remaining 8% other indirect systems) [114]. As of 2023, the list of countries with carbon pricing initiatives includes Europe, Mexico, most of South America, South Africa, Botswana, Morocco, some countries in Asia such as Chine, Japan and South Korea, Australia and Canada. A great absence one notices are USA where carbon pricing initiatives are only implemented in six states including California, Oregon and Hawaii (World Bank).

Currently, carbon tax values go up to over 100 USD/tonne depending on the country. Few countries already present prices above 100 USD/tonne, in particular Sweden, Switzerland, Liechtenstein and Uruguay. Few other European nations present values greater than 50 USD/tonne, while the remaining countries (the majority) have values below it (values from World Bank report about carbon pricing in 2023, Appendix Figure 3). However, it is important to underline that within a country not every sector is affected by the same value or affected at all.

As the World Bank states, overall carbon prices would need to rise in the longer term to drive investments into climate neutrality at the scale and pace required. The High-Level Commission on Carbon Prices concluded in 2017 that carbon prices needed to be at the level of 40–80 USD/tonne of CO_2 in 2020 and reach 50–100 USD/tonne of CO_2 by 2030 to be on track to keep temperatures below 2 °C - the upper end of the limit agreed upon in the Paris Agreement (2017 USD) [115].

In this study the carbon tax affects all countries worldwide at the same time and one single value is considered per time. Calculations are made for three different scenarios: no carbon tax, 50 EUR/tonne of CO_2 and 100 EUR/tonne of CO_2.

In addition to carbon taxes for productions within the country's borders, the European Commission has presented a carbon border adjustment mechanisms (CBAM) as part of the European Green Deal which basically imposes a carbon tax also to imported products. Five major commodity groups are currently included in the list of CBAM goods: iron and steel, fertilizers, cement, aluminum, and electricity. However, the list may be expanded in the future. The full implementation of CBAM is scheduled in 2026 and the goal is to penalize imported products that may be economically cheaper but not environmentally sustainable [116]. The presence of aluminum in the list of taxed products increases further the interest in the analysis of new production technologies like shown in the thesis.

In order to calculate the effects of a carbon tax on the production costs of the three processes analysed, the tables built in Chapter 3 have been adapted (Table 3.3, Table 3.6 and Table 3.8). Per each process, the specific emissions have been calculated based on the fossil fuel used with data collected in Table 3.9. The new production cost is obtained through Equation 5.1.

$$new\_PC_{i,j,k} = base\_PC_{i,j,k} + H_i \cdot E_k \cdot Tax \qquad \text{Equation 5.1}$$

Where:

- $new\_PC_{i,j,k}$ is the new production cost of process *i,* in the country *j,* using fuel *k*;
- $base\_PC_{i,j,k}$ is the production cost *i*,*j*,*k* in a zero-carbon tax scenario [EUR/tonne];
- H_i is the energy demand of process *i* supplied by fuel [kWh/tonne of product];
- E_k is the specific emission of fuel *k* [tonnes of CO_2/kWh];
- *Tax* is the carbon tax [EUR/tonne of CO_2].

In Figure 5.1 the graphs with the increasing production costs of the three processes using natural gas, heating oil and coal are reported. The graphs are based on productions in Mexico and one can observe that the interaction of the fuel-lines among the processes is the same, there is only a change of scale in the vertical axis: an oil kiln is always cheaper when the carbon tax is below 80 EUR/tonne and after this value the natural gas option becomes cheaper. This fact is because

the price of fuels is constant, what changes is the energy demand; in zinc production not so much fuel is used, resulting in a slight growth of costs with carbon tax, on the contrary, in aluminium and bricks production the energy demand in form of heat is high and this is reflected in a much stronger growth of costs with carbon taxes.

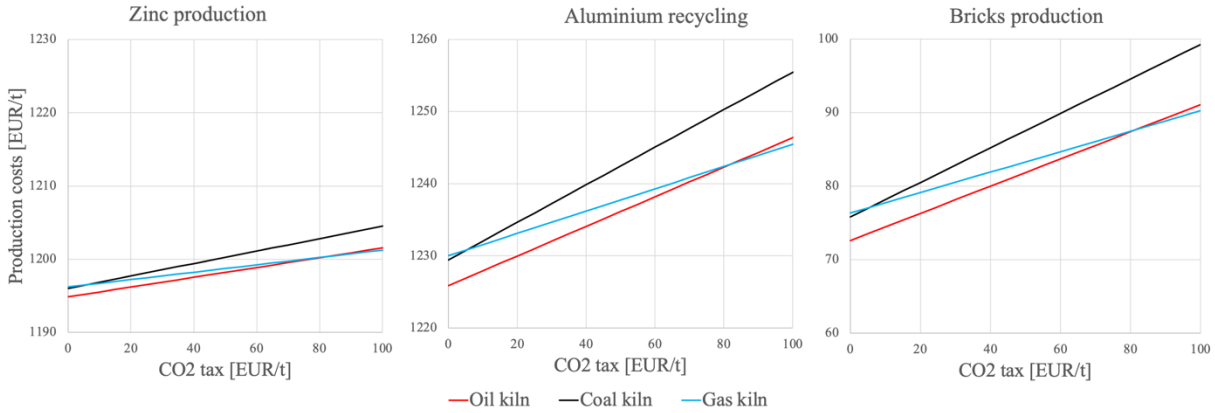

Figure 5.1: Production costs increase with carbon tax in the three processes (Mexico).

Further observations can be done on the graphs; the inclination of the different fuel options is depending on the emissions per kWh, therefore the black line corresponding to coal use has a sharper inclination than the red one (heating oil), which in turn has a greater inclination than the blue one (natural gas). Carbon tax has the ability to influence the cheapest fuel option; in the example heating oil is the less expensive choice until the tax reaches the value of around 80 EUR/tonne and after this value, natural gas becomes cheaper.

However, each country has different energy prices and the relative positions of the lines in the above graphs change based on the location. Where one fuel is much cheaper than the others, it can still remain the cheapest option even if its emissions are higher; this happens for example in Australia and Spain where coal is so cheap that even in a 200 EUR/tonne carbon tax scenario it remains cheaper than heating oil or natural gas.

5.2. CST production

In order to calculate the solar production cost, the most important element is to have an LCOH value, and particularly for this study, a geographical distribution of it. To obtain this, Equation 4.1 has been applied to the raster map of global distribution of annual DNI on the QGIS software. Each pixel consisting in a square with a resolution of around 7 km and containing an average annual value of solar irradiation, is associated with a value of heat production cost through CST solar tower technology. One simplification that is done is the consideration of the LCOH being only variable on the solar source and not with country specific costs. If on one side clear data of CST costs diversified per each country are not available, on the other side it is believed that the DNI parameter has a much bigger influence, as it is shown in Figure 4.2 and the work of Dersch et al. (Figure 4.1) where the location of the plants does not have a significant impact.

Because of the negative-logarithmic nature of the relationship, high LCOH costs are found in regions with low level of DNI and on the contrary, low costs are found in areas with a high solar source. In particular, the lowest values are found in the Andes region in the North of Chile where an absolute minimum of 0.017 EUR/kWh can be reached thanks to annual DNI values that are over 3500 kWh/m^2. Very low costs around 0.028 EUR/kWh can be found in several

countries around the world where the irradiance is above 2600 kWh/m^2, in particular in South-West USA, most of Mexico, South of the African continent, North Sahara region and Arabic peninsula, Himalayas region, and most of Australia. Medium-low costs around 0.045 EUR/kWh can be found in the rest of USA, Brazil, Southern Europe, Sub-Saharan region and India. It appears already interesting to have a first rough comparison of these costs with fuel prices in the different countries (Appendix Table 2); some locations present values very close or even greater than the solar ones such as in South European countries, and some locations on the contrary present values that are unable to be reached by the CST technology such as the extreme case of Iran where natural gas price is close to 0.001 EUR/kWh for businesses.

The global map has been cut based on country political borders and the 25 countries listed in Paragraph 3.1 have been taken into consideration for the following calculations. The world LCOH map with the selected countries highlighted is reported in Appendix Figure 2.

5.2.1. Calculation of CST production

As already mentioned, the three processes use fuel in different ways and the share of fuel used to provide heat differs. In the aluminium recycling process 100% of the fuel is used to provide heat in the kiln where the metal is melted at high temperature; the CST technology is therefore able to completely substitute the fossil source and consequently the emissions of the solar production are considered as zero. In reality, things are slightly different because there is no process which emits no CO_2, for example for the production of electricity that is intensively used. Although the carbon footprint of the CSP technology is reported to be as low as 20 g CO_2/kWh$_{el}$ [117] (thus, even lower for heat usage), it is also neglected. Nevertheless, including all the carbon sources present in an industrial process would have required many data and effort that are out of scope of this work; a simplification has been made and only the direct emissions from the fuel bought in the conventional production are taken into consideration.

In brick manufacturing, 70% of fuel is used to provide heat (50% at high temperature for the backing process and 20% at low temperatures for the drying process). The remaining 30% of fuel is not used to provide heat, therefore the CST technology cannot replace it and in the calculation of the solar production that percentage of fuel can increase the costs if a carbon tax is applied.

In zinc manufacturing, a total of 84% of fuel is used to provide heat (45% at high temperatures for roasting, 17% at medium temperatures for melting and 22% at low temperatures for the leaching phase). In this case the percentage of fossil fuel that is still used even in the solar production is 16%.

In order to calculate the solar production costs with a CST technology of the processes in the different locations, the following Equation 5.2 is applied considering the costs calculated in Chapter 3:

$$PC_{i,j,k} = NF_{i,j} + (1-\alpha)\cdot\left(F_{i,j,k} + H_i \cdot E_k \cdot Tax\right) + \alpha \cdot H_i \cdot LCOH(DNI) \qquad \text{Equation 5.2}$$

Where:

- $PC_{i,j,k}$ is the production cost of process i, in a location in country j, using fuel k
- $NF_{i,j}$ is the sum of non-fuels costs per tonne of product [EUR/tonne] (labour costs, maintenance, raw materials and all the items not changing with heat technology improvement)
- α is the share of fuel replaced by CST [%]

- $F_{i,j,k}$ is the cost of fuel per tonne of product in a 100% fossil scenario [EUR/tonne]
- H_i is the energy demand of process i supplied by fuel [kWh/tonne]
- E_k is the specific emission of fuel k [tonnes of CO_2/kWh]
- *Tax* is the carbon tax [EUR/tonne of CO_2]
- *LCOH(DNI)* is the heat cost provided by CST, in function of DNI [EUR/kWh]

By means of this equation, each cell of the map has been associated by the production costs of a process using CST, based on the local DNI value. This result will be compared to the corresponding fossil production of the cell.

5.3. PV comparison

In this section, a second solar technology (photovoltaics) is considered in order to provide thermal energy to the industrial processes.

5.3.1. From LCOE to LCOH map

Photovoltaic modules generate direct current, therefore an electrical heater is needed to provide heat for the industrial processes. Modern electric heaters reach efficiencies of up to 98%, while the power can be varied between 0 to 100% and a typical start up time of 1–5 min [118].

PV is by far one of the most spread and popular renewable technologies that has experienced a drastic drop of costs in the recent years. According to the IRENA 2023 report, between 2010 and 2022, the global weighted average LCOE of utility-scale photovoltaic plants declined by 89% from 0.445 USD/kWh to 0.049 USD/kWh. In Europe only, the cost of crystalline solar PV modules declined by 91% between the same period [78].

As opposed to CST that utilizes only the direct normal irradiance, PV can exploit both direct and diffuse irradiance. In 2020 Global Solar Atlas has published a study, in collaboration with the World Bank, about the Global Photovoltaic Power Potential by Country [119]. In particular, a global LCOE map has been elaborated with data from 2018 of large-scale ground-mounted PV power plants with the expected lifetime of 25 years. For the purpose of calculating the production costs in 2022, however, the map had to be updated. The following steps have been done:

- The raster map with LCOE data from 2018 [USD/kWh] has been firstly adjusted by inflation to 2022 values and then converted to Euro
- From the IRENA 2023 report, a decrease of 35% of PV LCOE has been observed from 2018 to 2022. Therefore, the map has been adjusted by this value (in its entirety)
- Country-based adjustment have been done based on values on the map and country-specific data provided in IRENA report.

The last step became necessary because the values obtained in some countries were slightly more expensive compared to those published by IRENA. In the report the average values of LCOE in the top 20 utility-scale markets are shown, Figure 5.2. In order to obtain a more realistic map, the average value of LCOE has been calculated per each considered country (namely the arithmetic mean of LCOEs of all the cells belonging to a country) and then the difference in percentage between it and IRENA´s values have been obtained. This percentage

has been used as a correction factor to be multiplied per each cell. The result is a map with LCOE values depending both on solar source and country characteristics.

Countries not present in IRENA dataset have been associated with LCOE average values of close and similar countries, in particular:

- Portugal has been associated with Spain´s value
- Angola, Botswana, Egypt, Iran, Israel, Madagascar, Morocco, Namibia, South Africa, Zambia and Zimbabwe have been associated with Saudi Arabia´s value
- Argentina, Bolivia and Peru have been associated with Chile´s value.

As an example, the average value of the cells in Australia was 0.067 EUR/kWh while according to IRENA the value is 0.041 EUR/kWh, corresponding to a 61% difference. This last value has been multiplied to all cells so that the new average value of the cells is updated and in line with the report.

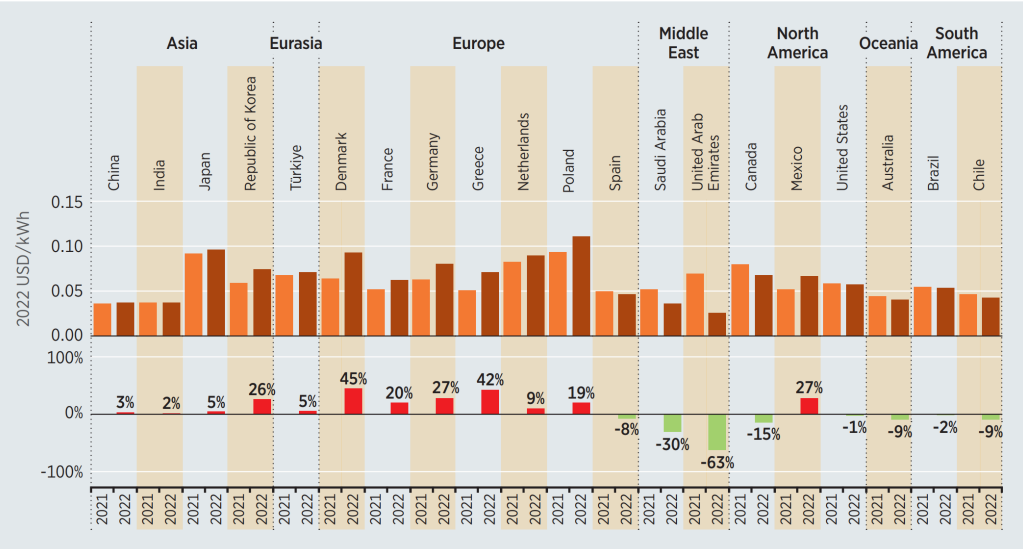

Figure 5.2: Utility-scale solar PV weighted average LCOE trends in some countries, 2021–2022 (IRENA, 2023 [78]).

LCOH values for PV are simply obtained considering a 98% efficiency of electricity-to-heat and LCOE values are multiplied by this factor. The value chosen is very high, especially in high temperature applications where heat losses are greater, however an optimistic scenario is considered in favor of PV to observe whether CST technology can still compete or not. This can then serve as a baseline for further studies, to narrow down the exact difference between both technologies.

5.3.2. Calculation of PV production

In order to calculate the production costs through PV technology, the same approach used for the CST case is used: solar energy, but this time via electrical heaters, provides the heat demand for a process. Equation 5.2 is therefore applied with the only difference of substituting *LCOH(DNI)* of CST, with *LCOH* values relative to PV plants.

After this calculation, each cell has been now associated with the production costs of three different heat-providing technologies: fossil fuel, concentrated solar energy and photovoltaics. As for the CST option, the emissions directly derived from the production and use PV panels

are neglected, since taking them into consideration would not change significantly the overall results.

5.4. Results

This section contains the results of previous calculations, in particular the maps showing the areas where a certain technology is the most appealing based on solar source, country parameters and carbon tax values. Specifically, the effects of emissions tax are deeply analysed.

5.4.1. Base scenario

The three maps graphically show the cheapest fuel option for the recycling of aluminium in some countries and under different carbon tax values. As will be shown later, these maps are also valid for the other production process of zinc and bricks, as the only relevant parameter is the utilized fuel.

There are three types of fossil fuel that are represented by a scale of grey, namely coal (the darkest), heating oil, and natural gas (the lightest). Solar is the cheapest option to provide heat in the red (CST technology) and yellow (PV technology) areas.

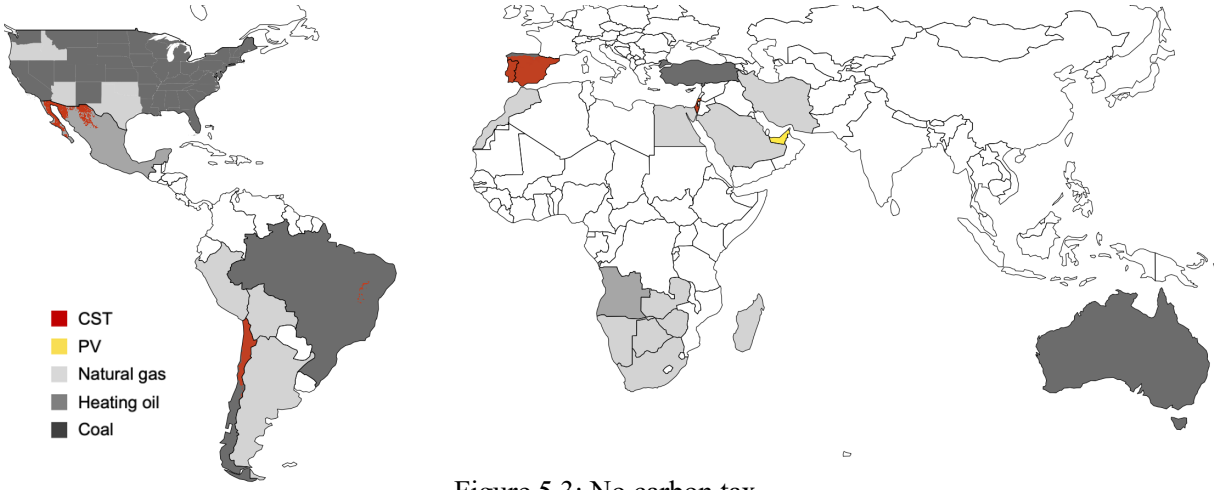

Figure 5.3: No carbon tax.

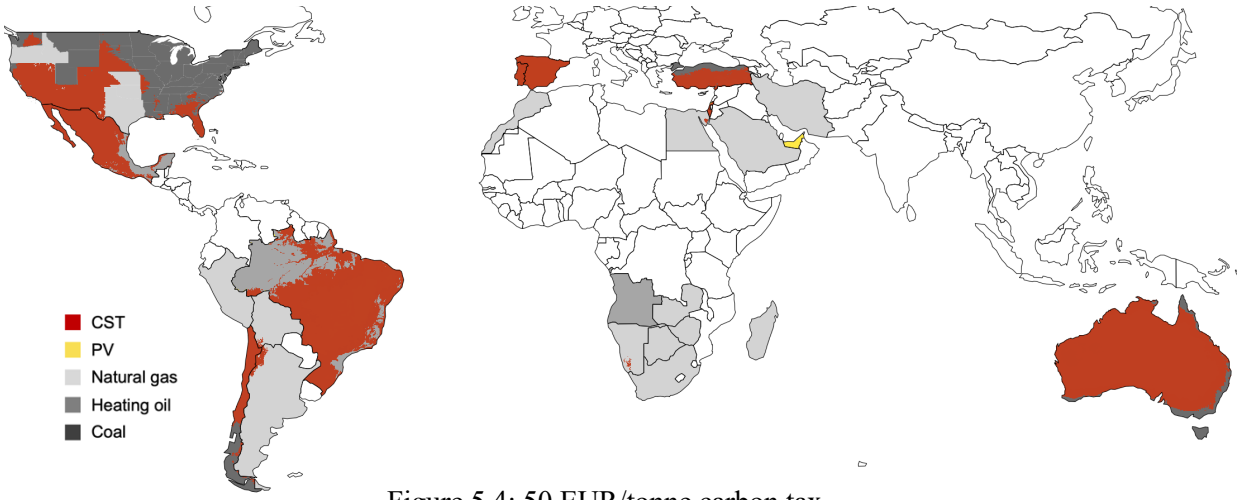

Figure 5.4: 50 EUR/tonne carbon tax.

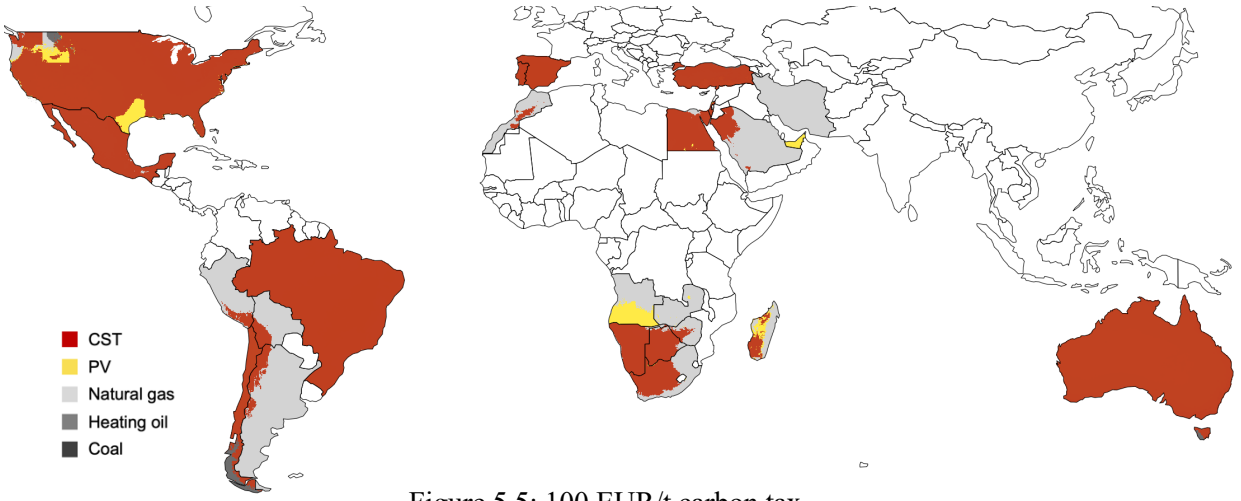

Figure 5.5: 100 EUR/t carbon tax.

It is possible to observe that when there is no carbon tax, fossil fuels are the cheapest option in most of the countries; CST is the cheapest option in large areas only in Spain, Portugal and Israel. In some locations of Mexico and Chile, the DNI is high enough that CST beats the other options. United Arab Emirates are the only country where PV are competitive.

When the tax is increased to 50 EUR/t, the situation improves drastically: CST starts to be the cheapest option in several countries and in large areas, for example, Australia turned almost completely red. PV technology still remains more expensive in every country (except UAE).

When the value of the tax is further increased to 100 EUR/t, solar production turns to be the best option for most of the countries. In Mexico, Brazil, Spain, Portugal, Israel, Turkey, Australia and Namibia, CST is the cheapest option in all of the territory. Areas where PV is competitive are found in the USA, Angola (where there are no locations where CST is the cheapest option), UAE, Madagascar and few points in Egypt.

The increasing of the carbon tax hugely affects production costs all over the world; even the fossil production is affected where “cleaner” fuels like natural gas become cheaper than coal or heating oil. Although PV production has been optimistically calculated (with a 98% efficiency and not considering any additional costs such as for the electrical heaters, heat storage etc.), CST seems to be more competitive in most of the countries.

5.4.2. Carbon tax and renewable production

Maps provide an easy-to-read global visualisation of where solar energy is competitive and even cheaper than the other available options, however they provide a static configuration of values based on a given carbon tax. In order to have a deeper understating of the effect of the tax, several maps should have been produced with a short enough step size in the value of the tax. The operation would have been costly and the results not so immediate to evaluate given the big number of maps produced.

A second approach to analyse the effect of the carbon tax is the analytical one, thanks to the equations describing the various production costs. In Figure 5.6 a graphical visualization of the production cost dependency on DNI and carbon tax values is reported. The grey function is the fossil option which is increasing linearly with the tax and remaining constant with DNI because independent from it. The yellow function, on the contrary, represents the solar production whose costs are decreasing with DNI, following the LCOH logarithmic relation, and staying constant with the tax. The shown case is for aluminium recycling where CST is able to replace 100% of the fossil fuel.

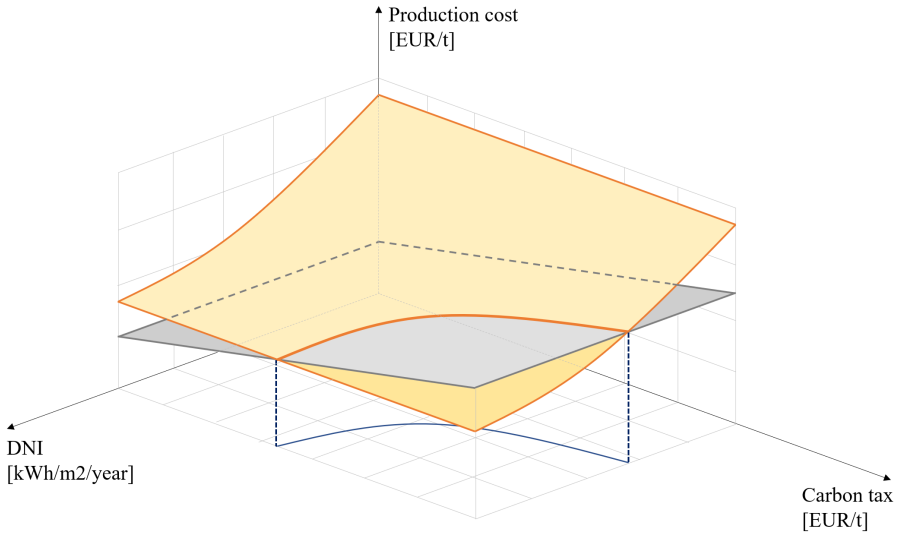

Figure 5.6: 3D visualization of the production cost dependency on DNI and carbon tax values for aluminium recycling.

The interesting part of the graph is where the grey function is above the yellow one, meaning the solar production via CST technology is cheaper than the fossil option. The projected blue line in the DNI-carbon tax plane represents the threshold among DNI-tax values for which one option is cheaper than the other. Its form is country dependent and it is obtained by the following simultaneous equation:

$$\begin{cases} \textit{Production costs with fossil fuel} & \text{Equation 5.1} \\ \textit{Production costs with CST} & \text{Equation 5.2} \end{cases}$$

The result is:

$$Carbon\ Tax_{i,j,k} = \frac{\alpha \cdot \left(H_i \cdot LCOH(DNI) - F_{i,j,k}\right)}{avoided\_emissions_i}$$ Equation 5.3

Where:

- *Carbon Tax*$_{i,j,k}$ is the value (coupled with the corresponding DNI) above which the solar production is cheaper in a process *i*, in country *j*, using fuel *k*;
- α is the share of fuel replaced by CST [%];
- H_i is the energy demand of process *i* supplied by fuel [kWh/tonne];
- *LCOH(DNI)* is the heat cost provided by CST, in function of DNI [EUR/kWh];
- $F_{i,j,k}$ is the cost of fuel per tonne of product in a 100% fossil scenario [EUR/tonne];
- *avoided_emissions*$_i$ is the specific amount of avoided CO_2 if CST is adopted in process *i*, which is conventionally using fuel *k* [tonnes of CO_2/tonne of product].

Noteworthy is the simplicity of this relationship which only depends on few factors: saved emissions, heat demand, fuel costs and share of heat by CST.

Figure 5.7 reports the graph with the cheapest production option per each couple of DNI-carbon tax values in Australia; the available DNI range of the country is also reported.

What can be seen in the graph for Australia (and verified with the maps) is that when there is no tax applied, coal is the cheapest option in every location of the country. However, if the price of carbon dioxide is increased, CST becomes more and more convenient; with a tax value of 50 EUR/t CST it is cheaper in every location with a DNI over 2000 kWh/m^2, which is very common in Australia. When the tax is above 70 EUR/t fossil fuel basically becomes more expensive in every location.

In countries like Spain or Portugal, CST is cheaper in many locations even if there is no tax and the solar source is not necessarily extremely high. This is the effect of fossil fuel prices that are changing country to country. The opposite case is verified for example in Iran, Morocco, Bolivia and South-African countries where the fuels are so cheap that CST is competitive only when both the tax and DNI are high. Appendix Figure 4 reports the graphs of six different countries and regions with their relative available DNI range.

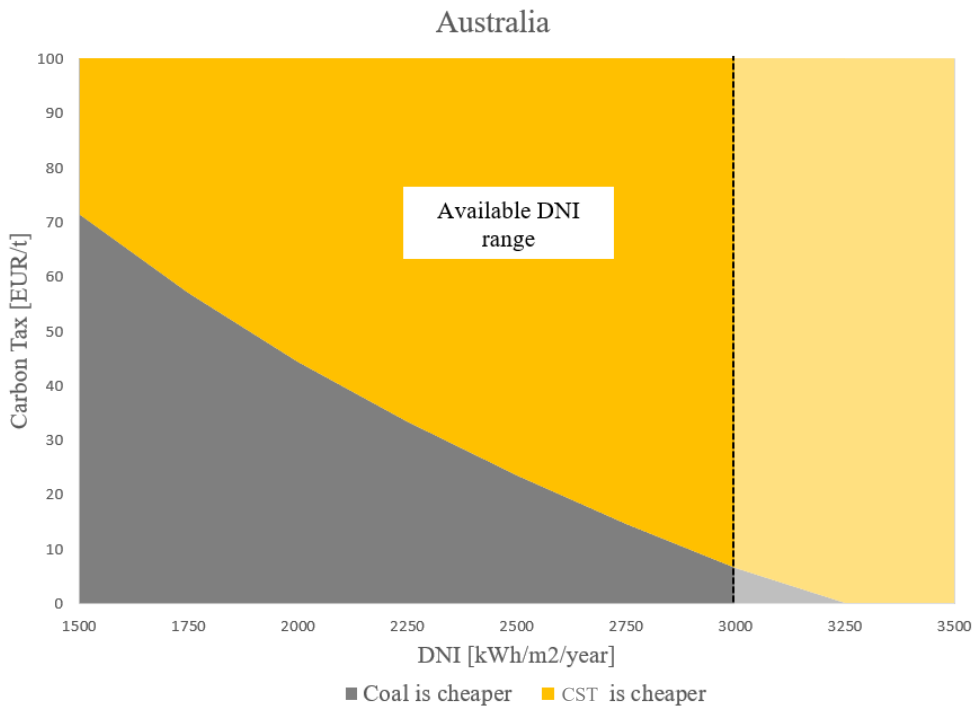

Figure 5.7: Carbon Tax vs DNI graph for Australia and its relative available DNI range which goes up to around 3000 kWh/m^2 per year, value represented by the dashed line.

The most interesting outcome that emerged from Equation 5.3 is that the obtained curve remains the same per every process considered, if the country and the fossil fuel are kept constant. In fact, the curve, given the nature of the equation, is only dependent on type of fossil fuel (that influences the emissions) and location (that influences the fuel price). This result is extremely important because once one curve is obtained, it can be valid for every other process with the mentioned constrains.

This means that the maps produced in QGIS for the aluminium process are also valid for the bricks and zinc production. In Appendix Figure 5 a graph showing the curves in different countries is reported. The cheaper the fuels in a location, the more the curve will be in the top-right area of the carbon tax-DNI plane. Therefore, the more difficult it is for CST to be competitive. Another graph was elaborated and reported in Appendix Figure 6 to analyse the effect of the fuel type. Two different countries using three types of fossil fuel are considered. If natural gas, heating oil and coal have similar prices within a country, the curves will be close to each other (see the case of Mexico, in the graph). On the contrary, if the prices differ a lot, the curves will be distant from each other (see the case of Egypt where natural gas is much cheaper than heating oil, which is itself much cheaper than coal).

In order to compare the two solar technologies on the same graph however, some changes are needed because there is no direct correlation of PV heat costs and DNI like for the concentrated solar technology. The parameter shared by both options is LCOH, and its relation to the carbon tax is linear as can be seen from Equation 5.4, which has been obtained by removing the dependency of DNI from Equation 5.3. For the PV case, LCOH is substituted by LCOE multiplied by 0.98.

$$Carbon\ Tax_{i,j,k} = \frac{\alpha \cdot \left(H_i \cdot LCOH - F_{i,j,k}\right)}{avoided\_emissions_i} \qquad \text{Equation 5.4}$$

Therefore, a carbon tax-LCOH representation has been established and the case for Australia is shown in Figure 5.8 where the LCOH value ranges for both solar technologies are highlighted and their distributions are reported to show that the values inside a price range are not homogenously spread, but rather asymmetrically and concentrated on cheaper values.

The main information that can be derived from the graph are:

- LCOH ranges and distributions of CST and PV are very similar, but the PV is shifted to the right meaning that overall, it is more expensive;
- CST can be the cheapest option if the carbon tax starts to be greater than 10 EUR/t and the asymmetrical distribution indicates that most of the locations have high DNI (resulting in low LCOH values);
- PV can be cheaper than fossil fuel only if the tax is very high (above 80 EUR/t) but CST performs better.

In Appendix Figure 7 the graphs of other countries are reported and once again, differences can be noticed due to the variability of fuel prices in the locations.

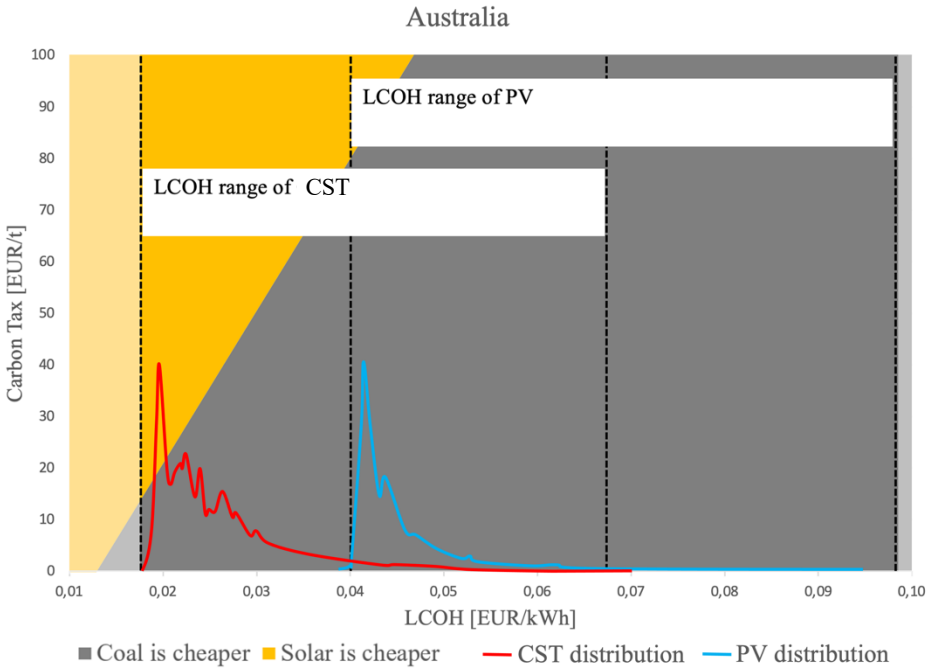

Figure 5.8: Carbon tax vs LCOH for Australia with the ranges reached by the two solar technologies and their distributions. Distributions are obtained through the *histogram visualization* tool in QGIS: they represent the distribution of cells having a certain cost value.

5.5. Sensitivity analysis

A sensitivity analysis has been done to assess the effects of an increase in the cost of CST technology and evaluate the extent to which it remains competitive. In particular, two additional groups of maps have been elaborated: one with a +25% of LCOH costs and the second with a +50% of LCOH costs, both with different carbon tax scenarios. The results are reported in Figure 5.9.

The main difference compared to the base scenario is that when the cost of CST increases, PV technology starts to be competitive, as it can be noted by the diffusion of yellow colour in the maps. In countries like Spain, Portugal, Brazil and Egypt, an increase of only 25% results in almost total disappearance of areas where CST is the cheapest option (in the base scenario the whole area was red (Figure 5.5)). In the +50% scenario the situation is even more pronounced. Considering the 100 EUR/t tax, CST is the best option only in few areas of Turkey, North of Chile, South West of USA and Australia.

In this instance, too, the circumstances in one country rely on its variables and, as it has been done for the base scenario, graphs have been elaborated to show for which couples of values of carbon tax and DNI the CST option is cheaper than fossil fuel. Figure 5.10 reports the case of South Africa where even in the base cost scenario, the solar technology needs high taxes and high DNI to be competitive. When the costs are increased by 25%, the availability range becomes smaller with DNI over 3000 kWh/m^2 and tax greater than 80 EUR/t. It should also be stressed, that the CST technology could be even cheaper than the base case assumption. This is supported by the fact, that the LCOH of the CentRec system is below the base case line, which was used as the reference for the sensitivity analysis (Figure 4.2).

In Appendix Figure 8 and Appendix Figure 9 the same type of graphs are reported for Spain and Mexico.

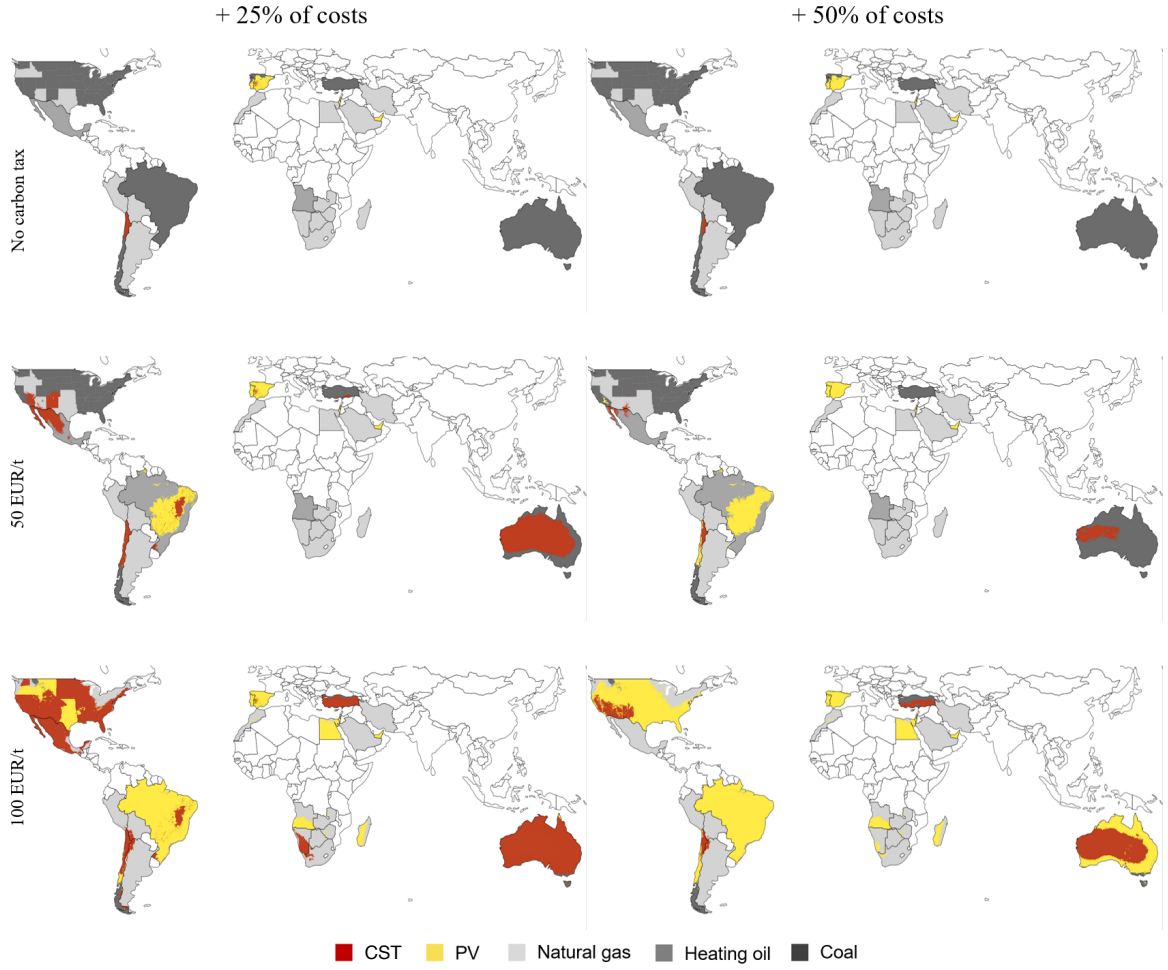

Figure 5.9: Sensitivity analysis on CST technology: on the left side maps with +25% increase of costs and on the right side with +50% increase, with three different carbon tax values.

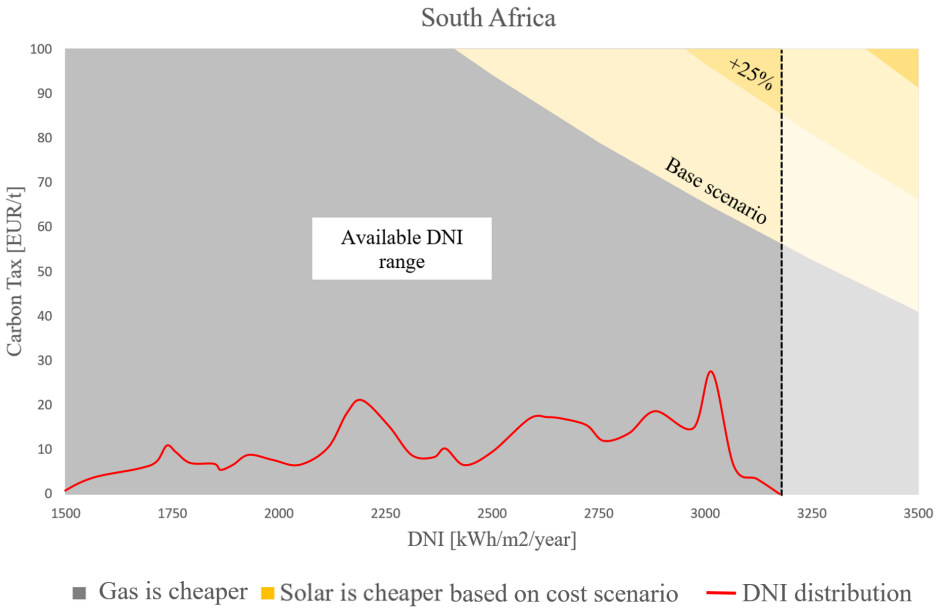

Figure 5.10: Carbon tax vs DNI graph of South Africa and its relative available DNI range and distribution. CST is cheaper in the yellow areas.

A final analysis that has been carried out, is how the comparison between CST and PV technologies is affected with an increase of costs. Figure 5.12 reports a carbon tax vs LCOH graph and the distribution of values obtained by both technologies: the more expensive CST becomes, the more on the right its distribution will be, until PV heat production becomes cheaper. When costs are 25% greater, photovoltaics is more convenient in most of the country (blue PV distribution is almost entirely on the left of CST distribution in +25% scenario).

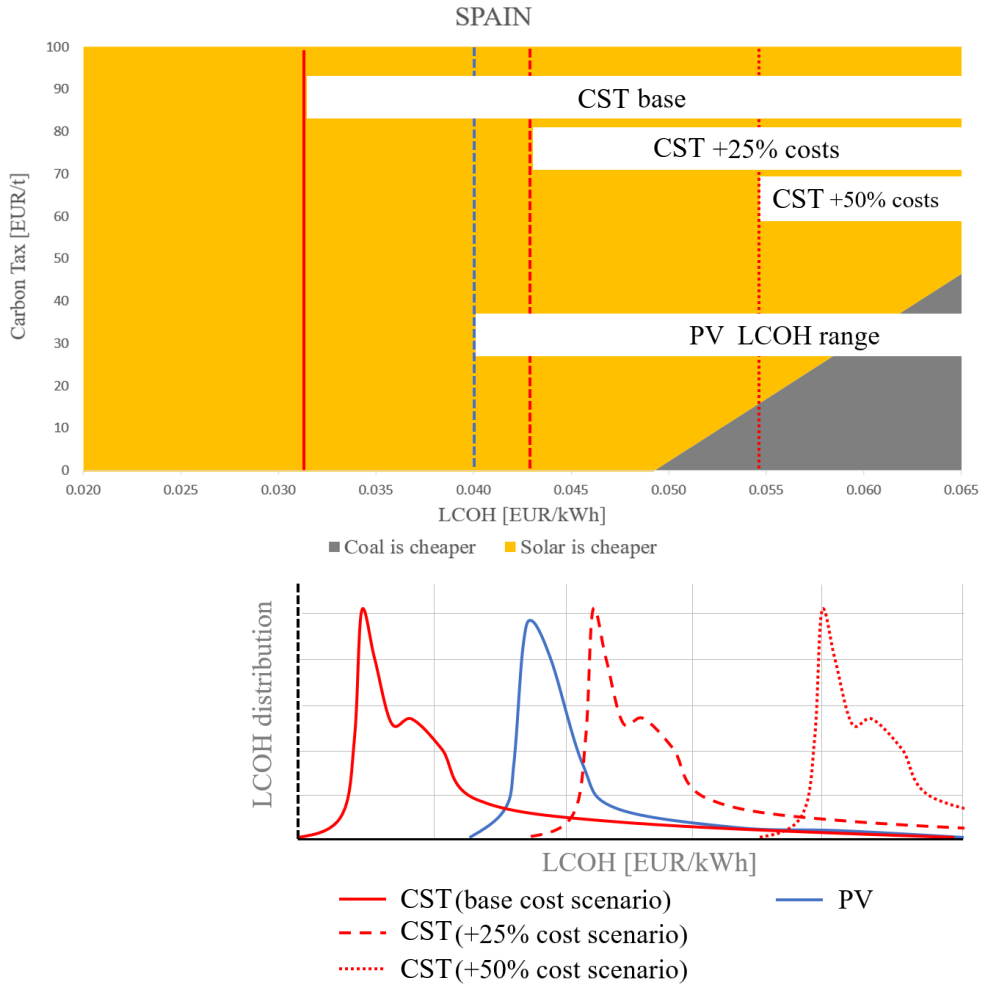

Figure 5.11: Comparison between CST and PV in Spain, in different cost scenarios for the CST technology. In the top part: a carbon tax vs LCOH graph where the values reached by both solar technologies are shown (three ranges for the CST based on the cost scenario). Below: LCOH distribution for PV and CST sources (three distributions for CST based on the cost scenario).

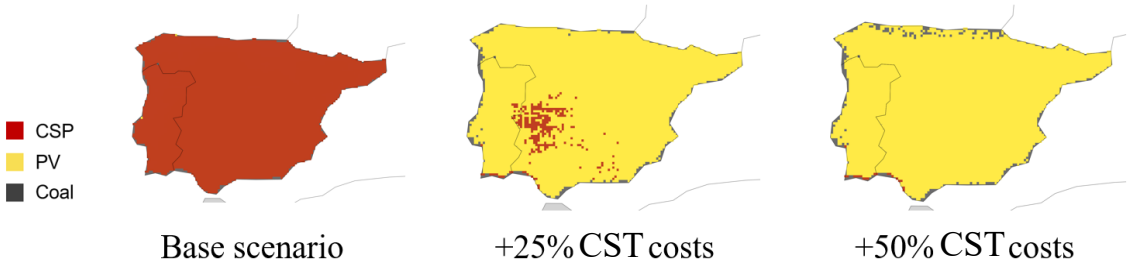

Figure 5.12: Maps showing the cheapest option in three cost scenarios.

6 Conclusion and future developments

Aluminium recycling, bricks and zinc production costs have been calculated in 24 countries that presented both high solar source and potential for these industries because of the presence of raw materials and existing facilities. The cheapest fossil fuel option, among natural gas, heating oil, and coal, of a certain location is compared with the production costs where the high temperature heat is provided by CST technology.

The LCOH values have been calculated as a function of DNI, obtained through an interpolation of literature data for existing plants.

A second renewable method for the provision of heat, through PV technology, is also compared throughout the countries. The influence of a carbon tax on the choice of the cheapest fuel option is extensively analysed, in particular with the changing values of DNI. Three maps have been elaborated for different tax values, namely 0, 50, and 100 EUR/t. Countries with high fuel prices showed the CST technology to be the best option even for very low carbon taxes, whilst for areas with cheaper fossil fuel, a high taxation on CO_2 is needed to make CST competitive. Despite the optimistic approach used to calculate the cost of heat provided by PV, this technology remained more expensive in most of the locations. Figure 6.1 summarizes the results in a map.

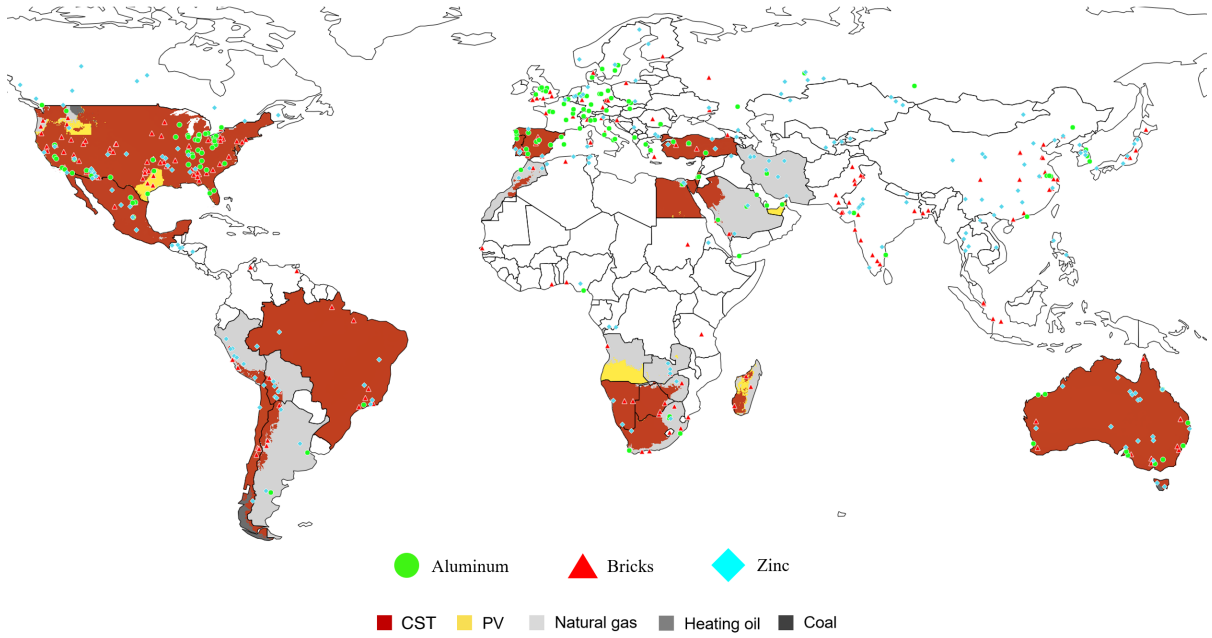

Figure 6.1: Cheapest option to provide heat in selected countries and main locations of the processes - base scenario for CST costs and carbon tax value equal to 100 EUR/t.

A sensitivity analysis on the LCOH from concentrated solar plants is done in order to investigate the effects in the different locations. In particular two new sets of maps have been elaborated: one with an increase of 25% of CST costs and one with a 50% increase, both with different carbon taxes. The overall outcome is that PV becomes more and more competitive and in the +50% case it dominates the map with only few areas with very high DNI maintaining the CST as cheapest option. Recent development shows however, that the cost of CST-heat could be even lower than what was assumed in the base case, caused by technologies such as particle-based receivers (CentRec).

The limitations of this study lay mainly on the LCOH approximation only based on DNI and the uncertainties related to fossil fuel prices. The latter have a big impact on the production costs and in particular in the comparison among the renewable sources of heat. Values are based on 2022 data, which was a peak year for most of commodity prices especially for energy in the Western countries. Possible future developments could be made in the direction of more accurate data both for CST technology and fuel prices around the world.

The operational hours have also not been considered in this study. The interaction of LCOH and operational hours would in fact vary with the solar resource, both for CST and PV technologies: this is considered as a task for future studies.

In conclusion, large amounts of CO_2 emitted by the industrial sector to provide heat can be avoided with the implementation of concentrated solar thermal technologies, which have proven to be competitive in several countries, especially when taxes on carbon emissions are raised, as it seems plausible by the international community.

References

[1] C. A. McMillan and M. Ruth, “Using facility-level emissions data to estimate the technical potential of alternative thermal sources to meet industrial heat demand,” *Applied Energy,* vol. 239, pp. 1077-1090, 2019.

[2] G. Thiel and A. Stark, “To decarbonize industry, we must decarbonize heat,” *Joule,* vol. 5, pp. 531-550, 2021.

[3] U. E. i. administration, “Annual Energy Outlook 2017,” Energy information administration, Washington, D.C., 2017.

[4] T. Naegler, “Quantification of the European industrial heat demand by branch and temperature level,” *International Journal of Energy Research,* 2015.

[5] M. Rehfeldt, T. Fleiter and F. Toro, “A bottom-up estimation of the heating and cooling demand in European industry,” *Energy efficiency,* vol. 11, pp. 1057-1082, 2018.

[6] Fernandez-Gonzalez et al., “Concentrated solar energy applications in materials science and metallurgy,” *Solar energy,* vol. 170, pp. 520-540, 2018.

[7] D. Fernandez-Gonzalez, “A state-of-the-art review on materials production and processing using solar energy,” *Mineral processing and extractive metallurgy review,* 2023.

[8] S. Wolf, “Resource-orientated overall view of material flows of metallic raw materials: the example of aluminium,” in *Lecture on the occasion of the 3A-Meeting on 19-06-1998*, Aachen, 1998.

[9] W. B. Frank, “Akuminum,” in *Ullmann´s Encyclopedia of Industrial Chemistry*, Wiley-VCH, 2009.

[10] “Aluminum,” Energy Education - University of Calgary, 2016. [Online]. Available: https://energyeducation.ca/encyclopedia/Aluminum. [Accessed July 2023].

[11] IAI - International Aluminium Institute, “Material flow analysis - A look at the numbers globally and in Asia,” 2023.

[12] J. Moya and A. Boulamati, “Energy efficiency and GHG emissions: prospective scenarios for the aluminium industry,” European Commission, JRC Scientific and Policy Reports, 2015.

[13] R. Quinkertz, G. Rombach and D. Liebig, “A scenario to optimise the energy demand of aluminium production depending on the recycling quota,” *Resources, Conservation and Recycling,* vol. 33, pp. 217-234, 2001.

[14] European Aluminium, “A strong, sustainable & complete European vale chain,” 2023. [Online]. Available: https://european-aluminium.eu/about-aluminium/aluminium-industry/. [Accessed July 2023].

[15] K. Funken, M. Roeb, P. Schwarzboelzl and H. Warnecke, “Aluminium remelting using directly solar-heated rotary kilns,” *Journal of Solar Energy Engineering (ASME),* vol. 123 (2), pp. 117-124, 2001.

[16] M. Roeb, M. Puttkamer, T. Beyer, J. P. Reinhold, C. Willsch, M. Thelen and et al., "Solares Recyceln von Aluminium in einem direckt bestrahlten Drehrofen," in *19. Kölner Sonnenkolloquium*, DLR - Cologne, Germany, 2016.

[17] P. Östborn and H. Gerding, "The diffusion of fired bricks in Hellenistic Europe: a similarity network analysis," *Journal of Archaeological Method and Theory,* vol. 22, pp. 306-344, 2015.

[18] C. Koroneos and A. Dompros, "Environmental assessment of brick production in Greece," *Building and Environment,* vol. 42, pp. 2114-2123, 2006.

[19] A. L. Murmu and A. Patel, "Towards sustainable bricks production: an overview," *Construction and Building Materials,* vol. 165, pp. 112-125, 2018.

[20] Mordor, "Brick market size & share analysis - growth trends & forecasts (2023 - 2028)," MordorIntelligence, 2023. [Online]. Available: https://www.mordorintelligence.com/industry-reports/brick-market. [Accessed August 2023].

[21] A. Vittoriosi and et al., "Monitoring of a MW class solar field set up in a brick manufacturing process," *Energy Procedia,* vol. 48, pp. 1217-1225, 2014.

[22] G. Villeda-Munoz and et al., "Clay-brick firing in a high temperature solar furnace," *Ingenieria Investigacion y Tecnologia,* vol. XII, pp. 395-408, 2011.

[23] S. Baily, "Properties and applications of Calcium (Ca)," AZO Materials, 2023. [Online]. Available: https://www.azom.com/article.aspx?ArticleID=9098. [Accessed July 2023].

[24] N. N. Greenwood and A. Earnshaw, in *Chemistry of the elements (2nd ed.)*, Butterworth-Heinemann, 1997, p. 198.

[25] T. Güthner and B. Mertschenk, "Cyanamides," in *Ullmann´s Encyclopedie of industrial chemistry*, Weinheim, Wiley-VCH Verlag GmbH & Co, 2012, pp. 645-667.

[26] Business Research , "Calcium cyanamide market size, share, growth and industry analysis by type," Businness Research Insights, October 2023. [Online]. Available: https://www.businessresearchinsights.com/market-reports/calcium-cyanamide-market-108577. [Accessed December 2023].

[27] G. Maduraiveeran and W. Jin, "Carbon nanomaterials: synthesis, properties and applications in electrochemical sensiors and energy conversion systems," *Materials Science and Engineering B,* vol. 272, 2021.

[28] M. Rahmati and M. Mozafari, "Biological response to carbon-family nanomaterials: interactions at the nano-bio interface," *Frontiers in Bioengineering and Biotechnology,* vol. 7, 2019.

[29] P. Bhatt and A. Goe, "Carbon fibres: production, properties and potential use," *Mat.Sci.Res.India,* 2017.

[30] Ellringmann et al., "Carbon fiber production costing: a modular approach," *Textile research journal,* vol. 86, no. 2, pp. 178-190, 2016.

[31] Energetics Incorporated, "Bandwidth study on energy use and potential energy savings opportunities in the manufacturing of lightweight materials: carbon fiber reinforced polymer composits," US Department of Energy, 2016.

[32] X. Hu, R. Zhang, Z. Wu and S. Xiong, "Concentrated Solar Induced Graphene," *ACS Omega,* vol. 7, pp. 27263-27271, 2022.

[33] L. Rodgers, “Climate change: the massive CO2 emitter you may not know about,” BBC News, 17 December 2018. [Online]. Available: https://www.bbc.com/news/science-environment-46455844. [Accessed July 2023].

[34] International Energy Agency, “Technology Roadmap - Low carbon transition in the cement industry: foldout,” IEA, 2023. [Online]. Available: https://www.iea.org/reports/cement-3. [Accessed December 2023].

[35] C. Shi and J. Qian, “High performance cementing materials from industrial slags - a review,” *Resources conservation & recycling,* vol. 29, pp. 195-207, 2000.

[36] J. G. J. e. a. Oliver, “Trends in global CO2 emissions - 2014 report,” PBL Publishers, The Hague, 2014.

[37] T. e. a. Czigler, “Laying the fundation for zero-carbon cement,” McKinsey & Company, 14 May 2020. [Online]. Available: https://www.mckinsey.com/industries/chemicals/our-insights/laying-the-foundation-for-zero-carbon-cement. [Accessed December 2023].

[38] G. Moumin, “Mineral treatment - CemSol,” DLR - Institute of Future Fuels, 2021. [Online]. Available: https://www.dlr.de/ff/en/desktopdefault.aspx/tabid-15591/29114_read-76597/. [Accessed December 2023].

[39] W. G. Davenport, M. King, M. Schlesinger and A. K. Biswas, Extractive metallurgy of Copper, Pergamon, 2002.

[40] R. R. Moskalyk and A. M. Alfantazi, “Review of copper pyrometallurgical practice: today and tomorrow,” *Minerals Engineering,* vol. 16, pp. 893-919, 2003.

[41] I. Cruz-Robles and et al., “Potential of solar central tower systems for thermal applications in the production chain of copper by pyrometallurgical route,” in *International Conference on Concentrating Solar Power and Chemical Energy Systems*, Santiago, Chile, 2018.

[42] Copper Alliance, “Copper recycling,” International Copper Association, 2021. [Online]. Available: https://copperalliance.org/resource/copper-recycling/. [Accessed July 2023].

[43] D. Streeter, “How is Copper Recycled,” Colling Recycling, July 2022. [Online]. Available: https://www.collinsrecycling.com.au/recycling-of-copper-how-its-done/. [Accessed July 2023].

[44] F. Gomez and et al., “Copper recycling and scrap availability,” *Resources Policy,* vol. 32, pp. 183-190, 2007.

[45] C. Samuelsson and B. Björkman, “Chapter 7 - Copper recycling,” in *Handbook of recycling*, Elsevier, 2014, p. 85.94.

[46] S. e. a. Moreno-Leiva, “Renewable energy in copper production: a review on systems design and methodological approaches,” DLR, Stuttgart, Germany, 2019.

[47] “Glass container recycling loop,” Glass packaging Institute, 2023. [Online]. Available: https://www.gpi.org/glass-recycling-facts. [Accessed August 2023].

[48] Global Market Inside, “Recycled Glass Market,” 2021. [Online]. Available: https://www.gminsights.com/industry-analysis/recycled-glass-market. [Accessed December 2023].

[49] “Glass producers and market studies,” Plants Glass Global, 2023. [Online]. Available: https://plants.glassglobal.com/login/. [Accessed July 2023].

[50] Ullmann´s Encyclopedia, Calcium Sulfate, Weinheim: Wiley-VCH Verlag GmbH & CO. KGaA, 2005.

[51] A. Augustyn, “Gypsum,” Britannica, December 2023. [Online]. Available: https://www.britannica.com/science/gypsum. [Accessed December 2023].

[52] Beidoou, “What is gypsum How gapsum is processed,” Beidoou, 2021. [Online]. Available: https://www.beidoou.com/materials/what-is-gypsum-how-is-gypsum-processed.html. [Accessed August 2023].

[53] M. e. a. Murariu, “Engineering Polypropylene - calcium sulfate (anhydrite II) composites,” *Polymers,* vol. 15, 2023.

[54] FLUORSID, “Bilancio di Sostenibilità 2021,” 2021.

[55] Fact.MR, “Anhydrite market growth accelerates,” GlobeNewswire, 02 May 2023. [Online]. Available: https://www.globenewswire.com/en/news-release/2023/05/02/2658887/0/en/Anhydrite-Market-Growth-Accelerates-at-a-4-1-CAGR-to-Reach-US-400-Billion-by-2033-Fact-MR-Report.html. [Accessed August 2023].

[56] Catalano at al., “An appraisal of the cradle-to-gate energy demand and carbon footprint of high-speed steel cutting tools,” *Procedia CIRP,* vol. 105, pp. 745-750, 2022.

[57] Mordor, “High speed steel market size & share analysis,” Moror Intelligence, 2023. [Online]. Available: https://www.mordorintelligence.com/industry-reports/high-speed-steel-market. [Accessed August 2023].

[58] Herranz et al., “Development of high speed steel sintered using concentrated solar energy,” *Journal of materials processing technology,* vol. 213, pp. 2065-2071, 2013.

[59] Garcia et al., “Effect of vanadium carbide on dry sliding wear behavior of powder metallurgy high speed steel processed by concentrated solar energy,” *Materials Characterization,* vol. 121, pp. 175-186, 2016.

[60] Fan et al., “Sustainable recycling technology for Li-Ion batteries and beyod: challenges and future prospects,” *Chemical reviews,* vol. 120, pp. 7020-7063, 2020.

[61] T. Junne, N. Wulff and T. Naegler, “Material demand in global energy scenarios, distribution of stocks and the role of recycling,” in *5th International conference on "Energy, Sustainability and Climate Change"*, DLR, 2018.

[62] American Iron and Steel Institute, “Steel Flowlines,” [Online]. Available: https://www.steel.org/steel-technology/steel-production/. [Accessed July 2023].

[63] C. Hoffmann, M. Van Hoey and B. Zeumer, “Decarbonization challenga for steel,” McKinsey & Company, 3 June 2020. [Online]. Available: https://www.mckinsey.com/industries/metals-and-mining/our-insights/decarbonization-challenge-for-steel. [Accessed July 2023].

[64] SSAB, “SSAB has launched an extensive research project in Finland to replace fossil fuels with renewable energy in steelmaking,” SSAB, 15 July 2021. [Online]. Available: https://www.ssab.com/en/news/2021/07/ssab-has-launched-an-extensive-research-project-in-finland-to-replace-fossil-fuels-with-renewable-en. [Accessed July 2023].

[65] The Essential Chemical Industry - Online, “Sulfuric Acid,” 9 October 2016. [Online]. Available: https://essentialchemicalindustry.org/chemicals/sulfuric-acid.html. [Accessed August 2023].

[66] H. Ogata and N. Tanaka, “Reduction of waste in semiconductor manufacturing plant (sulfuric acid recycling technology),” *Special Issue on Global Environment,* January 1998.

[67] Veoilia, “How sulfuric acid regeneration lowers refinery costs and environmental impact,” 26 Ausgust 2021. [Online]. Available:

https://blog.veolianorthamerica.com/how-sulfuric-acid-regeneration-lowers-refinery-costs-environmental-impact. [Accessed August 2023].

[68] Koltz, "Sulfuric acid waste recycling by regenerative process," United States Patent, 1998.

[69] United States Geological Survey, "Zinc: World Mine Production (zinc content of concentrate) by country," in *Minerals Yearbook: Zinc*, Washington, D.C., 2009.

[70] S. Srujan, "Mineral Commodity Summaries 2021: Zinc," United States Geological Survey, 2021.

[71] Nyrstar, "How is zinc produced?," 2023. [Online]. Available: https://www.nyrstar.com/products/zinc-zinc-alloys/how-is-zinc-produced. [Accessed August 2023].

[72] Qi et al., "Life cycle assessment of the hydrometallurgical zinc production chain in China," *Journal of Cleaner Production,* 2017.

[73] J. S. Roderick, The Extractive Metallurgy of Zinc, Carlton Victoria, Australia: The Australasian Institute of Mining and Metallurgy, 2005.

[74] D. Yadav and R. Banerjee, "Thermodynamic and economic analysis of the solar carbothermal and hydrometallurgy routes for zinc production," *Energy,* vol. 247, 2022.

[75] IRENA, "Renewable Capacity Statistics," The International Renewable Energy Agency, ABu Dhabi, 2022.

[76] K. Lovegrove and W. Stein, Concentrating solar power technology, Woodhead Publishing Limited, 2012.

[77] M. I. Khan, F. Asfand and S. Al-Ghamdi, "Progress in research and technological advancements of commercial concentrated solar thermal power plants," *Solar Energy,* vol. 249, pp. 183-226, 2023.

[78] IRENA, "Renewable Power Generation costs in 2022," Abu Dhabi, 2023.

[79] G. Moumin, "CSP/CSTE and its competitors," DLR, Group Meeting Carbon Management and Commodities, 2022.

[80] Pitz-Paal, "Status and Perspective of Concentrating Solar Tower Technologies. Center for Sustainable Systems, University of Michigan," *Photovoltaic Energy Factsheet,* 2021.

[81] Ong et al., "Land-use requirements for solar power plants in the United States," NREL - National Renewable Energy Laboratory, 2013.

[82] "Carbon Footprint of Heat Generation," *PostNote,* vol. 523, no. The Parliamentary Office of Science and Technology, p. 2, May 2016, London.

[83] Y. Gan and et al., "Greenhouse gas emissions embodied in the U.S. solar photovoltaic supply chain," *Environmental Research Letters,* vol. 18, 2023.

[84] C. Frantz, B. Reiner and A. Lars, "Design and cost study of improved scaled-up centrifugal perticle receiver based on simulation," in *14th International Conference on Energy Sustainability*, Denver, USA, German Aerospace Center (DLR) 2020.

[85] Pitz-Paal, "2nd Mena Emergy Meeting," 2021.

[86] R. Buck and M. Puttkamer, "Opportunities of applying concentrating solar solutions for process heat of up to 1000°C in South Africa," DLR - Institute of Solar Research, 2020.

[87] World Bank Group, ESMAP and SolarGis, "Global Solar Atlas," Energydata.info, 2023. [Online]. Available: https://globalsolaratlas.info/map?c=11.350797,8.613281,3. [Accessed October 2023].

[88] "World Population Review," [Online]. Available: https://worldpopulationreview.com/about. [Accessed 10 October 2023].

[89] V. Quaschning and B. Siegel, "Specific carbon dioxide emissions of various fuels," volker-quaschning.de, 2022.

[90] S. O. Alexopoulos, "Simulation of solar-heated rotary tube reactor for the remelting of aluminium," DLR, Cologne-Porz, Germany, 2003.

[91] M. Roeb, "Design and economic feasibility study of large-scale plant for solar aluminum recycling," DLR, Cologne-Porz, 2000.

[92] L. Deng, J. Sydney and G. Emre, "Environmental-techno-economic analysis of decarbonization strategies for the Indian aluminium industry," *Elsevier,* vol. Energy Conversion and Management, 2022.

[93] I. Dudman, "Fastmaket, European aluminium scrap and secondary prices," 7 January 2022. [Online]. Available: https://www.fastmarkets.com/insights/european-aluminium-scrap-and-secondary-prices-to-be-supported-participants-say-2022-preview/ . [Accessed October 2023].

[94] "Scrap Monster, Aluminium scrap prices," Scrap Monster, 2023. [Online]. Available: https://www.scrapmonster.com/scrap-prices/category/Aluminum-Scrap/116/1/1. [Accessed October 2023].

[95] I. Yüksek, S. K. Öztas and G. Tahtali, "The evaluation of fired clay brick production in terms of energy efficiency: a case study in Turkey," *Energy Efficincy,* 2020.

[96] S. Maithel and U. Heierli, "Brick by brick: the Herculean task of cleaning up the Asian brick industry," *Natural Resources and Environment Division (first ed.),* 2008.

[97] N. Youssef, Z. Lafhaj and C. Chapiseau, "Economic analysis of geopolymer brick manufacturing: a french case study," *Sustainability,* 2020.

[98] Linesight, "Country Commodity Reports," 2022.

[99] C. E. R. S.r.l., "Unipersonale," 2023. [Online]. Available: https://www.prezziariocer.it/. [Accessed November 2023].

[100] HomeAdvisor, "What are the typical brick prices?," August 2022. [Online]. Available: https://www.homeadvisor.com/cost/siding/brick-prices/. [Accessed November 2023].

[101] P. Turgut, "Manufacturing of building brick without Portland cement," *Journal of cleaner production,* vol. 37, pp. 361-367, 2012.

[102] I. Z. Association, "International Zinc Association 2022 to focus on zinc smelters´s outpu cuts," Fastmarkets, 2022. [Online]. Available: https://www.fastmarkets.com/insights/international-zinc-association-2022-to-focus-on-zinc-smelters-output-cuts/. [Accessed October 2023].

[103] A. Boulamanti and J. A. Moya, "Production costs of the non-ferrous metals in the EU and other countries: Copper and zinc," *Elsevier,* vol. 49, pp. 112-118, 2016.

[104] J. Dersch, "LCOE reduction potential of parabolic trough and solar tower technology in G20 countries until 2030," AIP Publishing, DLR, Köln, Germany, 2020.

[105] Australia Solar Thermal Research Institute (ASTRI), "Public dissemination report 2021," 2021.

[106] F. Cortes, "Techno-economical evaluation of parabolic trough collectors systems for steam processes in the Chilean industry," AIP Conference Proceedings, 2018.

[107] P. Kurup and C. Turchi, “Initial investigation into the potential of CSP industrial process heat for the Southwest United States,” NREL National Renewable Energy Laboratory, 2015.

[108] P. Kurup, C. Turchi and G. Zhu, “Solar process heat potential in California, USA,” ISES International Solar Energy Society, Palma de Mallorca (Spain), 2016.

[109] A. Mouaky, A. A. Merrouni, N. E. Laadel and E. G. Bennouna, “Simulation and experimental validation of parabolic trough plant for solar thermal applications under the semi-arid climate condistions,” *Solar Energy,* 2019.

[110] H. A. L. Ouali, S. Touili, A. M. Alami and I. Moukhtar, “Artificial neural Network-Based LCOH estimation for concentrated solar power plants for industrial process heating applications,” *Applied Thermal Engineering,* 2023.

[111] B. C. Riggs, R. Biedenharn, C. Dougher, Y. V. Ji, Q. Xu, V. Romanin, D. S. Codd, J. M. Zahler and E. D. Matthew, “Techno-economic analysis of hyvrid PV/T systems for process heat using electricity to subsidize the cost of heat,” *Applied Energy,* 2017.

[112] S. Akkaya and U. Bakkal, “Carbon leakage along with the green paradox against carbon abatement? A review based on carbon tax,” *Folia Oeconomica Steninensia,* vol. 20, no. 1, pp. 25-44, 2020.

[113] Clark Center Economic Experts Panel Methodology, “Climate change policies,” ChicagoBooth, 13 November 2018. [Online]. Available: https://www.kentclarkcenter.org/surveys/climate-change-policies/. [Accessed December 2023].

[114] World Bank, “What is Carbon pricing?,” 2023. [Online]. Available: https://www.worldbank.org/en/programs/pricing-carbon. [Accessed December 2023].

[115] World Bank Group, “State and Trends of Carbon Pricing 2023,” WorldBank.org, Washington, 2023.

[116] Knoema, “International Carbon Tax: who will pay for the EU´s Green future?,” Knomea, 29 July 2021. [Online]. Available: https://knoema.de/infographics/pgtukpc/international-carbon-tax-who-will-pay-for-the-eu-s-green-future. [Accessed December 2023].

[117] O. Edenhofer, R. Pichs-Madruga, Y. Sokona, K. Seyboth, P. Matschoss, S. Kadner, T. Zwickel, P. Eickemeier and G. Hansen, “IPCC, 2011: Summary for Policymakers. In: IPCC Special Report on Renewable Energy Sources and Climate Change Mitigation,” Cambridge University Press, Cambridge, United Kingdom and New York, NY, USA, 2011.

[118] T. Oltmann, Techno-economic comparison of different path for solar generation of process heat at a temperature level of 130°C, Aachen, 2022.

[119] Global Solar Atlas, World Map Group and ESMAP, “Global Photovoltaic Power Potential by Country,” 2020. [Online]. Available: https://globalsolaratlas.info/global-pv-potential-study. [Accessed November 2023].

[120] Nicolas Youssef, Zoubeir Lafhaj, Christophe Chapiseau, “Economic analysis of geopolymer brick manufacturing: a French case study,” *Sustainability,* 9 September 2020.

[121] V. Quasching, Regenerative Energiesysteme, München: Hanser, 2015.

A Appendix A

A.1. Supplementary tables

In this section the tables are reported that have been created during the analysis with data coming from own calculations and data from literature containing valuable information.

Appendix Table 1: Extraction of dataset with industry locations around the world (27 points out of 577).

CODE	PROCESS	COMPANY	COUNTRY	REGION	LAT	LONG
BR01	BR	ACME	USA	Alabama	33.5	-86.8
BR02	BR	ACME	USA	Alabama	32.4	-86.3
BR03	BR	ACME	USA	Arkansas	35.5	-93.5
BR04	BR	ACME	USA	Arkansas	35.4	-94.4
BR05	BR	ACME	USA	Arkansas	35.8	-90.7
BR06	BR	ACME	USA	Arkansas	34.4	-92.8
BR07	BR	ACME	USA	Oklahoma	35.5	-97.5
BR08	BR	ACME	USA	Oklahoma	36.2	-96.0
BR09	BR	ACME	USA	Texas	33.2	-97.1
AL01	AL	Real Alloy	USA	Illinois	41.5	-87.6
AL02	AL	Real Alloy	USA	Michigan	41.9	-85.0
AL03	AL	Real Alloy	USA	Michigan	41.9	-85.0
AL04	AL	Real Alloy	USA	West Virginia	39.5	-81.1
AL05	AL	Real Alloy	USA	Tennessee	35.7	-84.3
AL06	AL	Real Alloy	USA	Ohio	41.3	-81.5
AL07	AL	Real Alloy	CANADA	Mississauga	43.7	-79.7
AL08	AL	Real Alloy	MEXICO	Frontera	26.9	-101.5
AL09	AL	Real Alloy	USA	Kentucky	37.2	-86.7
ZN01	ZN	ALZINC	ALGERIA	Tlemcen	34.9	-1.3
ZN02	ZN	Teck	PERU	Antamina	-9.4	-77.0
ZN03	ZN	Teck	CANADA	Trail	50.6	-124.2
ZN04	ZN	Teck	USA	Alaska	68.3	-153.1
ZN05	ZN	HudBay	CANADA	Snow Lake	54.8	-100.0
ZN06	ZN	Nevsun	ERITREA	Bisha	16.0	37.6
ZN07	ZN	South32	USA	Arizona	31.5	-110.7
ZN08	ZN	South32	AUSTRALIA	Cannington	-21.9	140.9
ZN09	ZN	Norzinc	CANADA	Praire	58.4	-113.3

ACME: ACME brick.com
Real Alloy: Realalloy.com
ALZINC: Spa-alzinc.dz
Teck: Teck.com
HudBay: Hudbayminerals.com
Nevsun: Zijinmining.com
South32: South32.net
Norzinc: Norzinc.com

Appendix Table 2: Energy prices in the countries in 2022. When a certain price was not found, it was used the one of a similar/close country indicated with a letter (the legend is reported below).

Country	**Electricity**		**Natural gas**		**Heating oil**		**Coal**		**Diesel**	
-	EUR/kWh		EUR/kWh		EUR/kWh		EUR/kWh		EUR/l	
Angola	0,011	[1]	0,014	[1]	0,008	[1]	0,029	(SA)	0,154	[1]
Argentina	0,038	[1]	0,012	[1]	0,040	[1]	0,033	(C)	0,946	[1]
Australia	0,249	[1]	0,089	[1]	0,074	[1]	0,023	[2]	1,175	[1]
Bolivia	0,050	[1]	0,011	[1]	0,015	[1]	0,033	(C)	0,510	[1]
Botswana	0,100	[1]	0,014	(A)	0,034	(Z)	0,029	(SA)	1,219	[1]
Brazil	0,132	[1]	0,126	[1]	0,037	[1]	0,034	[3]	1,151	[1]
Chile	0,118	[1]	0,050	[1]	0,068	[1]	0,033	[3]	1,094	[1]
Egypt	0,035	[1]	0,017	[1]	0,022	[1]	0,029	(SA)	0,252	[1]
Iran	0,002	[1]	0,000	[1]	0,001	[1]	0,028	(T)	0,005	[1]
Israel	0,149	[1]	0,120	[1]	0,130	[1]	0,049	(EU)	1,589	[1]
Madagascar	0,093	[1]	0,014	(A)	0,034	(Z)	0,029	(SA)	1,025	[1]
Mexico	0,189	[1]	0,034	[1]	0,029	[1]	0,029	[3]	1,255	[1]
Morocco	0,099	[1]	0,013	[1]	0,022	(E)	0,029	(SA)	1,287	[1]
Namibia	0,100	(B)	0,014	(A)	0,034	(Z)	0,029	(SA)	1,162	[1]
Peru	0,161	[1]	0,013	[1]	0,051	[1]	0,033	(C)	1,068	[1]
Portugal	0,128	[1]	0,159	[1]	0,179	[1]	0,049	[4]	1,706	[1]
Saudi Arabia	0,065	[1]	0,012	[1]	0,020	[1]	0,028	(T)	0,189	[1]
South Africa	0,067	[1]	0,012	[1]	0,057	[1]	0,029	[5]	1,332	[1]
Spain	0,140	[1]	0,127	[1]	0,119	[1]	0,049	[4]	1,626	[1]
Tanzania	0,090	[1]	0,014	(A)	0,034	(Z)	0,029	(SA)	1,200	[1]
Turkey	0,143	[1]	0,043	[1]	0,098	[1]	0,028	[3]	1,270	[1]
UAE	0,104	[1]	0,076	[1]	0,020	[1]	0,028	(T)	0,881	[1]
USA	0,092	[1]	0,040	[1]	0,075	[1]	0,026	[6]	1,113	[1]
Zambia	0,037	[1]	0,014	(A)	0,034	[1]	0,029	(SA)	1,287	[1]
Zimbabwe	0,014	[1]	0,014	(A)	0,034	(Z)	0,029	(SA)	1,693	[1]

[1]: GlobalPetrol (https://it.globalpetrolprices.com)
[2]: Energy Council (https://www.energycouncil.com.au/analysis/high-prices-cured-high-prices/)
[3]: Medium (https://medium.com/intratec-products-blog/coal-price-turkey-q1-2023-d102f1294bcb)
[4]: IEA Coal Market update July 2023 (https://iea.blob.core.windows.net/assets/6d364082-35fc-49cf-bf3e-c06a05a3445d/CoalMarketUpdate_July2023.pdf)
[5]: Reuters (https://www.reuters.com/world/africa/safricas-exxaro-resources-annual-profit-surges-hot-coal-prices-2023-03-16/)
[6]: IEA Coal 2023 Analysis and forecast (https://iea.blob.core.windows.net/assets/a72a7ffa-c5f2-4ed8-a2bf-eb035931d95c/Coal_2023.pdf)

(A): Angola
(B): Botswana
(C): Chile
(E): Egypt
(EU): Europe
(SA): South Africa
(T): Turkey
(Z): Zambia

Appendix Table 3: Raw materials prices in countries in 2022.

Country	**Aluminium scrap**	**1000 bricks**	**Zinc raw material**
-	EUR/t	EUR	EUR/t
Angola	900	100	121
Argentina	1000	404	121
Australia	1100	983	187
Bolivia	900	404	121
Botswana	900	100	121
Brazil	900	404	121
Chile	1000	404	121
Egypt	900	100	121
Iran	900	100	121
Israel	1100	830	280
Madagascar	900	100	121
Mexico	1000	404	121
Morocco	900	404	121
Namibia	900	100	121
Peru	900	404	121
Portugal	1100	850	280
Saudi Arabia	900	404	121
South Africa	1000	404	121
Spain	1100	850	280
Tanzania	900	100	121
Turkey	900	404	121
UAE	900	450	121
USA	1100	778	187
Zambia	900	100	121
Zimbabwe	900	100	121

Aluminium scrap: Fastmarkets [93], Scrapmonster [94]
1000 bricks: Linesight Global Country Commodity Reports Q4 2022 [98]
Zinc raw material: International Zinc Association

Appendix Table 4: US states energy prices 2022.

Country	**Electricity**	**Natural gas**	**Heating oil**	**Coal**	**Diesel**
-	EUR/kWh	EUR/kWh	EUR/kWh	EUR/kWh	EUR/l
Arizona	0,091	0,025	0,070	0,026	1,061
Arkansas	0,083	0,035	0,065	0,026	1,113
California	0,192	0,045	0,060	0,020	1,307
Colorado	0,096	0,033	0,060	0,026	1,008
Idaho	0,076	0,017	0,070	0,026	1,061
Kansas	0,089	0,028	0,055	0,026	1,113
Montana	0,086	0,030	0,065	0,013	1,113
Nevada	0,102	0,027	0,070	0,024	1,113
New Mexico	0,066	0,032	0,050	0,026	1,061
Oklahoma	0,080	0,024	0,060	0,024	1,113
Oregon	0,068	0,021	0,075	0,026	1,113
Texas	0,076	0,022	0,050	0,023	0,921
Utah	0,070	0,026	0,065	0,013	1,061
Wyoming	0,071	0,028	0,065	0,013	1,113

Source EIA U.S. Energy Information Administration
https://www.eia.gov/electricity/monthly/epm_table_grapher.php?t=epmt_5_6_a
https://www.eia.gov/dnav/ng/NG_PRI_SUM_A_EPG0_PIN_DMCF_A.htm
https://www.eia.gov/todayinenergy/prices.php

Appendix Table 5: Direct operating costs for a 100000 t/a zinc plant ([73]).

	Personnel	**Labour cost**	**Maintenance materials**	**Electricity**	**Fuel**	**Materials and supply**	**SUM**	
Plant section	USD/t	USD/t	USD/t	USD/t	USD/t	USD/t	USD/t	
Concentrate handling	8	4.00	1.20	0.40	0.45	0.80	6.85	1.5%
Roasting	35	17.50	5.40	4.40	1.20	3.50	32.00	7.0%
Acid plant	25	12.50	6.00	8.00		1.00	27.50	6.0%
Leaching / iron separation	45	22.50	6.00	4.00	0.60	7.50	40.60	8.9%
Purification	30	15.00	4.00	1.20		2.75	22.95	5.0%
Cadmium production	12	6.00	0.80	0.60	0.01	0.60	8.01	1.8%
Gypsum removal		0.00	1.00	1.20		0.10	2.30	0.5%
Electrolysis	60	30.00	11.60	132.00		12.00	185.60	40.7%
Melting and casting	50	25.00	3.60	6.00	0.45	6.00	41.05	9.0%
Effluent treatment	10	5.00	0.80	0.80		1.80	8.40	1.8%
Residue disposal	10	5.00	1.20	0.40		2.00	8.60	1.9%
Administration	60	45.00	1.25	0.40		25.00	71.65	15.7%
TOT	**345**	**187.50**	**42.85**	**159.40**	**2.71**	**63.05**	**455.51**	
		41.2%	9.4%	35.0%	0.6%	13.8%	100%	

A.2. Supplementary figures

In this section are reported additional figures, maps and graphs that have being used as source of information or have been created during the calculations. In the caption the source is given, if not present it means it is an image created by the author.

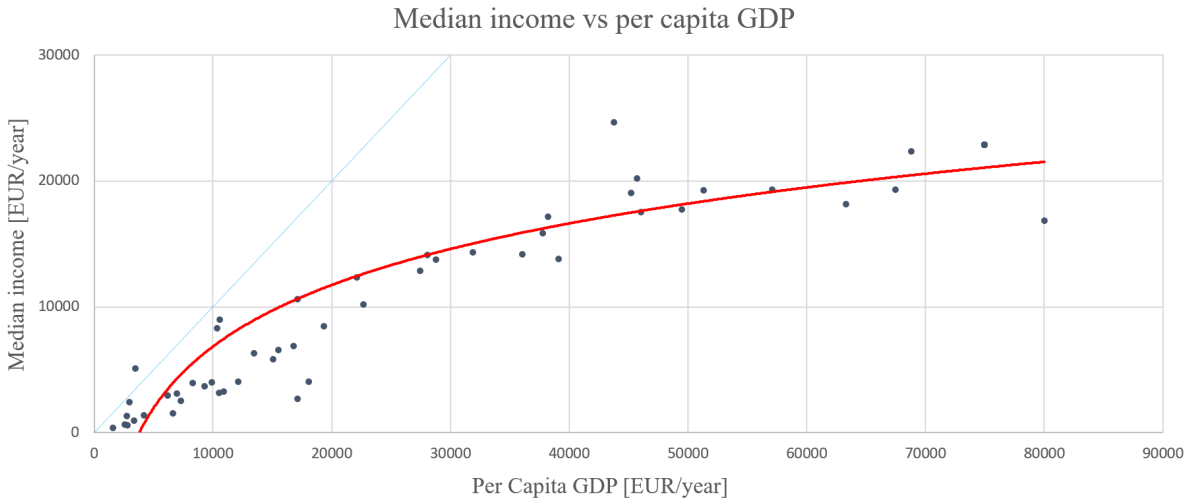

Appendix Figure 1: Non-linear relationship between per capita GDP and median income in some countries around the world (data from *World Population Review* [88]).

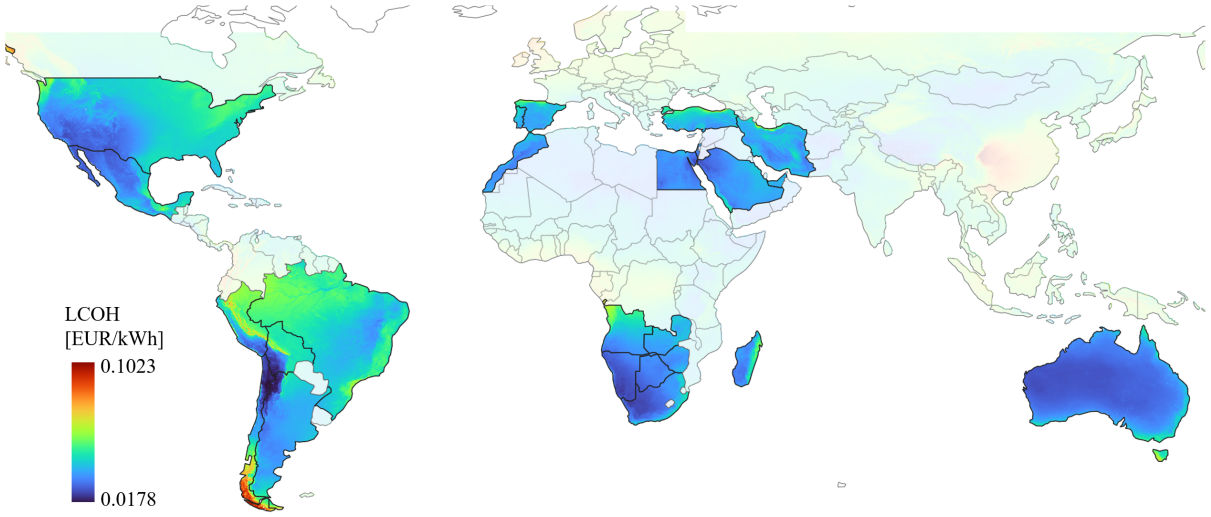

Appendix Figure 2: World LCOH map with the countries analysed in the thesis being highlighted.

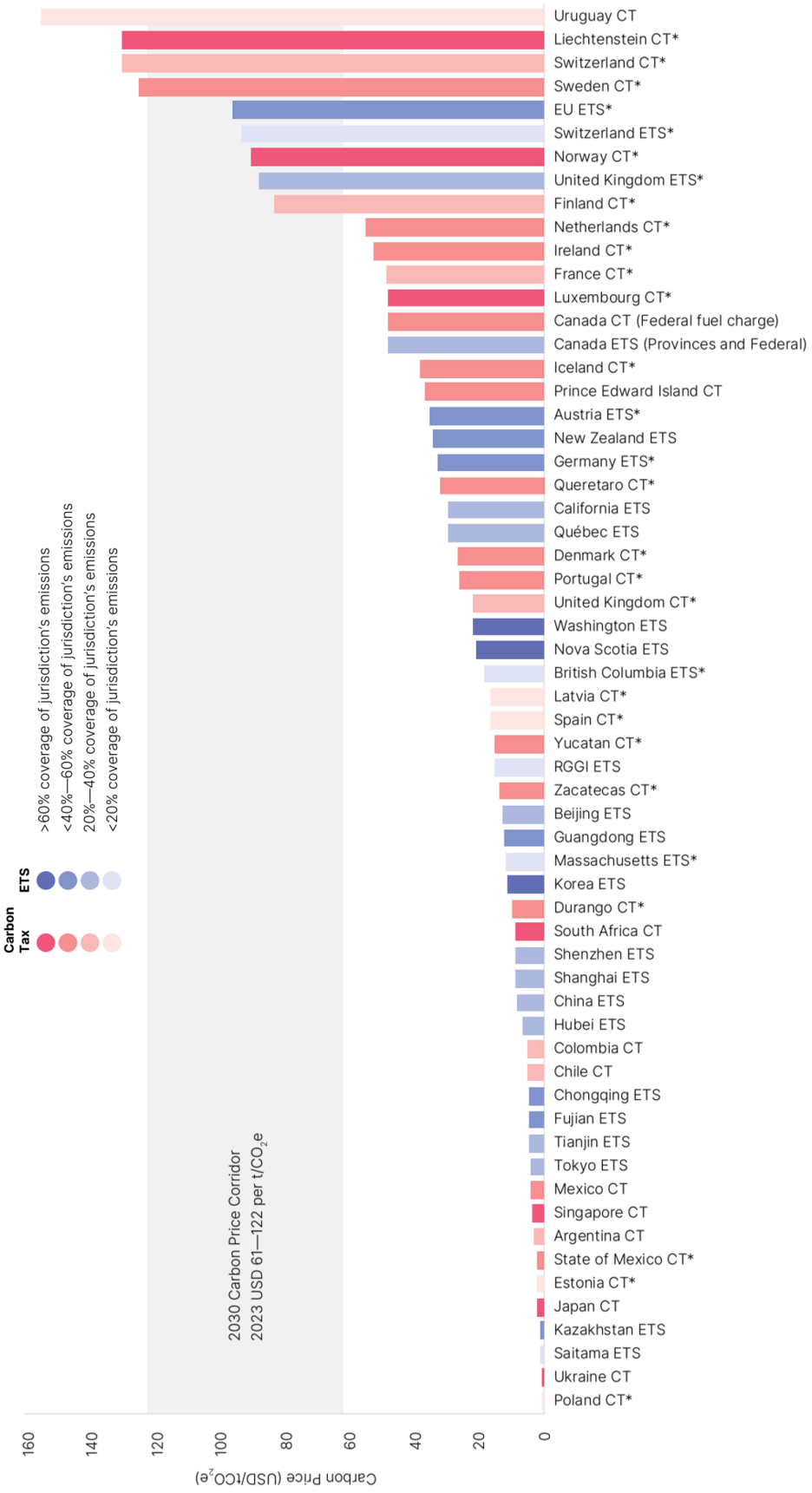

Appendix Figure 3: Prices and coverage across ETs and Carbon taxes (World Bank [115]).

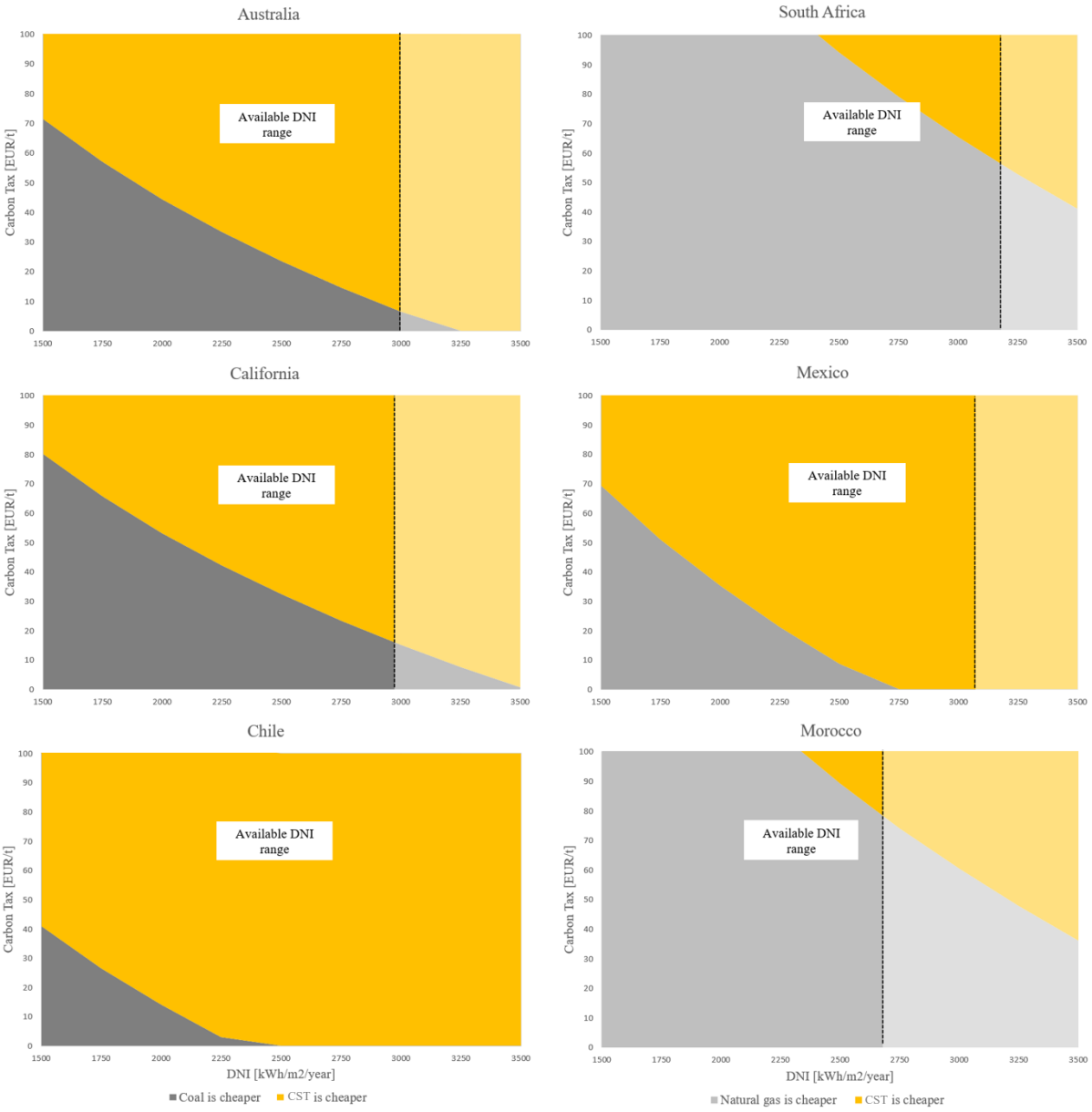

Appendix Figure 4: Carbon Tax vs DNI graphs of six different countries and regions with their relative available DNI range.

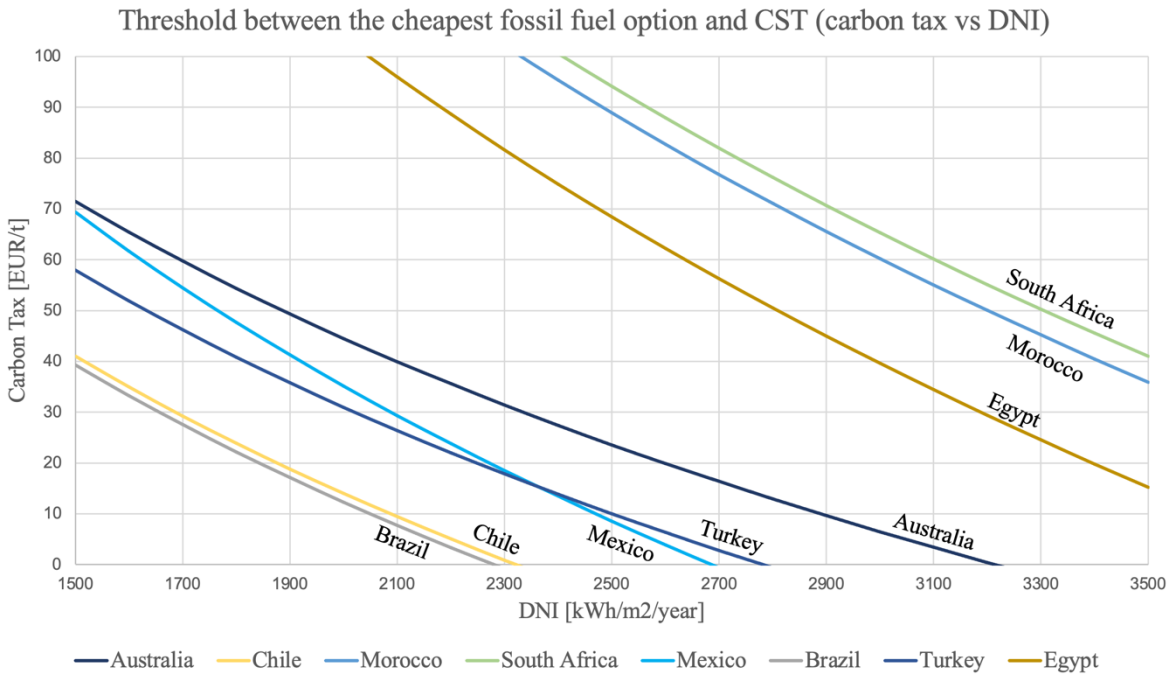

Appendix Figure 5: Carbon Tax vs DNI in eight different countries (calculations made with the cheapest fossil fuel relative of the location). Considering a country, above the line there are the couples of DNI and CO_2 values that permit the CST to be cheaper than fossil fuel.

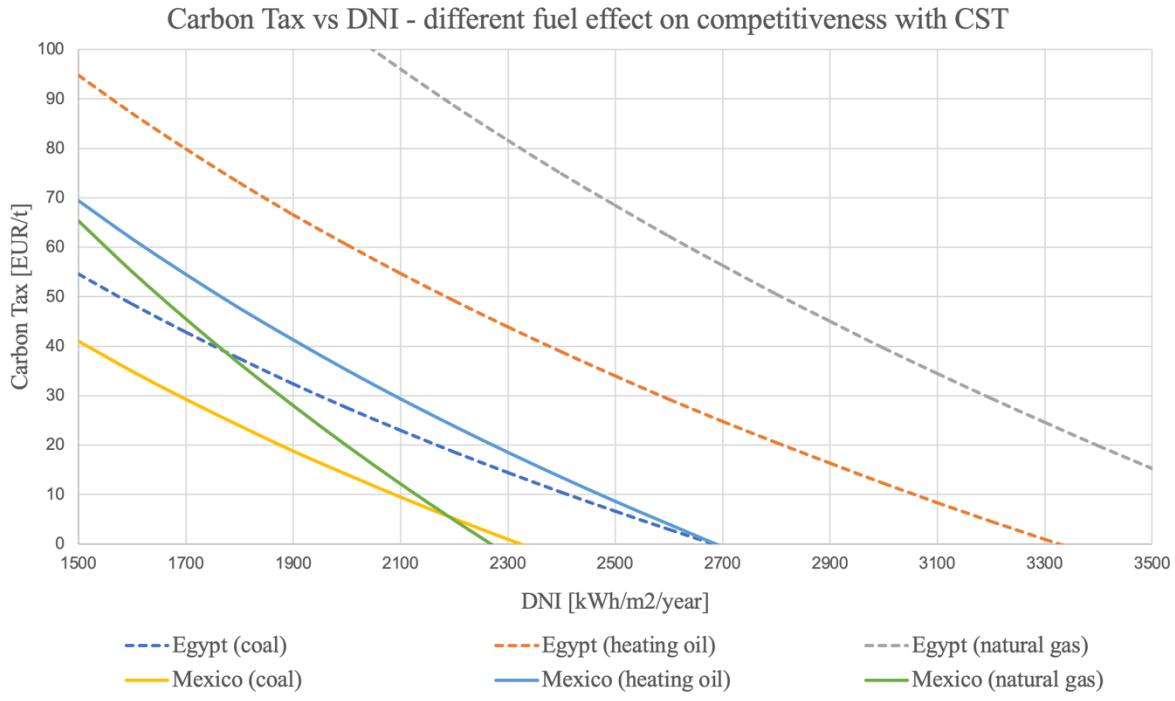

Appendix Figure 6: Carbon Tax vs DNI in two different countries with fuel type options. Again, above a certain line corresponding to a country and a fossil fuel used, CST option is the cheapest option.

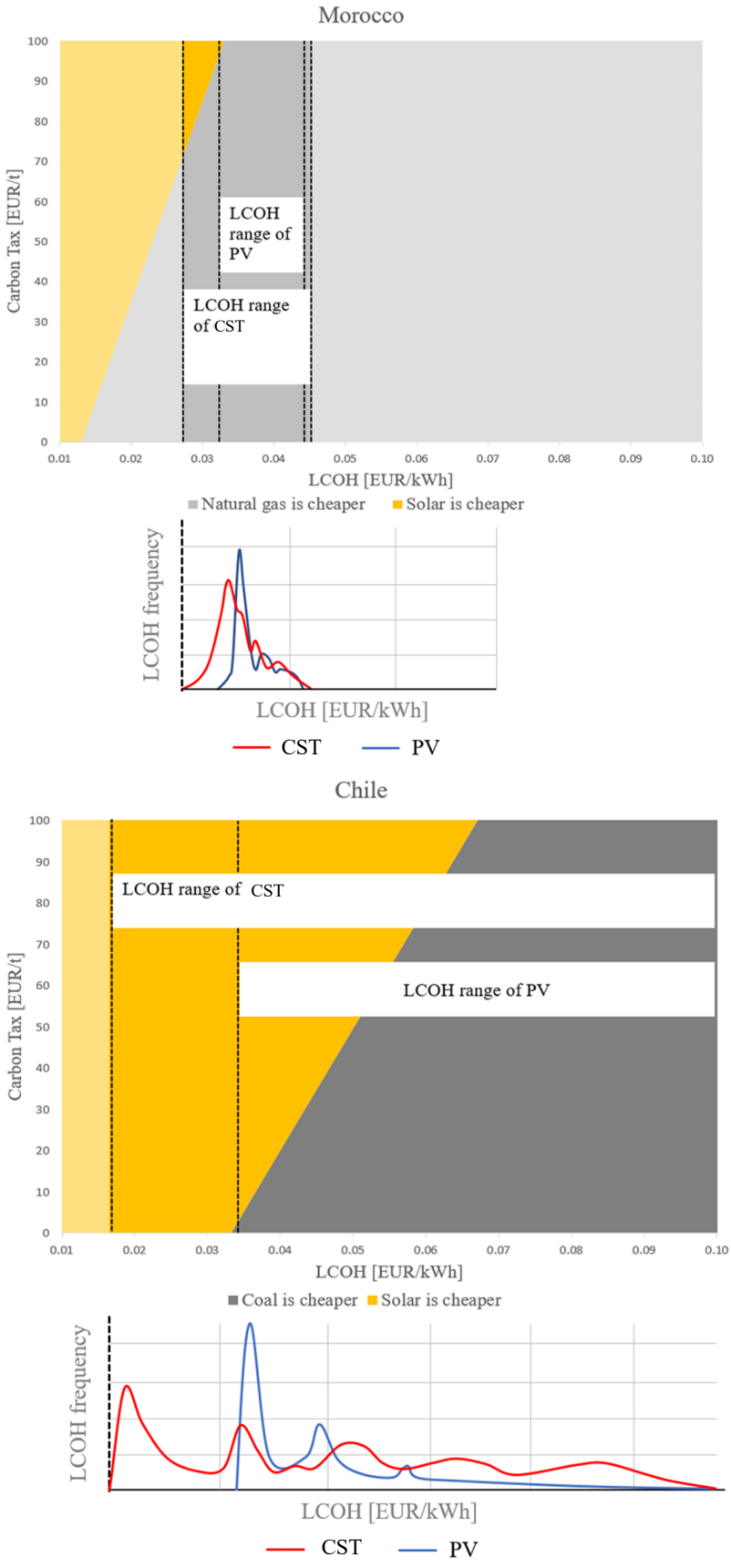

Appendix Figure 7: Carbon tax vs LCOH graph of two countries with the ranges reached by the two solar technologies and their distributions.

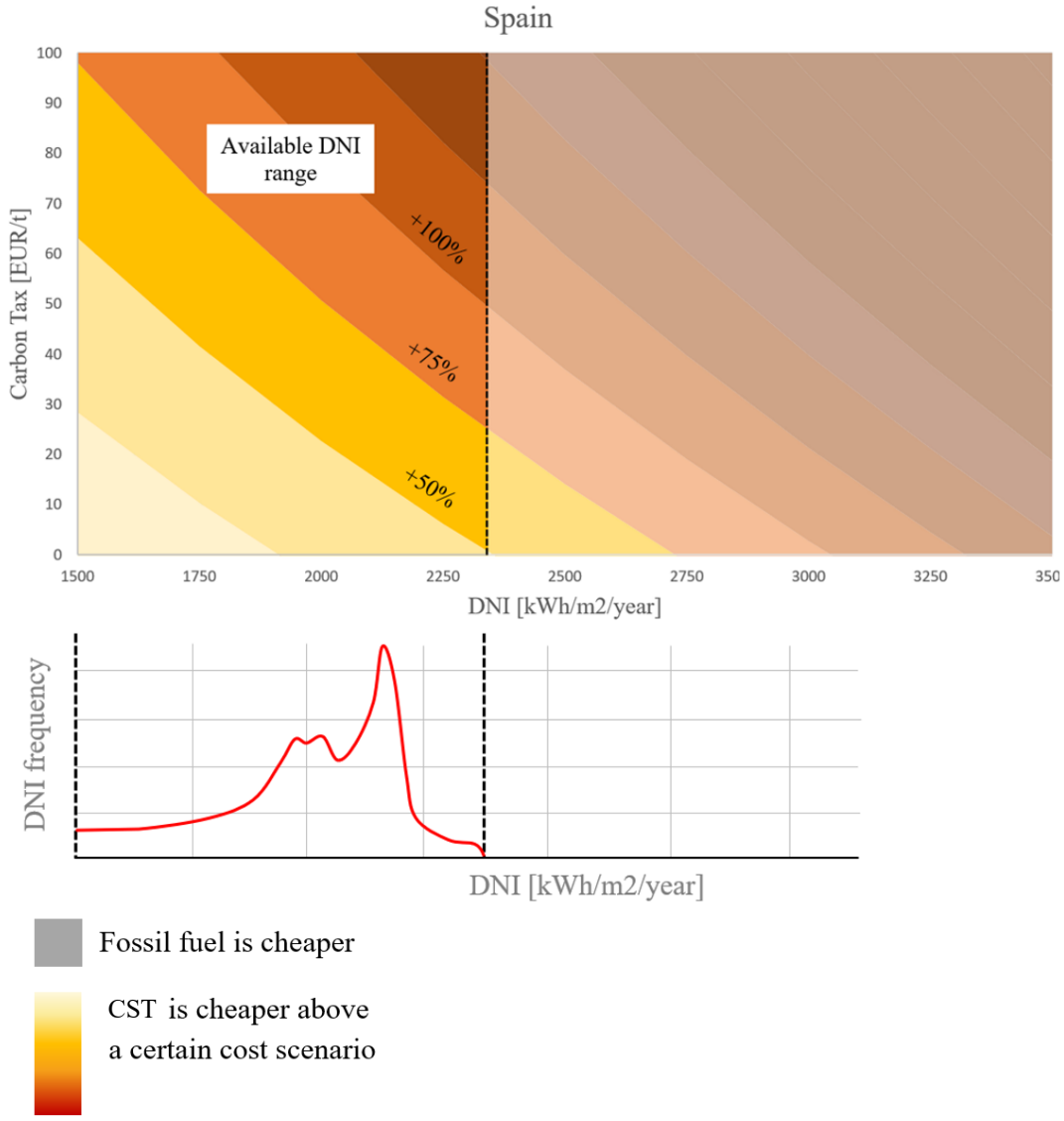

Appendix Figure 8: Carbon tax vs DNI graph of Spain and its relative available DNI range and distribution. CST is cheaper in yellow-red areas based on its costs.

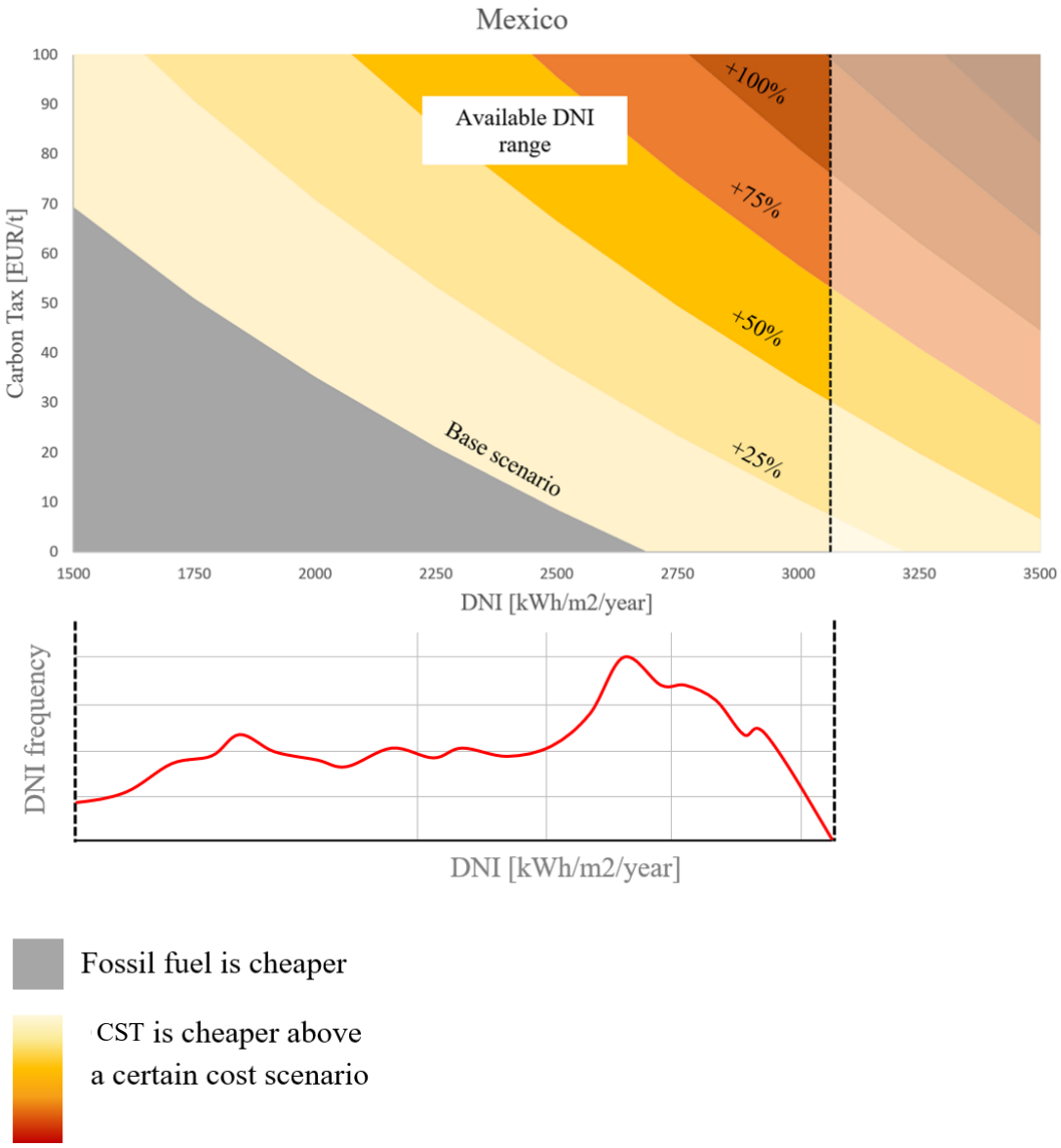

Appendix Figure 9: Carbon tax vs DNI graph of Mexico and its relative available DNI range and distribution. CST is cheaper in yellow-red areas based on its costs.

List of Figures

Figure 1.1: Total final energy consumption world-wide in 2015 (EPP 2017). 3
Figure 1.2: Schematic drawing based on the system designed by Munoz (2011). 7
Figure 2.1: Configuration of the four CST technologies: (1) Parabolic Trough, (2) Solar Tower (3) Parabolic dish and (4) Linear Fresnel. In black the physical components (mirrors, tower), in blue the receiver, and in yellow solar radiation. 23
Figure 2.2: Basic concept of CentRec receiver (Frantz et al., 2020 [83]). 25
Figure 3.1: World map showing areas with DNI over 2000 kWh/m^2 and the main locations for the three industrial processes. 27
Figure 3.3: Cost breakdown of Western refineries of secondary aluminium (Moya, 2022 [12]). 30
Figure 4.1: LCOE and DNI resource of different plants with potential law fit curves (Dersch et al.) 38
Figure 4.2: Graph with literature data and interpolation line. Different technologies are highlighted (Solar Towers in blue circle and Parabolic Trough in red squares) and the plant studied by Frantz et al. is the yellow circle (not included in the interpolation). 40
Figure 5.1: Production costs increase with carbon tax in the three processes (Mexico). 43
Figure 5.2: Utility-scale solar PV weighted average LCOE trends in some countries, 2021–2022 (IRENA, 2023 [78]). 46
Figure 5.3: No carbon tax. 47
Figure 5.4: 50 EUR/tonne carbon tax. 48
Figure 5.5: 100 EUR/t carbon tax. 48
Figure 5.6: 3D visualization of the production cost dependency on DNI and carbon tax values for aluminium recycling. 49
Figure 5.7: Carbon Tax vs DNI graph for Australia and its relative available DNI range which goes up to around 3000 kWh/m^2 per year, value represented by the dashed line. 51
Figure 5.8: Carbon tax vs LCOH for Australia with the ranges reached by the two solar technologies and their distributions. 52
Figure 5.9: Sensitivity analysis on CST technology: on the left side maps with +25% increase of costs and on the right side with +50% increase, with three different carbon tax values. 53
Figure 5.10: Carbon tax vs DNI graph of South Africa and its relative available DNI range and distribution. CST is cheaper in the yellow areas. 54
Figure 5.11: Comparison between CST and PV in Spain, in different cost scenarios for the CST technology. In the top part: a carbon tax vs LCOH graph where the values reached by both solar technologies are shown (three ranges for the CST based on the cost scenario). Below: LCOH distribution for PV and CST sources (three distributions for CST based on the cost scenario). 55
Figure 5.12: Maps showing the cheapest option in three cost scenarios. 55
Figure 6.1: Cheapest option to provide heat in selected countries and main locations of the processes - base scenario for CST costs and carbon tax value equal to 100 EUR/t. 57

List of Tables

Table 1.1: Synthesis of high temperature industrial processes information (source for the data are specified in the previous sections)..... 20
Table 3.1: Specific carbon dioxide emissions of various fuels (Quaschning and Siegel, 2022 [88]). 28
Table 3.2: Production costs for a fossil fuel plant in Spain, 2000 (Roeb, 2000 [90]). 29
Table 3.3: Production costs calculation based on country and fuel used for a 15000 t/year plant. 30
Table 3.4: Comparison of kilns in terms of energy consumption (Maithel and Heierli 2008 [95]). 32
Table 3.5: Production costs for a clay-fired brick plant in France, 2020 (Youssef, 2020 [96]). 33
Table 3.6: Production costs calculation based on country and fuel used for a 25220 t/year plant. 34
Table 3.7: Direct operating costs for an 100,000 t/a zinc plant (in USD as at June 2000, [73]). 35
Table 3.8: Production costs calculator based on country and fuel used for a 100,000 t/year plant. 36
Table 3.9: Specific emissions for the three processes based on fuel used (no electricity)..... 37
Table 4.1: Dataset used for the interpolation LCOH vs DNI..... 39